TECHNISCHE UNIVERSITÄT MÜNCHEN

Lehrstuhl für Allgemeine Lebensmitteltechnologie

Determinations of the configurations of mercaptoalkanone enantiomers and analytical/sensory characterizations of 2-mercapto-4-alkanones

Christiane Kiske

Vollständiger Abdruck der von der Fakultät Wissenschaftszentrum Weihenstephan für Ernährung, Landnutzung und Umwelt der Technischen Universität München zur Erlangung des akademischen Grades eines

Doktors der Naturwissenschaften

(Dr. rer. nat.)

genehmigten Dissertation.

Vorsitzender:	Prof. Dr. Rudi F. Vogel
Prüfer der Dissertation:	1. Prof. Dr. Karl-Heinz Engel
	2. Prof. Dr. Peter Schieberle

Die Dissertation wurde am 13.06.2019 bei der Technischen Universität München eingereicht und durch die Fakultät Wissenschaftszentrum Weihenstephan für Ernährung, Landnutzung und Umwelt am 22.07.2019 angenommen.

ACKNOWLEDGMENTS

The present work was carried out under the supervision of Prof. Dr. Karl-Heinz Engel at the Chair of General Food Technology of the Technical University of Munich.
I thank Professor Engel for giving me the opportunity to work on this interesting and challenging subject, for his scientific support as well as his guidance and confidence.

My special thanks go to apl. Prof. Dr. Wolfgang Eisenreich (Chair of Biochemistry) for the provision of the infrastructure for NMR measurements as well as the scientific discussions and for the kind help. I also want to thank Christine Schwarz for recording the NMR spectra and her kind support.

Particular gratitude is owed to Prof. Dr. Kenji Monde and Dr. Tohru Taniguchi for the valuable collaboration regarding the VCD measurements and our joint publications.

Prof. Dr. Peter Schieberle is gratefully acknowledged for the examination of this thesis and Prof. Dr. Rudi Vogel for chairing the thesis committee.

I want to thank Dr. Kathrin Jung and Dr. Svenja Nörenberg for the great time in the aroma team, their help, and especially their friendship. Particularly, I want to thank Svenja for the good training and the familarization with the topic at the beginning of my work and for her great support during the whole time.

I want to thank all former colleagues at the Chair of General Food Technology, Dr. Birgit Scholz, Sophia Goßner, Dr. Chenguang Zhou, Anja Devenie Riegel, Veronika Stiegler, Dr. Stefan Wocheslander, Dr. Alexandra Lanzinger, Dr. Rebecca Esche, Dr. Walter Weiss, Dr. Thomas Frank, Iulia Poplacean, Oxana Fastowski, Verena Breu, Gabriele Pawlowski, Claudia Steinmetz, and Dr. Ludwig Ziegler.

I would like to thank my former students Miriam Ecker, Xingyue Ma, Ronja Hopf, and Franziska Groß for their valuable work.

TABLE OF CONTENTS

ABBREVIATIONS

AcS	acetylthio
AEDA	aroma extract dilution analysis
ANL	*Aspergillus niger* lipase
c	conversion rate
CAL-B	*Candida antarctica* lipase B
cAMP	adenosine 3,5-cyclic monophosphate
CD	cyclodextrin
CH_2Cl_2	dichloromethane
CRL	*Candida rugosa* lipase
DCC	*N*,*N*'-dicyclohexylcarbodiimide
DFT	density function theory
DMAP	4-(dimethylamino)pyridine
E	enantioselectivity
ee_P/ee_S	enantiomeric excess of product/substrate
EI	electron ionization
eq.	equivalent
Et_2O	diethyl ether
EtOAc	ethyl acetate
eV	electron volt
FD	flavor dilution
FID	flame ionization detector
GC	gas chromatography
GC/O	gas chromatography/olfactometry
HCl	hydrochloric acid
HPLC	high performance liquid chromatography
HTA	hydratropic acid (2-phenylpropionic acid)
i.d.	inner diameter
IR	infrared spectroscopy
LRI	linear retention index
M*α*NP	2-methoxy-2-(1-naphthyl)propionic acid
MeOH	methanol

Mio.	million
MPA	2-methoxy-2-phenylacetic acid
MS	mass spectrometry
NMR	nuclear magnetic resonance
OAV	odor activity value
PLE	porcine liver esterase
PLE imm.	porcine liver esterase, immobilized
PPL	porcine pancreatic lipase
R_f	response factor
RT	room temperature
SD	standard deviation
TBDMS	*tert*-butyldimethylsilyl
TLC	thin layer chromatography
VCD	vibrational circular dichroism
WGL	wheat germ lipase

1. INTRODUCTION AND OBJECTIVES

Sulfur-containing volatiles play outstanding roles in the flavors of various foods and beverages and have been widely explored (Boelens and van Gemert, 1993b; Mussinan and Keelan, 1994; Vermeulen *et al.*, 2005). Due to their low odor thresholds, polyfunctional thiols contribute significantly to the overall aroma of many foods and beverages and are characterized by distinct odor qualities (Blank, 2002; Mestres *et al.*, 2000; Vermeulen and Collin, 2006). Sensory properties can be affected by concentration as well as by structural characteristics. One important structural feature is the 1,3-oxygen-sulfur function, the so-called 'tropical olfactophore' (Rowe, 2002). Compounds fulfilling this structural requirement are associated with fruity, tropical, and vegetable odor notes. Important examples have been shown for the longer chain homologs of 3-mercaptoalkanols (C6-C9) and for branched representatives like 3-mercapto-2-methylpentanol (Vermeulen and Collin, 2002; 2006; Vermeulen *et al.*, 2003). Another prominent example is 4-mercapto-4-methyl-2-pentanone which has been described as black currant-like (Buettner and Schieberle, 1999) and tropical (Munafo *et al.*, 2014).

β-Mercaptoalkanones and *β*-mercaptoalkanols are representatives of these naturally occurring polyfunctional thiols; for example, 4-mercapto-2-heptanone and 4-mercapto-2-heptanol as well as their positional isomers, and 4-mercapto-2-nonanol have been isolated from cooked red bell pepper (Naef *et al.*, 2008; Nörenberg *et al.*, 2017a). The C5-homolog 4-mercapto-2-pentanone has been reported in aged Cheddar cheese (Kleinhenz *et al.*, 2006; Kleinhenz *et al.*, 2007).

The influence of the stereochemistry on the odor thresholds and qualities has been shown by Wakabayashi *et al.* (2015) for the homologous series of the enantiomers of 4-mercapto-2-alkanones and the corresponding 4-acetylthio-2-alkanones. They demonstrated that the odor qualities of the (*S*)-mercapto-compounds were more pleasant and fruity than those of the (*R*)-enantiomers. Differences of the odor thresholds were only significant for 4-mercapto- and 4-acetylthio-2-hexanone.

The main objectives of this thesis were the determination of the absolute configurations of *β*-mercaptoalkanone enantiomers and the analytical as well as sensory analysis of a homologous series of 2-mercapto-4-alkanones and the corresponding 2-acetylthio-4-alkanones, respectively. To this end, the acetylthio-alkanones should be synthesized

by Michael-type addition of thioacetic acid to the respective 2-alken-4-ones and 3-alken-2-ones (Naef *et al.*, 2008; Wakabayashi *et al.*, 2011) and subsequent transesterification to the mercaptoalkanones.

A thorough reinvestigation of the assignments of the configurations of *β*-mercaptoalkanones, using the C5-compound 4-mercapto-2-pentanone **11**, the C7-representative 4-mercapto-2-heptanone **12**, and its positional isomer 2-mercapto-4-heptanone **2** as examples, should be performed. The assigned configurations based on the ^{1}H-NMR anisotropy method using (*S*)-M*α*NP as chiral derivatizing agent should be compared to the results obtained by investigation of the respective diastereoisomeric thioesters of (*R*)-hydratropic acid (HTA) as well as (*R*)- and (*S*)-2-methoxy-2-phenylacetic acid (MPA).

After establishment of the methods for determining the absolute configurations, the homologous series of 2-mercapto-4-alkanones (**1**, **3**-**5**) and the corresponding 2-acetylthio-4-alkanones (**6**, **8**-**10**) should be separated via GC using a chiral stationary phase, and the orders of elution (GC) should be determined. To this end, enantiomers were obtained via enzyme-catalyzed kinetic resolutions. In order to find suitable enzymes, an enzyme screening with three commercial lipases was performed with respect to conversion rate, enantiomeric excess, and enantioselectivity. Additionally, optimal reaction conditions were determined. Subsequently, the enantiomers were analyzed via the ^{1}H-NMR anisotropy method using different chiral derivatizing agents, i.e. (*R*)-HTA, (*R*)- and (*S*)-MPA, and (*S*)-M*α*NP.

In the last part, sensory evaluations of the 2-mercapto-4-alkanones (C5-C10) and the corresponding 2-acetylthio-4-alkanones were performed by determining the odor thresholds and odor qualities via GC/O. The impact of stereochemistry and chain length on sensory properties should be evaluated, and a structure odor relationship should be established by comparing the sensory data to those of their positional isomers 4-mercapto- and 4-acetylthio-2-alkanones previously examined by Wakabayashi *et al*. (2015).

2. BACKGROUND

2.1. Flavor Compounds

Flavor is a major quality criterion of many foods and beverages and can be decisive for their acceptance or rejection by consumers. The term flavor comprises smell, taste, and tactile sensations including mouth feel, temperature, and even pain when consuming food. Taste and tactile sensations are associated with non-volatile compounds whereas smell is linked to volatile constituents. Regarding the smell of foods, the orthonasal perception, which means smelling of the food before eating can be distinguished from the retronasal perception, which plays a role when flavor compounds are released during eating and drinking food and beverages (Blank, 1997; Shankaranarayana *et al.*, 1974). By the interaction of a variety of volatile compounds with odorant receptors in the nasal cavity, the olfactory perception is created which is a very complex and the least understood sense. The volatile compounds have to meet the following requirements/properties for odor perception: surface activity, low polarity but high lipophilicity, high vapor pressure, and a molecular weight lower than 300 Da (Ohloff, 1994). When a volatile compound reaches an odorant receptor (expressed by the olfactory sensory neuron) in the olfactory epithelium, a heterotrimeric G-protein is activated. Thereby, activation of adenylyl cyclase (type III) catalyzes the cAMP production, which opens a cyclic nucleotide-gated channel and leads to a depolarization of the neuron by opening ion channels (influx of Na^+ and Ca^{2+}). Amplification of this depolarization is reached by the activation of Ca^{2+}-activated Cl^--channels and the efflux from Cl^- from the cell. These changes in the neuron membrane potential generate an electrical signal (action potential) which propagates along the sensory neuron's axon into the glomeruli in the olfactory bulb. From there, the olfactory information is transmitted to the primary frontal cortex and further to the brain where the olfactory information is processed (Brand, 2006; DeMaria and Ngai, 2010; Tromelin, 2016). The odor perception is dependent on the odor threshold and concentration of the respective compound. A distinction is made regarding recognition threshold (lowest concentration of a compound that is sufficient for its odor recognition) and detection threshold (the concentration at which the compound is detectable but an odor quality cannot be assigned). However, neither the concentration nor the odor threshold itself provides information about the contribution to the aroma of foods (Belitz *et al.*, 2009; Hatt, 2010). Therefore, the concept of the odor activity value (OAV) has

been introduced in order to estimate the sensory contribution of a compound. The OAV is defined as the quotient of the concentration and the odor threshold (Grosch, 1990; Patton and Josephson, 1957; Rothe and Thomas, 1963). In principle, the higher the OAV, the higher is the sensory contribution, whereby a value ≥1 has to be reached. However, this value is regarded as an approximation because the threshold value is determined subjectively and the complexity of odor perception is not considered. Nonetheless, this led to the identification of 226 key food odorants out of 10,000 volatile food ingredients, which means that only 3% of volatiles contribute to characteristic aromas (Dunkel *et al.*, 2014). This result is in accordance with that of Grosch (2001) who stated that: *"<5% of the volatiles identified in foods contributed to aromas*." In their meta-analysis, Dunkel *et al.* (2014) examined 119 publications referring to 227 different food products. The 226 key food odorants were graded according to their frequency of occurrence in foods and revealed 16 "generalists", 57 "intermediaries", and 151 "individualists". The "generalists" were identified in 25% of the 227 foods and are characterized by the ability to contribute to different food products. 3-Methional (odor of cooked potato) and 2- and 3-methylbutanal (malty odor) contribute to the aroma of 50% of all foods. The "generalists" are widespread and are normally generated by ubiquitously occurring, biosynthetic precursors like carbohydrates, amino acids, and unsaturated fatty acids during enzymatic (e.g. fermentation) or non-enzymatic (e.g. Strecker or Maillard reaction) reactions. The "intermediaries" contribute to the aromas of 5-25% of all foods and the most abundant "individualists" to 5%. The latter ones are generated by the conversion of specific precursors, such as polyphenols or isoprenoids and are characterized by their distinct aroma contribution to one or a few foods as well as by their extremely low odor thresholds (ppb-ppt). The wine lactone (3*S*,3a*S*,7a*R*)-3a,4,5,7a-tetrahydro-3,6-dimethylbenzofuran-2(3*H*)-one, for example, with its coconut-like smell contributes to the aroma of red and white wine as well as orange juice, and exhibits an odor threshold of 0.02 ppb. The omission of the wine lactone from a model experiment for the wine "Gewürztraminer" revealed a lower degree of similarity with the original (Guth, 1997). The meta-analysis of these 227 foods revealed odor codes with 3 (sour-cream butter) to 36 (cognac) key odorants with distinct concentration ratios, corresponding to 1-16% of all 226 key food odorants.

In another study (Weiss *et al.*, 2012) it was shown that it is possible to create a so-called "olfactory white" flavor impression corresponding to the color percept of white or "white noise". Two conditions have to be met: first, mixtures with ~30 components with

equal intensities and second, these components have to span the stimulus space, meaning good distribution of components in the olfactory space. This means that mixtures of different components, assuming that they comply with both conditions, will have a very similar smell and will not be distinguishable.

2.1.1. Sulfur-Containing Volatile Compounds

About 10% of all volatile compounds have been identified as organic sulfur-containing compounds (Blank, 2002; Boelens and van Gemert, 1993b). The contribution of sulfur-containing volatiles to characteristic flavors and off-flavors in foods and beverages is of vital importance. They are characterized by low odor thresholds, low concentrations (down to ppt level), and sensitivity to oxidation. At higher concentrations (ppm) their smell is strongly sulfurous and obnoxious whereas at low concentrations (ppb-ppt) it can vary from empyreumatic to herbaceous up to fruity and tropical (Goeke, 2002; McGorrin, 2011; Vermeulen *et al.*, 2005). Some sulfur compounds rank among the character-impact compounds, meaning they constitute the characteristic sensory property of a certain food; examples are given in Table 1 (Blank, 2002; McGorrin, 2011). Character-impact compounds and other sulfur-containing volatiles, especially thiols, can be found in seafood, cheese and dairy products, herbs and seasonings, beverages, fruits, cooked and processed foods, as well as vegetables. Their occurrence and important roles have been demonstrated in various reviews (Blank, 2002; Boelens and van Gemert, 1993b; Goeke, 2002; Maga, 1976; Mottram and Mottram, 2002; Mussinan and Keelan, 1994; Shankaranarayana *et al.*, 1974; Vermeulen *et al.*, 2005).

Table 1. Character-impact sulfur-containing volatiles in foods.

character-impact compound	**occurrence**
propyl propanethiosulfonate	raw onion
2-(propyldithio)-3,4-dimethylthiophene	fried onion
diallyl thiosulfinate	garlic
allyl isothiocyanate	mustard
2-methyl-4-propyl-1,3-oxathiane	passion fruit
methyl thioacetate	strawberry
ethyl 3-(methylthio)-propanoate	pineapple
3,5-dimethyl-1,2,4-trithiolane	durian
S-methyl methanethiosulfinate	sauerkraut, cabbage
1,2,4-trithiolane	white truffle
2-*iso*-butylthiazol	fresh tomato

Sulfur-containing compounds can be found in processed foods, e.g. cooked, fried, roasted, or fermented. The Maillard reaction plays an important role within this category. This reaction occurs between amino compounds, for example thiamine or sulfur-containing amino acids like cysteine, cystine, and methionine, and reducing sugars. The reaction starts with the condensation of the sugar's carbonyl group with the amino group to give a glycosylamine. Due to rearrangement and dehydration, via deoxyosones, various dehydration and degradation products like furfural and furanone derivatives, hydroxyketones and dicarbonyl compounds are generated and can further react with compounds like amines, amino acids, aldehydes, hydrogen sulfide, or ammonia (Mottram and Mottram, 2002). The dicarbonyls (deoxyosones), generated during the Maillard reaction, catalyze the Strecker degradation to produce mercaptoacetaldehyde, acetaldehyde, hydrogen sulfide, and other compounds.

Thiols can also be formed by secondary metabolism of microorganisms or plants. During fermentation, e.g. wine production, volatile thiols are released by the enzyme *β*-lyase from precursors like cysteine-*S*-conjugates which are derived from glutathione-*S*-conjugate precursors (Cooper, 1998; Starkenmann *et al.*, 2008; Vermeulen *et al.*, 2005). The biosynthesis of these conjugates and the release of volatile organo-sulfur compounds by C-S-lyases have been extensively studied in *Allium* species. Vegetables and herbs like onion, shallot, garlic, leek, spring onion, and chives are representatives of this group. The volatiles are generated from non-volatile precursors like alliin ((+)-*S*-2-propenyl-L-cysteine-*S*-oxide) in garlic and related *S*-alkenyl-L-

cysteine-*S*-oxides. These precursors are found in the cytoplasm in an intact cell whereas the allinase (C-S-lyase, enzyme) is located in the vacuole. During cell rupture, allinase is released and subsequent *α*,*β*-elimination of the *S*-oxides results in volatile organo-sulfur compounds like allicin (diallyl thiosulfinate, in garlic) or propyl propanethiosulfonate (in raw onion) with an intense smell (Block, 1992). In numerous foods, thiols are derived by this formation process including asparagus, cheese, bell pepper, passion fruit, and wine (Starkenmann *et al.*, 2008). 3-Mercaptohexan-1-ol and 3-mercaptohexyl acetate, for example, play important roles in passion fruit (Engel and Tressl, 1991) and in white wines from *Vitis vinifera* (Tominaga *et al.*, 1996; Tominaga and Dubourdieu, 2000; Tominaga *et al.*, 1998). They exhibit odors reminiscent of citrus, grapefruit, and tropical/passion fruit as well as boxwood and passion fruit, respectively (Tominaga *et al.*, 2006).

An interesting flavor is blackcurrant or cassis. Different compounds can impart this flavor and have been found in different plants, however, they all reveal a catty odor in higher concentrations. 4-Methoxy-2-methyl-2-butanethiol is one of those compounds found in blackcurrant buds (Rigaud *et al.*, 1986) as well as in blackcurrant berries (Jung *et al.*, 2016) with an odor threshold of 10^{-3} µg/kg in water and 0.00008-0.0003 ng/L in air (Guth and Grosch, 1991). The second one is 4-mercapto-4-methyl-2-pentanone which has been identified in Sauvignon wines with an odor threshold ranging from 0.066 to 0.165 ng/L in water (Darriet *et al.*, 1995). The odor of this compound is also described as boxtree or broom; it has indeed been isolated from both plants by Tominaga and Dubourdieu (1997). The concentration differences are considerable. The quantities found in wines were between 1 and 15 ppt and thus lower (factor ~1000) than in boxtree where they ranged between 5 and 22 ppb. In comparison, the threshold value in water is around 0.1 ppt. The third compound is 8-mercapto-*p*-menthan-3-one, firstly isolated from Buchu leaf oil by Lamparsky and Schudel (1972). Sundt *et al.* (1971) determined the smell as intense fruity cassis with minty and burnt nuances, and a panel favored the *trans*- over the *cis*-isomer because of its typical cassis note. Nijssen and Maarse (1986) described it to possess a much sweeter catty odor than the sharper 4-methoxy-2-methyl-2-butanethiol.

But thiols can also give a desired flavor in one food or beverage while they contribute to an off-flavor in another one. Methional (cooked potato), for example, contributes to the aroma of coffee (Mayer *et al.*, 2000), cooked American lobster tail meat (Lee *et al.*, 2001), lychees (Mahattanatawee *et al.*, 2007), or different cheese varieties (Milo and

Reineccius, 1997; Preininger *et al.*, 1994; Qian and Reineccius, 2003). As an off-flavor, it can be found in oxidized white wine with a cooked vegetables note, in aged orange juice with a cooked potato note, and in UHT-milk with the scent of potatoes (McGorrin, 2011). Another off-flavor comes from 3-methyl-2-butene-1-thiol (prenyl mercaptan) which is responsible for the typical "light-struck" off-flavor with skunky and plastic odor notes. It is generated when beer is exposed to sunlight (Gunst and Verzele, 1978), but it is also reported as being likely important to light-protected beer (Vermeulen *et al.*, 2006). Boelens and van Gemert (1993b) reported that about 100 ng/L in beer seems to be necessary for the typical flavor. Holscher *et al.* (1992) identified prenyl mercaptan in roasted coffee with an odor threshold of 0.2-0.4 ng/L. It was also found in several Prieto Picudo wines at concentrations around the odor threshold of 0.5-1 ng/L in wine (San-Juan *et al.*, 2012). However, the contribution of this thiol to the wine aroma could not be determined.

It often depends on the concentration whether a thiol compound imparts a pleasant or unpleasant flavor to a food or beverage and it also depends on its odor threshold. Normally, lower concentrations reveal pleasant and desired aromas whereas higher concentrations the unpleasant and objectionable ones. Because of this reason, thiols are normally found in low concentrations (sometimes around the odor threshold) in foods and beverages.

2.1.2. Structure-Odor Correlations in Thiols

Olfactory research has been neglected for a long time but it is becoming more and more important. Scientists have been dealing with challenging questions like: 'How do we recognize and discriminate between different odors?' or 'Which molecular properties are responsible for similar or different smells?' Different theories were stated at the beginning of the 20th century, for example, the vibrational theory which was postulated by Dyson and later investigated by Wright (Rossiter, 1996). This theory implies a relation between odor and characteristic molecular vibration which are assigned to certain Raman frequencies ("osmic frequencies") (Wright, 1954). Amoore postulated an alternative theory in 1952, namely the 'stereochemical theory' of olfaction which stated a dependence of the odor on size and shape of molecules (Amoore, 1963).

Sensory characteristics have further been studied with respect to their structure-odor relationship. Wannagat *et al.* (1987) examined the exchange of an OH- by an SH-group within isosteric molecules. They could show a drastic change in the odor from floral for carbinols to nauseating in thiocarbinols and thereby queried the theory of Amoore (1963). In 2002, Sakoda and Hayashi investigated this relationship using 1- and 2-alkyl alcohols and thiols by principal component analysis without determining the odor thresholds (Sakoda and Hayashi, 2002). Showing a dependence of the odor properties in a homologous series on the chain length and on the exchange of OH by SH, they could also find some correlations between alcohols and thiols. However, the change of odors within the 1-alkanols to 1-alkanethiols was similar to those of 2-alkanols and 2-alkanethiols. In a recent study, Polster and Schieberle (2015) showed that the odor threshold is significantly influenced by the presence of the free mercapto-group. They examined different alkanols and alkanethiols and demonstrated that alkanols have higher odor thresholds than the corresponding alkanethiols (factors up to 1.2 Mio. for tertiary thiols) except for higher chain lengths (C9 and C10). Also the odor qualities were found to be different; the examined alcohols showed mainly fruity and flowery odor notes for the shorter chain lengths (C4-C8) and increasing fatty and soapy odor notes starting at C7 to C10. In contrast, the respective thiols were described as garlic, sulfury, and burned (C3-C5), roasty and mushroom-like (C6-C9) and as fatty/soapy (C10). These descriptions for odor qualities were different to those of Sakoda and Hayashi (2002). The 1-alkyl alcohols have been described as more oily for shorter chain lengths (C5-C8) and fresher for the longer chain lengths (C9-C11), whereas the 2-alkyl alcohols have been shown a sweet factor for C5-C8 and little odor for C9-C11. 1-Alkyl thiols have been described as fruity, tropical, and oily (C5 and C6), fishy and oily (C7 and C8) and as spicy, roasty, and oily (C9-C11), whereas 2-alkyl thiols have been shown fishy factors for C5 and C6, sweet, fruity, tropical, floral, and fresh notes for C7 and C8, and sweet and fresh factors for C9-C11. Nonetheless, the used principal component analysis for the investigation of structure-odor relationships also revealed differences between alcohols and the respective thiols. Additionally, Schoenauer and Schieberle (2016) demonstrated the impact of the OH-SH-exchange on the odor threshold. (*R*)-*p*-Menthene-8-thiol ($9.0 \cdot 10^{-5}$ ng/L air) showed a 51 Mio. times lower odor threshold than the corresponding (*R*)-*α*-terpineol (4600 ng/L) and (*S*)-*p*-menthene-8-thiol ($6.6 \cdot 10^{-6}$ ng/L air) revealed an odor threshold 86 Mio. times lower than that of (*S*)-

α-terpineol (570 ng/L air). Different odor qualities could also be identified for mercapto-containing *p*-menthene derivatives and the respective alcohols.

By blocking the SH-group via methylation or acetylation, the importance of the free thiol group was also proven by different research groups (Nörenberg *et al.*, 2013; Polster and Schieberle, 2015; Wakabayashi *et al.*, 2012; Wakabayashi *et al.*, 2015). Examining the odor thresholds of 4-mercapto-2-heptanol and 4-acetylthio-2-heptanol, Nörenberg *et al.* (2013) could show differences in the odor thresholds of factors between 9 and 60 for the diastereoisomers and differences for the enantiomers (2*R*,4*R*) with a factor of 172 and (2*R*,4*S*) with a factor of 16. The sensory evaluation of the homologous series of 4-mercapto-2-alkanones (C5-C10) and the respective 4-acetylthio-2-alkanones by Wakabayashi *et al*. (2015) revealed pronounced differences for both compound classes. The 4-acetylthio-derivatives showed higher odor thresholds up to a factor of 1571 for the (*S*)-C8-homolog compared to the respective mercapto-compound. The methylation of the SH-group within different alkanethiols performed by Polster and Schieberle (2015) showed the same result; significantly lower odor thresholds for the alkanethiols than for the methylated derivatives.

The position of the free thiol group within a molecule was also shown to be important. In 1975, Meilgaard has already shown that tertiary thiols have lower odor thresholds than their corresponding secondary and primary derivatives. Extremely pronounced were the differences for the *sec*-isoamyl mercaptan (0.2 ppb) and the respective *tert*-amyl mercaptan (0.00007 ppb) with a factor of 2875. This was confirmed in two studies by Polster and Schieberle (2015, 2017). In the first one (2015), alkane-1-thiols, alkane-2-thiols, alkane-3-thiols, and 2-methylalkane-2-thiols were examined. It was found that the primary thiols showed the highest and the tertiary thiols the lowest odor thresholds for short chain lengths (C3-C6). With elongation of the chains (C7-C10), the secondary alkane-2-thiol revealed the lowest threshold value compared to the respective homologs. In the second study (2017), another functional group was introduced (alcohol moiety) and the odor thresholds of 1-mercapto-alkan-3-ols, 3-mercapto-alkan-1-ols, and 3-mercapto-3-methylalkan-1-ols were examined. For chain lengths C3/4 to C8, the tertiary mercapto-alcohols showed distinct higher threshold values than the secondary and primary homologs. The highest difference could be found for C6 and C7 compounds with one and two orders of magnitude, respectively. For the higher chain lengths C9 and C10, the tertiary mercapto-alcohol revealed the highest whereas

the primary one showed the lowest odor threshold. In contrast to the shorter chain lengths, the differences were not so pronounced.

The investigation of different sulfur-containing compounds revealed specific chemical structures exhibiting certain odor impressions (Dimoglo *et al.*, 1988; Rowe and Tangel, 1999; Rowe, 2002; Vermeulen *et al.*, 2003). In 2002, Rowe developed the model of a so-called “tropical olfactophore”, possessing a 1,3-oxygen-sulfur function relationship (Figure 1). Compounds fulfilling this structural feature are associated with fruity, tropical, and vegetable odor notes.

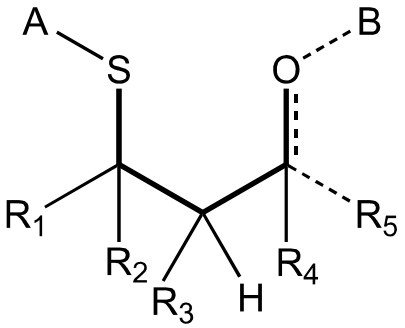

A: H, SCH_3, ring
B: H, CH_3, acyl, absent if carbonyl
R_1, R_2: H, alkyl
R3: H, alkyl, ring
R_4: H, CH_3, OR, ring
R_5: H, absent if carbonyl

Figure 1. The ‘tropical olfactophore’ adapted from Rowe, 2002.

In the same work, Rowe also presented a “catty olfactophore” with similar structural features and catty as well as black currant odor notes. Prerequisite for this structure is a tertiary mercaptane. In Table 2, compounds fulfilling the structural requirements of the different olfactophores are presented.

Table 2. Examples of compounds showing an 1,3-oxygen-sulfur function.

‘tropical olfactophore’	structure	flavor description
3-mercaptohexanol	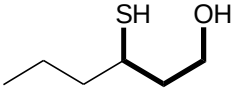	lime, rhubarb[1] citric and fruity notes, flowery and caramel notes[2]
3-mercaptoheptanol	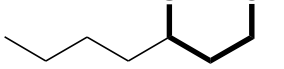	citrus fruit, vinaigrette, carrot[1] green, ink, rhubarb, grassy, vegetal, bitter grapefruit[3]
4-mercapto-3-methylpentan-2-ol	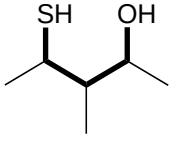	sweat, cooked milk (diastereomer)[1] onion, leek, sweat, soup (diastereomer)[1]

Table 2. continued

‘tropical olfactophore’	structure	flavor description
3-mercapto-2-methylpentanol	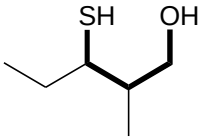	meat broth, onion, sweaty leek (racemate: 0.5 ppb)[4]
4-mercapto-2-alkanones (C5-C10)	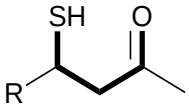	fruity, fresh ((*S*)-enantiomer); sulfury, catty, peel oil ((*R*)-enantiomer)[5]
3-acetylthiohexanal	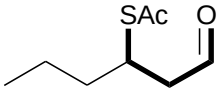	grapefruit, citrus peel, sweet (racemate: 0.1 µg); sulfurous, roasted, citrus peel ((*R*)-enantiomer: 1 µg); fruity, sweet grapefruit ((*S*)-enantiomer: 1 µg)[6]
3-acetylthio-2-alkyl alkanals	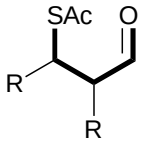	fruity, tropical, grapefruit (at 0.5-5 mg/mL in water)[7]
4-acetylthio-2-alkanones (C5-C10)	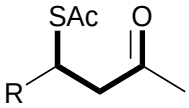	Sulfury, oily, fruity ((*S*)-enantiomer); Fruity, sweet, citrus, peely ((*R*)-enantiomer)[5]
‘catty olfactophore’	structure	flavor description
4-mercapto-4-methyl-2-pentanone	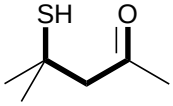	black currant-like[8] tropical[9]

[1] Vermeulen *et al.* (2003); [2] Ferreira *et al.* (2002); [3] Escher *et al.* (2006); [4] Widder *et al.* (2000); [5] Wakabayashi *et al.* (2015); [6] Wakabayashi *et al.* (2003); [7] Robert *et al.* (2004); [8] Buettner and Schieberle (1999); [9] Munafo *et al.* (2014)

Robert *et al*. (2004) and Wakabayashi *et al*. (2003) showed that the “tropical/vegetable olfactophore” can also be applied to the general structure with an acetyl group at substituent A (Figure 1). Later on, Wakabayashi *et al*. (2015) demonstrated that odor can also be dependent on stereochemistry which should also be taken into account when establishing olfactophore models.

2.2. Chirality

2.2.1. Definition and Importance

Chirality is derived from the Greek word “cheir” and means handedness. Louis Pasteur was the first one to discover molecular chirality when examining tartaric acid. Chirality describes the properties of two molecules of the same molecular formula, the so-called enantiomers, without a rotary mirror axis. Four different substituents at a carbon atom (C-atom) meet these requirements. That means, the two molecules are image and mirror image and cannot be superimposed by rotation or translation. Chirality is ubiquitous in nature, e.g. amino acids, sugars, nucleosides as well as various alkaloids and hormones are chiral compounds. Thus, biological processes can result in optically pure products whereas synthetic chemical procedures generate racemates, i.e. a 1:1 mixture of the respective enantiomers, unless specific catalysts are employed. Physical properties are identical for enantiomers despite the rotation of the plane of polarized light in opposite directions (optical activity). They also show identical chemical properties, except for their reactivity in a chiral environment. This fact is very important for biochemistry, pharmaceutical, agrochemical, and food industry as enantiomers can show different biological activities resulting in different interactions with receptors, biocatalysts (enzymes), and transport systems (Bentley, 2006; Brenna *et al.*, 2003; Gal, 2013; Marchelli *et al.*, 1996; Nguyen *et al.*, 2006; Prelog, 1976).

The relationship between stereochemistry and bioactivity has been widely studied since the 19th century regarding, for example, amino acids or microorganisms (Gal, 2013) as well as pheromones (Mori, 1996). D-Asparagine was found to be intensively sweet whereas L-asparagine showed no taste (Gal, 2012). Further taste differences of enantiomers are shown by monosodium L-glutamate (umami) and the respective D-enantiomer (no taste) as well as for the LL-aspartame (very strong sweetness) and the DD-enantiomer (bitter taste) (Bentley, 2006).

Regarding semiochemicals, i.e. biomolecules needed for information exchange between individuals, pheromones were studied with respect to synthesis, stereochemistry, and bioactivity. The pheromones are divided into ten categories depending on their structure-bioactivity relationship. The most important category is characterized by bioactivity of one single enantiomer without inhibition through the opposite enantiomer. About 60% of the chiral pheromones belong to this category. For example, (+)-*exo*-brevicomin is the bioactive pheromone of the western pine beetle

(*Dentroctonus brevicomis*) whereas the (-)-enantiomer is completely inactive. The female sex pheromone of the Japanese beetle (*Popilla japonica*) belongs to the second category, i.e. only one enantiomer is bioactive, and the opposite enantiomer inhibits the response to the pheromone. An example is (*S*)-japonilure, strongly inhibiting the bioactivity of the (*R*)-enantiomer (Brenna *et al.*, 2003; Mori, 1996; 2000).

Another important field is the pharmaceutical industry. More than 50% of the drugs are chiral and the body may metabolize each enantiomer via different pathways resulting in different pharmacological activities and effects. That means, one enantiomer can have the desired therapeutically effect while the opposite enantiomer can be inactive or it can have an undesired or even toxic effect. The most prominent example of such a toxic effect was the drug contergan® which was used as a sedative but also as a drug against morning sickness during pregnancy. The active substance is thalidomide, and it was used as a racemic drug. It was withdrawn from the market in the 1960s because it causes severe teratogenic effects like phocomelia and amelia (Mane, 2016; Nguyen *et al.*, 2006). It was found that only the (*R*)-thalidomide is active whereas the (*S*)-enantiomer has the toxic effect. Further studies showed that the toxic side effect could not have been avoided by using the pure (*R*)-enantiomer due to the rapid interconversion of the enantiomers in biological media (Waldeck, 2003). There are a lot of other examples for racemic drugs with pharmacologically different effects; an overview of some drugs is given by Mane (2016) who classified them into five categories. Nowadays, new chiral drugs are developed as pure enantiomers to overcome the negative aspects and to achieve higher efficacy, improved pharmacokinetics, and to eliminate adverse side effects. The already existing racemic drugs are re-evaluated in order to explore if there can be a gain by switching from a racemate to the enantiomer. This is what has been done with ketamine. It was found that (*S*)-(+)-ketamine should be preferred over (*R*)-(-)-ketamine because it is more potent regarding the analgesic and anaesthetic effect and it is eliminated more rapidly. But it was shown that the (*S*)-enantiomer also has similar psychotomimetic side effects as the racemate (Waldeck, 2003). Another example is the use of racemic Dopa (dihydroxy-3,4-phenylalanine), a precursor of dopamine, which was used for the treatment of Parkinson's disease. Because of the tremendous side effects, such as nausea, anorexia, and agranulocytosis, only L-Dopa is now used with decreased side effects and also the dose could be halved (Hutt and Valentova, 2003). This chiral

switch has been launched 15 times during 1994 and 2011 (Calcaterra and D'Acquarica, 2018).

2.2.2. Chiral Flavor Compounds

Another important field for chiral compounds is the food industry. Normally, enantiomers have different odor qualities and intensities, only 5% of chiral compounds have the same odor (Brookes *et al.*, 2009). To date, more than 700 enantiomeric pairs with odor descriptions (and odor thresholds if available) are given by Leffingwell (2018). Rienacker and Ohloff (1961) published the first data on odor perception of chiral compounds. They examined the synthesis of optically active *β*-citronellol and described the odor of the (*S*)-(-)-enantiomer as reminiscent of geranium oil. The (*R*)-(+)-enantiomer was found to be like citronella oil. Another prominent example for different odor qualities and thresholds is carvone. Its (*R*)-(-)-enantiomer exhibits a spearmint odor with a threshold in water of 2 ppb while its (*S*)-(+)-enantiomer shows a caraway note with a threshold of 85-130 ppb in water (Leitereg *et al.*, 1971). An overview of odor qualities and thresholds of different chiral odorants is given by Boelens and van Gemert (1993a); Brenna *et al.* (2003); Koppenhoefer *et al.* (1994).
Sulfur-containing chiral compounds can also exhibit huge differences regarding odor properties and/or qualities. A remarkable example is 1-*p*-menthene-8-thiol which was identified in grapefruit juice (*Citrus paradise* MACFAYDEN) as powerful flavor impact constituent by Demole *et al.* (1982). They determined the odor thresholds in water with $2 \cdot 10^{-4}$ ppb for the (*R*)- and $8 \cdot 10^{-4}$ ppb for the (*S*)-enantiomer and stated that both enantiomers have a similar flavor of fresh grapefruit juice. Later, Lehmann *et al.* (1995) examined the odors of the single enantiomers using enantioselective GC/O and discovered a specific difference, namely that only the (*R*)-enantiomer reveals the grapefruit-like, strong odor while the (*S*)-enantiomer is nearly odorless. Polyfunctional thiols also play important roles as chiral odorants. The investigation of the juice of yellow passion fruit (*Passiflora edulis* f. *flavicarpa*) revealed sulfur-containing compounds; many of them with one or two chiral centers (Engel and Tressl, 1991; Werkhoff *et al.*, 1998; Winter *et al.*, 1976). Determinations of the absolute configurations, isomeric distributions, and odor qualities were performed and revealed mostly different odor notes for the enantiomeric pairs (Heusinger and Mosandl, 1984;

Weber *et al.*, 1992; Weber *et al.*, 1995). The (*R*)-enantiomers of 3-mercapto- and 3-methylthiohexanol and their esters exhibit a typical fruity aroma whereas the (*S*)-enantiomers show unpleasant and herbaceous odor notes. This perception is reversed for 3-methylthiohexanol; the (*S*)-enantiomer has an exotic and fruity odor and was found to occur as (*S*)-enantiomer in passion fruit (Bentley, 2006; Weber *et al.*, 1995). 3-Mercaptohexanol is the only compound identified with no odor difference; both enantiomers have an intense sulfur odor note. Mercaptoalkanones and further mercaptoalcohols have been identified in foods, e.g. 4-mercapto-2-pentanone in cheddar cheese (Kleinhenz *et al.*, 2006; Kleinhenz *et al.*, 2007) and 4-mercapto-2-heptanone, 4-mercapto-2-heptanol, 2-mercapto-4-heptanone and 2-mercapto-4-heptanol in cooked red bell pepper (Naef *et al.*, 2008; Nörenberg *et al.*, 2017a). Wakabayashi *et al*. (2015) investigated the odor properties of the enantiomers of 4-mercapto-2-pentanone and 4-mercapto-2-heptanone. The odor thresholds showed no significant difference between the (*S*)- and (*R*)-enantiomers of the C5 homolog (1.1 and 1.3 ppt, respectively), or the C7 homolog (0.6 ppt and 0.2 ppt, respectively). However, both compounds revealed differences for the odor qualities between the enantiomers. The (*S*)-enantiomers of both homologs were attributed with grapefruit and sweet whereas the (*R*)-enantiomers showed a more unpleasant odor described as catty with fruity notes. The enantiomers of 4-mercapto-2-heptanol also showed small differences of the odor thresholds, except for the (2*R*,4*R*)-enantiomer. The values determined in air for the enantiomers are 0.1 ppt (2*S*,4*S*), 0.01 and 0.05 ppt (2*R*,4*R*), 0.2 ppt (2*R*,4*S*), and 0.3 ppt (2*S*,4*R*). The odor qualities showed differences but not so pronounced as for other polyfunctional thiols. They were described as fruity with a sulfur note for the (2*S*,4*S*)-enantiomer, as onion for (2*R*,4*R*) and (2*R*,4*S*), and as savory with a green note for the (2*S*,4*R*)-enantiomer (Nörenberg *et al.*, 2017b)

2.2.3. Chiral Analysis of Flavor Compounds

Chirality plays an important role in the perception of odors and flavors. Separation of enantiomers and determinations of the enantiomeric ratios (er) or enantiomeric excesses (ee) are of great importance. Thus, it is possible to detect adulteration of natural flavors and essential oils in the authenticity control, to monitor raw materials used in food and beverage industry, and it is also possible to get access to biogenetic

information on a compound. Additionally, the sensorial properties of the respective enantiomers can be evaluated (Armstrong *et al.*, 1990; Bicchi *et al.*, 1999; Bicchi *et al.*, 1995; Koenig and Hochmuth, 2004).

Enantioseparations can be differentiated into two categories, the indirect and the direct method. The indirect approach utilizes a stereoisomerically pure derivatization reagent in order to derivatize both enantiomers of a racemic mixture. Thus, the obtained diastereoisomers can be separated in an achiral environment. For the direct methods, the enantiomers need to be separated in a chiral environment in which the analyte forms a transient diastereoisomeric complex with the chiral selector in thermodynamic equilibria. The chiral selector can be fixed to an immobile support (e.g. stationary phase) or added to the mobile phase (LC) (Scriba, 2012). Due to several disadvantages of the indirect method (e.g. requirement of complete optical and chemical purity of the derivatization reagents), the direct method is mainly used today; more than 90% of the racemates are separated without derivatization (Bicchi *et al.*, 1999; Schreier *et al.*, 1995). For the chiral analysis of flavor compounds, gas chromatography is the preferred method. The availability of enantioselective GC was a breakthrough in chirospecific analysis. Prerequisites are volatility, thermal stability, and resolvability of the chiral analyte. Three different types of chiral stationary phases (CSPs) are used for separation differing in their selector-selectand interaction: (i) chiral amino acid derivatives resolving enantiomers by H-bonds, (ii) chiral metal coordination compounds resolving enantiomers by complexation, and (iii) cyclodextrins resolving enantiomers by inclusion (Mosandl, 1992; Nowotny *et al.*, 1989; Schurig, 2001).

2.2.3.1. Cyclodextrins

Cyclodextrins (CD) are cyclic oligosaccharides consisting of D-glucopyranose units which are connected via *α*-1,4-glycosidic bonds. The major industrially manufactured and applied CDs are *α*-, *β*-, and *γ*-CDs, differing in their number of glucose molecules, namely six, seven, and eight, respectively. The molecular structure of *β*-CD is shown in Figure 2a. It is a truncated cone-shaped molecular structure due to the free rotation of the primary hydroxyl groups reducing the diameter of the cavity (narrow side). The glucose molecules are arranged in a chair conformation. Due to these $^4C_1$ conformations all secondary hydroxyl groups (in positions 2 and 3) are located on the

wider edge of the ring, whereas all primary ones (position 6) are situated on the narrower edge (Figure 2b and c). A *β*-CD has a rather rigid structure, as the C2- and C3-OH-groups of two adjacent glucopyranose units can form H-bonds resulting in a complete secondary belt. The CD has a hydrophobic cavity at the inside due to the H-atoms and glycosidic O-bridges. It also shows a Lewis base character inside because the free electron pairs of the oxygen bridges are directed toward the inner cavity producing a high electron density. Its outer surface, however, is hydrophilic due to the orientation of the hydroxyl-groups (Scriba, 2012; Szejtli, 1998; Szente and Szeman, 2013).

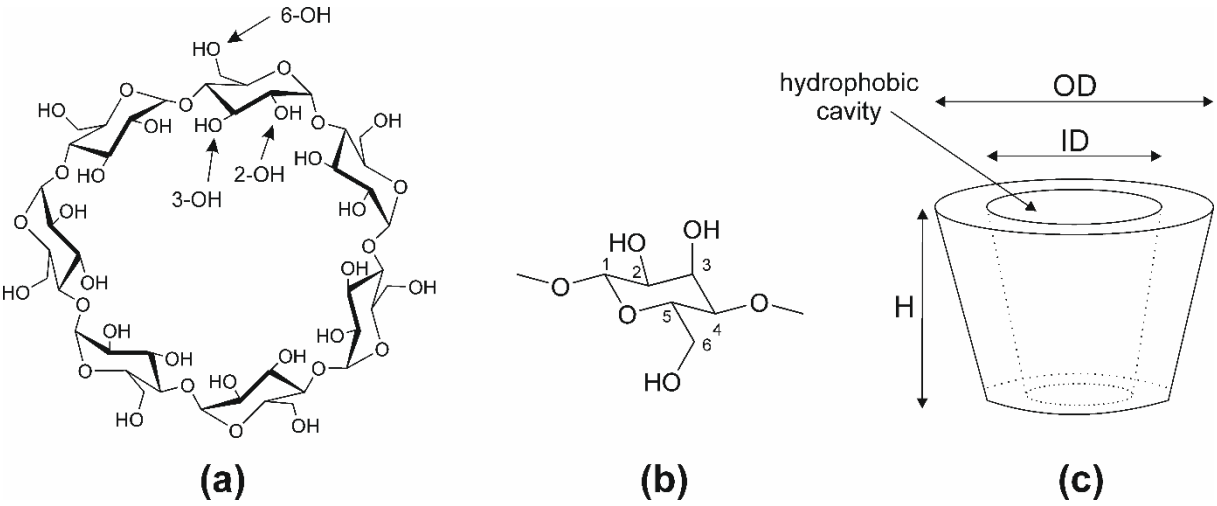

Figure 2. (**a**) Molecular structure of *β*-cyclodextrin; (**b**) glucopyranose unit with its orientation in the truncated cone-shape; (**c**) schematic model of a cyclodextrin with its hydrophobic cavity, H: height, ID: inner diameter, OD: outer diameter (modified after Szejtli, 1997 ()and Dodziuk, 2008).

A characteristic property of CDs is the ability to form inclusion or so-called host-guest complexes. The guest molecules can be organic or inorganic, neutral or ionic but also noble gases. The most important requirement for the complexation is that the guest molecule fits into the chiral cavity of the CD. The binding forces of these complexes can be of different nature, for example van der Waals (hydrophobic) interactions or hydrogen bonds between the hydroxyl-groups. The stability of the inclusion complex is determined by the geometric capability and polarity of the guest molecule, the medium, and temperature. They can be formed in solution as well as in crystalline state, but usually they are formed in the presence of water (Li and Purdy, 1992). The complexation mechanism in CSP has to be different because no water is involved but it is not fully understood. Many contributions to the intermolecular interactions between

host and guests have been discussed, inter alia: steric/induced fit, different interactions (van der Waal, H-bonds, charge transfer, electrostatic, etc.), or depletion of ring strain of the cyclodextrin (Schurig and Nowotny, 1990). The enantiomeric separation is claimed to be based on energetic differences during the host-guest interactions that each enantiomer of a racemate generates with the chiral selector (CD) (Bicchi *et al.*, 2011).

2.2.3.2. Cyclodextrins in Gas Chromatography

Gil-Av *et al.* (1966) were the first who successfully separated enantiomers by GC on chiral stationary phases made up of amino acid derivatives. CD derivatives have been used for the first time as chiral stationary phases in GC by Koscielski *et al.* (1983) in order to separate *α*- and *β*-pinene. To this end, a packed column coated with a mixture of native *α*-CD in a formamide solution was used. The next progress was the discovery that derivatized cyclodextrins are more stable with respect to temperature as well as lifetime, and that they are also able to resolve enantiomers. In *β*-CD, 21 hydroxyl groups (three in every glucose molecule) can be modified. Thereby, the H atom or the hydroxyl group can be substituted by a wide variety of groups, e.g. alkyl, carboxyalkyl, hydroxyalkyl, thiol, tosyl, amino, esters, ethers, etc. The substitution of the primary C6-hydroxyl group with a bulky group like *tert*-butyldimethylsilyl (TBDMS) has a strong impact on enantioselectivity. This bulky substituent influences the conformation of the CD and blocks the entrance of the smaller rim. A second important progress was the use of siloxane polymers by dissolving the CD derivative in polysiloxane. A further improvement was the covalently anchoring of the CD to the polysiloxane followed by immobilization. By now, there are more than 50 CD derivatives employed in chiral GC (Bicchi *et al.*, 2011; Juvancz and Petersson, 1996; Mosandl, 1992; Schurig, 1994; 2001; Szejtli, 1998; Szente and Szeman, 2013).

2.2.3.3. Sensory Analysis via Gas Chromatography/Olfactometry

Gas chromatography/olfactometry (GC/O) combines the conventional chromatography (instrumental-analytical method) with the sensory method. The volatile compounds are

separated in a suitable capillary column; afterwards the gas stream is split by a column flow splitter in order to reach the conventional detector and the sniffing port simultaneously. A human assessor is employed as detector in parallel to the conventional detector like FID or MS (Figure 3). This enables the identification of aroma-active compounds and also their evaluation in complex mixtures, i.e. food matrices or essential oils as well as the determination of odor thresholds and odor qualities (Brattoli *et al.*, 2013; Delahunty *et al.*, 2006).

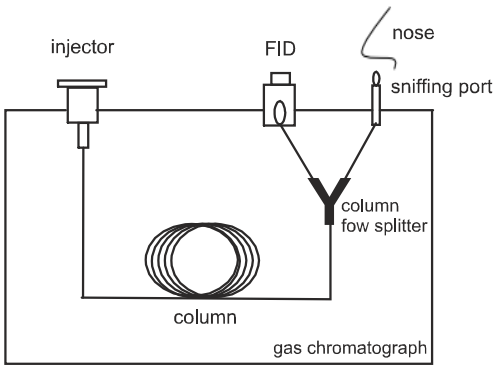

Figure 3. Schematic representation of a GC/O system.

Three types of GC/O-methods are classified: (i) detection frequency, (ii) dilution to threshold, and (iii) direct intensity.

Detection frequency, originally used by Linssen *et al.* (1993), is a simple method without requiring much training of the assessors. It is based on a panel of 6-12 assessors each carrying out GC/O runs on the same extract in order to provide the percentage of people who sensed an odor compound at a specific retention time.

Dilution to threshold is divided into two methods: “Aroma Extract Dilution Analysis” (AEDA) (UIlrich and Grosch, 1987) and “Combined Hedonic Aroma Response Measurement” (CharmAnalysis™) (Acree *et al.*, 1984). Both methods can quantify the odor potency of a compound depending on the ratio of its concentration to its odor threshold in air. They also include the preparation of a dilution series of an extract or a compound and the assessment of every dilution by GC/O. The difference between both methods is that AEDA determines the highest dilution of a perceived odor reporting it as the flavor dilution (FD) factor and CharmAnalysis™ records the duration of an odor quality which is then plotted against the dilution value.

Direct intensity methods involve a scale to measure the perceived intensity of the eluting compound. It can also be divided into two approaches: a single time-averaged

measure (e.g. posterior intensity) whereby the maximum intensity is scaled after elution of the compound, and a dynamic measure (e.g. Osme) whereby onset, maximum intensity, and decay of the eluting odor are recorded continuously (Brattoli *et al.*, 2013; Delahunty *et al.*, 2006; Van Ruth, 2001).

2.3. Enantioselective Biocatalysis

Biocatalysis describes a process that utilizes enzymes, enzyme complexes, a cell organelle, or a whole cell as catalysts for chemical synthesis under controlled conditions. Biocatalysts can be used in purified form or as whole-cell catalysts as well as free or immobilized. The source of biocatalysts can be of microbial, plant, or animal origin. They play important roles for the interactions between microorganisms and their environment and have traditionally been used for the production and preservation of foodstuffs (e.g. bread, dairy and meat products) and alcoholic beverages (e.g. beer and wine). Nowadays, biocatalysts are used for the production of fine chemicals, pharmaceuticals, and agrochemical intermediates, exploiting the desired properties regarding chemo-, regio-, and stereoselectivity at ambient temperatures, pressure, and pH-values (Buchholz and Poulsen, 2000; Nestl *et al.*, 2011; Schulze and Wubbolts, 1999; Turner, 2003). Major drawbacks were the lacking discovery of efficient enzymes for many reactions and the limitation of biocatalysis due to the instability of the biocatalysts regarding temperature, pressure, pH, and organic solvents, as well as the limited substrate range. Therefore, a basic prerequisite for biocatalysis was, and still is, the increase of the catalytic efficiency of natural enzymes under process conditions (Badenhorst and Bornscheuer, 2018; Nestl *et al.*, 2011). Great progress in this field was made through the three waves of technological research and innovations. The first wave started more than a century ago. During this period, scientists discovered the applicability of living cell components for chemical transformations, e.g. the synthesis of (*R*)-mandelonitrile by benzaldehyde and hydrogen cyanide using plant extracts or the usage of proteases in laundry detergents (Bornscheuer *et al.*, 2012). A huge step was the immobilization of enzymes, which increased their stability, but only in a moderate and often insufficient way for most chemical transformations. At the end of this period, the rational design was developed which allowed the design of enzymes with a certain functionality and predictable properties (Bommarius, 2015). The second

wave was characterized by the directed evolution, meaning the use of genetic and protein engineering technologies. This included random mutagenesis and recombination combined with screening or selection of enzymes by enrichment cultures (Bommarius, 2015; Bornscheuer *et al.*, 2012). As a result, a wide DNA sequence space was established and therefore, large libraries of mutants were accessible. As this innovation was also not that successful, because it required high-throughput equipment and did not lead to the desired hit rates, the search continued for better controllable techniques and protocols. That was the beginning of the third wave, the data-driven protein engineering (Bommarius, 2015; Bornscheuer *et al.*, 2012). In this period, the link of all available information led to the establishment of so-called “small, but smart” libraries. Therein, protein structures were combined with sequence comparison and experimental data by appropriate software in order to obtain reliable mutant libraries and to reduce intensive laboratory work (Bornscheuer, 2015). There has been a great progress in directed evolution in protein engineering like stability of the protein against temperature, organic solvents, and other factors or the improved characterization for enhanced protein design (Bommarius, 2015). An overview of the progress in the individual areas is given in different reviews (Badenhorst and Bornscheuer, 2018; Bommarius, 2015; Bornscheuer *et al.*, 2012; Bornscheuer and Kazlauskas, 2004; Nestl *et al.*, 2011; Reetz, 2013; Turner, 2003). Despite these advances there are still limitations to overcome; for example, customized enzyme engineering needs to be accelerated and smaller and smarter libraries have to be designed through advanced DNA synthesis technologies (Badenhorst and Bornscheuer, 2018).

The directed evolution methods are also applicable to improve enzyme enantioselectivity. The stereoselective synthesis of chiral organic compounds is not only of academic but also of great industrial interest in the fields of pharmacy, foods, flavors and fragrances (see chapters 2.2.1. and 2.2.2.). Enzymes can operate enantioselectively and thus, generate predominantly one enantiomer. There are three methods for the enantioselective synthesis depending on the starting material (Figure 4).

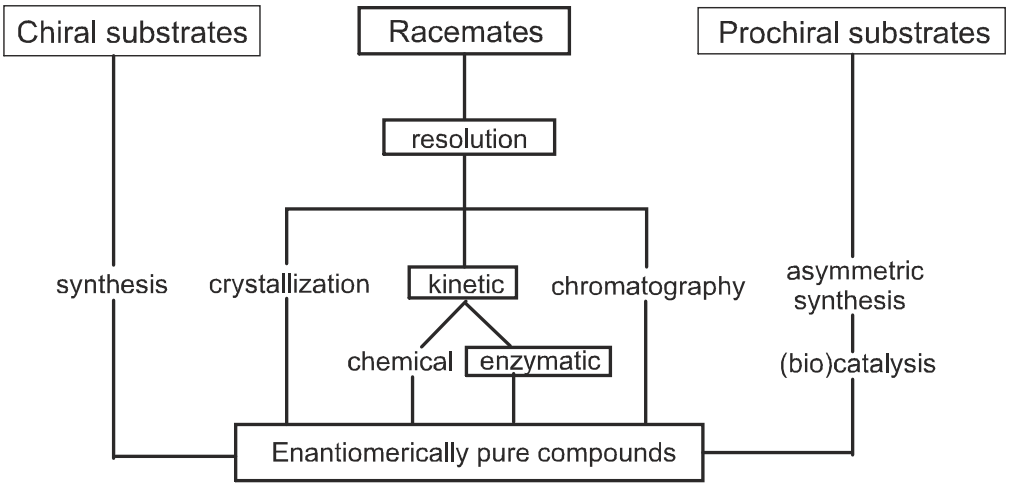

Figure 4. Methods for the production of enantiomerically pure compounds (according to Ghanem and Aboul-Enein, 2005).

One method is to chemically synthesize the enantiomerically pure compounds starting with chiral substrates. The other two methods rank among enantioselective biocatalysis. One is the asymmetric synthesis using prochiral substrates. The disadvantage of this method is the application of rare metals as chiral catalysts (Badenhorst and Bornscheuer, 2018). The other is the resolution of racemates either by crystallization, chromatography, or kinetically. The commonly used method is the enzyme-catalyzed kinetic resolution, which is also applied in this thesis. The enzyme transforms both enantiomers at different rates, this only occurs when the individual rate constant $k_R \neq k_S$. Ideally, only one enantiomer (e.g. (*R*)) reacts with the enzyme, then $k_S = 0$ and the yield would be 50% of enantiomerically pure product P and at the same time, 50% pure substrate (*S*) would remain (Figure 5). The major drawback of this kinetic resolution is a maximum theoretical yield of 50% (Schulze and Wubbolts, 1999).

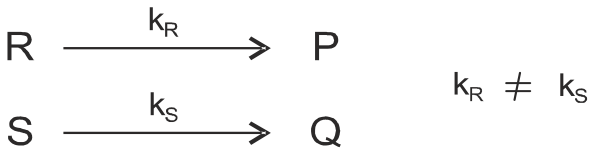

Figure 5. Principle of an enzyme-catalyzed kinetic resolution of a racemate (according to Ghanem and Aboul-Enein, 2005).

To overcome this limitation, the dynamic kinetic resolution can be employed. Therein, the enantiomers of the substrate are in an equilibrium and continuously isomerized (racemized) during the resolution. That means, all of the (*R*) substrate can be

transformed into the enantiomerically pure product P resulting in a theoretical yield of 100% (Ghanem and Aboul-Enein, 2005; Stecher and Faber, 1997).

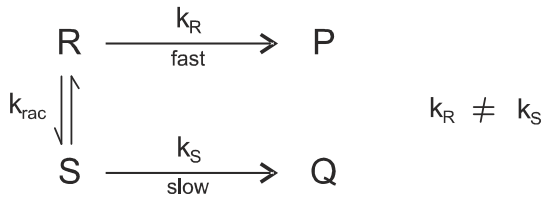

Figure 6. Principle of a dynamic kinetic resolution (k_{rac}: racemization constant; according to Stecher and Faber, 1997).

2.4. Enzymes

Enzymes are biocatalysts as they accelerate biochemical reactions by decreasing the activation energy and by stabilizing the respective transition state without changing the position of the chemical equilibrium. They are chiral polypeptides consisting of L-amino acids, whereby they are able to catalyze reactions stereoselectively. Normally, they are proteins, but there are also catalytic active RNA-molecules. Enzymes are highly specific regarding the respective type of reaction as well as the substrate. Many of them need cofactors for their catalytic activity, meaning coenzymes or metal ions.

The first step of catalysis is the formation of an enzyme-substrate complex. In this step, the enzyme binds the substrate in the gap of its active site, whereby specific bonds are polarized or weakened. Some of these interactions appear preferentially in the transition state that is thereby stabilized and thus, the reaction is initiated. As the transition state is labile, the enzyme-substrate complex disintegrates to form either product or substrate again depending on Δ*G* of the reaction. The kinetics of enzyme-catalyzed reactions depends on the occupancy of the active site with enzyme-substrate complex. It can be explained by the Michaelis-Menten-model in which the enzyme-substrate-complex [ES] is able to degrade into product [P] after forming or to dissociate into [E] and [S] again. k_{cat}, the turnover number, determines the number of substrate molecules converted to product per enzyme molecule per second.

Most of the time, the reaction rate is proportional to the substrate's concentration at the beginning and gets close to a maximum value with an asymptotical curve progression. The velocity v_0 of product formation can be calculated by the Michaelis-Menten equation.

$$v_0 = v_{max} \frac{[S]}{[S] + K_M}$$

The maximum rate (v_{max}) is achieved at saturating substrate concentration. K_M, Michaelis constant, is the substrate concentration at which the reaction rate is at half-maximum. The term k_{cat}/K_M is a significant measure for enzyme activity.

Specific small molecules or ions can inhibit enzymes. These molecules or ions prevent the binding of the substrate to the active site of the enzyme. A reversible bond between inhibitor and enzyme, leading to a decreased reaction rate, characterizes the competitive inhibition. The desired reaction can be controlled by the inhibitor concentration. In contrast, the non-competitive inhibition includes a covalent or very strong and thus irreversible bond between inhibitor and enzyme, and the substrate is not able to form the enzyme-substrate complex.

The product itself can also act as the inhibitor. This product-inhibition is of importance as it can control the extent of a reaction. In this manner, an undesired concentration of the product can be prevented in a cell and a reaction sequence with several steps can be controlled. It is called feedback-inhibition and is also used in the cell to manage the produced amount of substances (Berg *et al.*, 2013; Mortimer and Müller, 2010; Nelson and Cox, 2009).

2.4.1. Lipases

Lipases are triacylglycerol hydrolases [EC 3.1.1.3] that hydrolyze long-chain acyl glycerols. These enzymes are found in many microorganisms, plants, and animals. They play manifold roles in fat digestion and mobilization of stored triacylglycerols; therefore, they have pharmacological potential. Besides their physiological function, lipases play important roles in several fields of industry (e.g. manufacture of foods, cosmetics, leather, pharmaceuticals, etc.) and biotechnology (as detergent additives, catalysts for the manufacture of specialty chemicals). Their importance in organic

synthesis is due to their stability against organic solvents and the fact that they exhibit a broad range of substrate specificity, e.g. aliphatic, alicyclic, bicyclic, and aromatic esters. In addition, their high stereoselectivity towards a broad range of substrates is of great value, as it enables the generation of enantiomerically pure compounds from racemates that are normally difficult to synthesize by chemical processes. Most of the commercially available lipases are of microbial origin, from extracts of stomach and pancreas. Nowadays, also a spectrum of recombinant lipases obtained by using genetic engineering techniques is available (Kovac *et al.*, 2000; Schmid and Verger, 1998).

2.4.1.1. Structure

Despite significant differences in the amino acid sequences, the topology and three-dimensional structures are quite similar and characteristic for all lipases and even esterases. The folding pattern was named '*α*/*β*-hydrolase fold' by Ollis *et al.* (1992) and is characterized by a central, predominantly parallel *β*-sheet consisting of eight strands. The second strand is arranged in an antiparallel manner and the parallel strands *β*3 to *β*8 are connected by *α*-helices (Jaeger *et al.*, 1999; Kazlauskas, 1994).
The active site contains three catalytic residues and is denoted as catalytic triad. It consists of (i) a nucleophilic residue, which can be serine, cysteine, or aspartate, (ii) a catalytic residue that can be aspartate or glutamate, and (iii) a histidine residue. As lipases are serine-hydrolases, the catalytic triad consists of serine, aspartate or glutamate, and histidine. The catalytic nucleophile (serine) is located in a highly conserved pentapeptide, Gly-X-Ser-X-Gly. This pentapeptide forms a sharp *γ*-like turn between the *β*5-strand and the following *α* helix. This strand-nucleophile-helix arrangement is the "nucleophile elbow" where the nucleophile is positioned at the sharp turn that allows easy access to the histidine, on the one side, and to the substrate on the other. The nucleophile is also optimally positioned at the N–terminal end of the following helix so that the helix dipole can help stabilizing the tetrahedral intermediate and the ionized nucleophile's form as well. This structural feature is also called 'oxyanion hole'. This hole is characterized by two NH groups, one is from the residue just behind the serine and the other from the residue of strand *β*3 (Jaeger *et al.*, 1999; Ollis *et al.*, 1992; Schrag and Cygler, 1997).

2.4.1.2. Catalytic Mechanism

The mechanism of lipase-catalyzed hydrolysis and esterification is based on the catalytic triad of serine, histidine, and aspartate or glutamate, which are interconnected via hydrogen bonds (Figure 7). The tetrahedral intermediate is stabilized by the oxyanion hole as explained in 2.4.1.1.

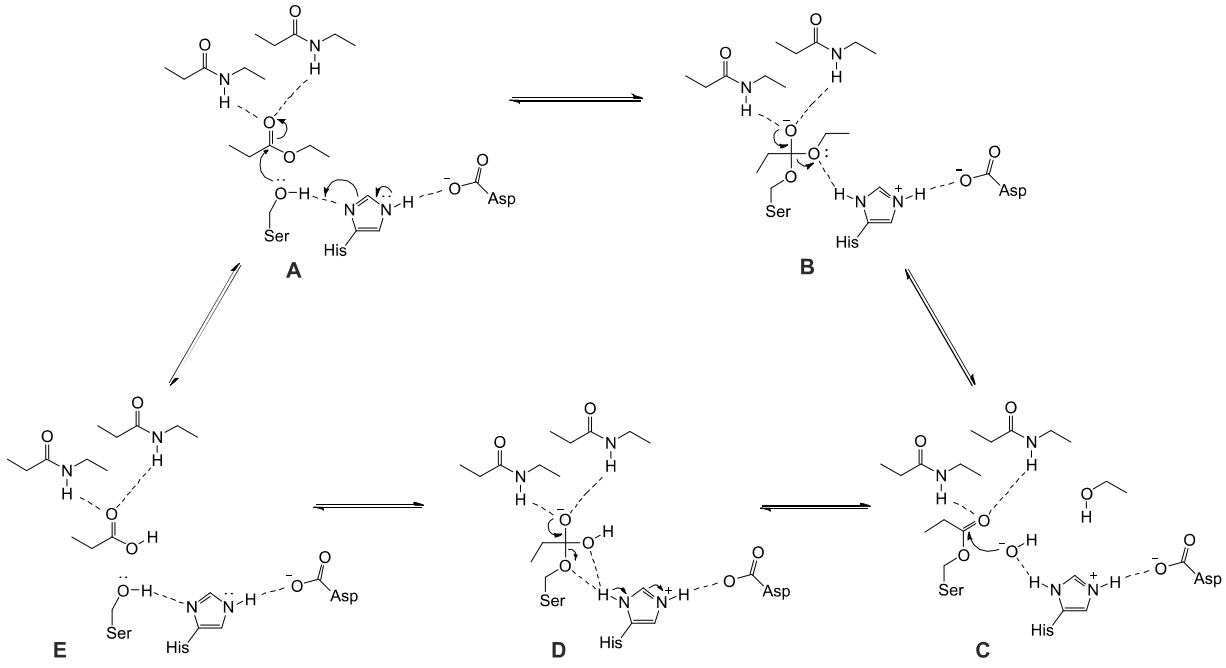

Figure 7. Reaction mechanism of lipases (adepted from Jaeger *et al*., 1999 and Kazlauskas, 1994).

The catalytic mechanism proceeds as follows.

[A] It starts with the binding of the lipid in the oxyanion hole by H-bonding, and the nucleophilic serine residue is activated by a proton transfer to the neighboring imidazole of the histidine. The Ser-O^- attacks the substrate's carbonyl C-atom in a nucleophilic manner.

[B] A tetrahedral intermediate is formed which is stabilized by two peptide NH-groups. The histidine donates a proton to the alcohol to spun off and the alcohol is released as the first product. Simultaneously, the acid component of the substrate is esterified with the enzyme's serine residue and the "acyl enzyme", a covalent intermediate, is generated.

[C] The entering H_2O molecule is activated by the transfer of its proton to the histidine and the resulting hydroxyl anion performs a nucleophilic attack to the carbonyl atom of the acyl enzyme.
[D] The resulting tetrahedral intermediate is stabilized by interactions with the oxyanion hole. The histidine residue transfers a proton to the active serine residue, whereby the ester bond between serine and acyl component is cleaved.
[E] The carboxylic acid is released as the second product. Consequently, the lipase is regenerated and the mechanism can start from the beginning (Jaeger *et al.*, 1999).

2.4.1.3. Interfacial Activation

The phenomenon of the ‘interfacial activation’ was considered as typical for lipases for a long time and was one criterion for the definition of a “true” lipase. The second criterion was the existence of a ‘lid’-structure.
Sarda and Desnuelle (1958) observed an increased activity of lipases when acting at a lipid-water interface of micellar or emulsified substrates. This is triggered by a structural feature, the so-called lid. It is an amphiphilic peptide segment, which covers the active site of the lipase and thus, makes it inaccessible for substrates. By accumulation on a lipid-water interface, the lid experiences a conformational change and opens up in order to give access to the substrate to the catalytic residues. It turned out to be not applicable to all lipases as there are lipases without this lid or bearing only a ‘mini-lid’ instead, e.g. cutinase or guinea pig (phospho)lipase (Hjorth *et al.*, 1993; Martinez *et al.*, 1992) but also lipases with a lid which do not show an interfacial activation, e.g. CAL-B (Uppenberg *et al.*, 1994). This means that both criteria are not sufficient to classify an esterase as lipase. Therefore, lipases are defined as carboxylesterases catalyzing the hydrolysis as well as the synthesis of long-chain acylglycerols (the length is not accurately specified). Any acyl chain lengths of ≥10 carbon atoms are regarded as lipase substrates. A trioleoylglycerol is regarded as standard substrate (Jaeger *et al.*, 1999; Schmid and Verger, 1998).

2.4.1.4. Enantioselectivity

Lipases are powerful biocatalysts in organic synthesis due to their stereoselectivity. They are widely used for the preparation of optically active carboxylic acids, esters, alcohols, amino acids, and amides. Stereoselectivity of a lipase is mostly dependent on the structure of the substrate and therefore its interaction with the active site of the lipase. Thereby, two determining factors play important roles. Firstly, the orientation of both enantiomers in the active site and secondly, the energetic states of the tetrahedral intermediates as well as of the ground states. Only if the substrate binds favorably to the active site of the lipase, the potential energy of the tetrahedral intermediate can be decreased and the respective enantiomer can be converted more rapidly (Ema *et al.*, 1998; Haeffner *et al.*, 1998; Orrenius *et al.*, 1998).

Some improvements were made in the last years for enhancing the stereoselectivity; on the one hand, by immobilization of lipases (Cassimjee *et al.*, 2017; Hanefeld *et al.*, 2009; Kirk and Christensen, 2002) and on the other hand by studying the influence of solvents, water, and reaction conditions (Hansen *et al.*, 1995; Hult and Norin, 1992; Muralidhar *et al.*, 2002; Reetz, 2002). By molecular modeling and simulations, it was possible to examine and to predict the enantioselectivity of respective lipase-catalyzed reactions (Haeffner *et al.*, 1998). By medium, substrate, and enzyme engineering it is even possible to create enantioselectivity for enzymes (Magnusson *et al.*, 2001; Tsai, 2016).

Despite much research and many improvements, the “Kazlauskas-rule”, a rule to predict the fast-reacting enantiomer of racemic secondary alcohols in enzyme-catalyzed reactions using cholesterol esterase (CE), lipase from *Pseudomonas cepacia* (PCL), and from *Candida rugosa* (CRL), is still applicable for the prediction. On the basis of an enzyme with two different sized pockets and a secondary alcohol with two different sized substituents, one large (L), the other smaller (M), the rule says that the enantiomer reacts faster (often (*R*)) that fits better into the catalytic site of the enzyme. This means, the larger substituent accommodates into the larger pocket and the smaller group accommodates into the smaller pocket of the enzyme, as is depicted in Figure 8a (Kazlauskas *et al.*, 1991). The catalytic mechanism was studied and proven by Cygler *et al.* (1994) with CRL as lipase and menthyl phosphonate inhibitors as substrate. They also described this phenomenon for other lipases. Ghanem and Aboul-Enein (2005) reviewed lipase-catalyzed reactions with different substrates.

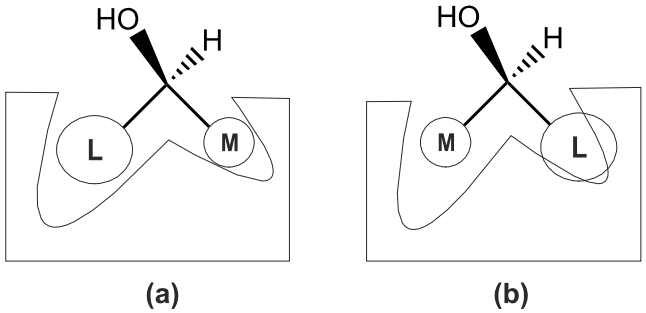

Figure 8. Schematic representation of the active site of a lipase for the 'Kazlauskas rule'. (a) preferred and fast reacting enantiomer; (b) unpreferred and slow reacting enantiomer (according to Ghanem and Aboul-Enein, 2005).

2.4.1.5. *Candida Antarctica* Lipase B (CAL-B)

Candida antarctica is a basidiomyceteous yeast which produces two different lipases, A and B. Both lipases are highly stable in an immobilized form and over a relatively broad pH range but they can also be very different. CAL-A is extremely thermostable and calcium dependent, whereas CAL-B is less thermostable and calcium independent. The specificity of both lipases is also different. CAL-A shows a preference for the *sn*-2 position in triglycerides. It was found to exhibit a unique activity towards diverse sterically hindered alcohols and amines including secondary and even tertiary alcohols. In the esterification of *cis*/*trans*-isomers of unsaturated fatty acids, CAL-A shows a clear preference for the *trans*-isomer. In contrast, other lipases prefer the esterification of *cis*-fatty acids (Kirk and Christensen, 2002). CAL-B however, shows less preference for large triglycerides but a very high activity towards a broad range of esters, amides, and thiols. It exhibits a high stability in water as well as in organic solvents and also a high substrate-selectivity with respect to regio- and enantioselectivity in hydrolysis and organic synthesis. Thus, CAL-B found the widest application in many industrial processes and biocatalysis (Anderson *et al.*, 1998; Stauch *et al.*, 2015).

CAL-B consists of 317 amino acids and has a molecular weight of 33 kDa. It is a globular protein and belongs to the *α*/*β*-hydrolase fold family. The difference is that CAL-B has only seven *β*-strands. Moreover, CAL-B differs in its pentapeptide sequence resulting in a bend, slightly more away from the strand. This provides more space for the threonine residue lying in the middle of *β*4. The catalytic triad of the active site consists of Ser-His-Asp and therefore reveals the same sequential order of the

catalytic residues as for other lipases. Although CAL-B shows no interfacial activation (Martinelle *et al.*, 1995), there is a small helix (*α*5) which has long been supposed to act as a lid (Uppenberg *et al.*, 1994). Recently, Stauch *et al*. (2015) examined the structure of CAL-B regarding an open and closed state, again. They described the structure as a pocket with the amino acid residues Asp 145 and Lys 290 at the opening and with Ser105 at the inner bottom. In the open state, a series of aliphatic residues (*α*-helix) line the channel that leads to the active site with only one polar residue (Asp145). In this state, a triacylglycerol molecule can pass and is hydrolyzed to diacylglycerol and monoacylglycerol. In the closed state, the *α*-helix 5 undergoes a drastic conformational change where the carboxylic acid group of Asp145 gets close to the side chain of Lys290, thus forming a salt bridge and resulting in an unstructured loop. To complete the closure of the catalytic cavity, the *α*-helix 10 is brought closer to the new lid region by the spatial rearrangement of Lys290. By unfolding the *α*-helix 5, the lid is closed over the cavity and no substrate can access the catalytic site. Stauch *et al*. (2015) stated: "*The interfacial activation phenomenon is then the convolution of the properties of the substrate, the media, and the enzyme with its amino acid sequence*." They also suggested that interfacial activation should not be discussed based on the presence or absence of a lid region. In 2017, Luan and Zhou discovered a "true" open state of CAL-B in water and they stated that the lid *α*5 is held by a "lid-holder" consisting of *α*6 and *β*8 which uses a salt bridge between *α*5 and *β*8 and hydrophobic attraction between *α*5 and *α*6. This provides a wider and more stable entrance to the catalytic site. They postulate a novel self-activation mechanism by spontaneous switching between the opened and closed state resulting in an open lid in water allowing a hydrophilic substrate to enter the catalytic site. However, this can only happen if the binding energy between the lid and a hydrophobic surface is larger than the binding energy between the lid and lid-holder (critical value: 4.0 kcal/mol).

Uppenberg *et al.* (1995) examined the stereospecificity of CAL-B with respect to secondary alcohols as it was found that CAL-B exhibits a high enantioselectivity towards these substrates. The study revealed a preference for the (*R*)-enantiomer during esterification of an alcohol as well as hydrolysis of a glycerol monoester. This presupposes that the alcohol or the ester reveal two different sized substituents (a medium and a large one) as postulated by Kazlauskas (see 2.4.1.4). Uppenberg *et al*. (1994, 1995) have already described the active site as a flat hydrophobic region with the active serine residue at the bottom of a narrow and deep pocket. This active site

pocket can be divided into two channels, an acyl side and an alcohol side in which the corresponding substituents of the substrate will be located during catalysis. The alcohol side additionally contains a stereospecificity pocket consisting of Thr42, Ser47 and Trp104, in which only a substituent of the size of ethyl or smaller can be comfortably hosted. Two different orientations are possible for the binding of secondary alcohols. In the first mode, the medium-sized group of the fast-reacting enantiomer (normally (*R*)) is positioned in the stereospecificity pocket whereas the large group substituent is located at the entrance of the active site pointing out towards the enzyme's surface. In the second mode, the medium-sized group of the slow-reacting enantiomer (*S*) is oriented towards the entrance of the active site while the large group is forced into the smaller stereospecificity pocket. In both modes, the hydrogen bonding pattern essential for catalysis, especially the hydrogen bond between the histidine residue of the catalytic triad and the oxygen atom of the alcohol, is present (Haeffner *et al.*, 1998; Magnusson *et al.*, 2005; Orrenius *et al.*, 1998; Rotticci *et al.*, 1998). Haeffner *et al*. (1998) and Orrenius *et al*. (1998) additionally examined the energetic states of the tetrahedral intermediates. Orrenius *et al*. found that the tetrahedral intermediate of the fast-reacting (*R*)-enantiomer has the lowest potential energy in the first docking-mode and the slow-reacting (*S*)-enantiomer has the second lowest potential in the second docking-mode. Haeffner *et al.* (1998) developed a method for calculating the enantioselectivity by molecular modeling and also found the (*R*)-enantiomer as the faster reacting one.

Due to the limited size of the stereospecificity pocket, the excellent enantioselectivity is restricted to secondary alcohols with a medium and a large substituent. This also explains why primary and tertiary alcohols are not suitable for CAL-B as lipase (Magnusson *et al.*, 2005; Orrenius *et al.*, 1998; Rotticci *et al.*, 1998). Other substrates like for example esters, amines, or thiols and thioacetates can also be catalyzed by CAL-B with obtaining mostly the (*R*)-enantiomer (Anderson *et al.*, 1998; Tsai, 2016).

3. MATERIALS AND METHODS

3.1. Materials

3.1.1. Chemicals

The following chemicals were used:

Acetaldehyde	Merck Schuchardt OHG, Hohenbrunn, Germany
n-Alkane standard solution (C8-C20 und C21-C40)	Sigma-Aldrich, Steinheim, Germany
Ammonium chloride (p.a.)	VWR, Darmstadt, Germany
Ammonium sulfate (technical ≥ 99%)	Sigma-Aldrich, Steinheim, Germany
Celite® 503	Sigma-Aldrich, Steinheim, Germany
Chloroform (≥ 99.5%)	Sigma-Aldrich, Steinheim, Germany
(*E*)-2-Decenal (≥ 95%)	Sigma-Aldrich, Steinheim, Germany
Deuterated chloroform (99.96 atom% D)	Sigma-Aldrich, Steinheim, Germany
Dichloromethane (AnalaR Normapur)	VWR, Darmstadt, Germany
N,*N'*-dicyclohexylcarbodiimide	Sigma-Aldrich, Steinheim, Germany
Diethyl ether (AnalaR Normapur)	VWR, Darmstadt, Germany
4-(Dimethylamino)pyridine	Sigma-Aldrich, Steinheim, Germany
2,2-Dimethyl-1,3-dioxan-4,6-dione (Meldrum's acid)	Sigma-Aldrich, Steinheim, Germany
Ethanol (reinst, ≥ 99.5%)	Carl Roth GmbH, Karlsruhe, Germany
Ethyl acetate (Chromasolv)	Sigma-Aldrich, Steinheim, Germany
Ethyl acetate	Sigma-Aldrich, Steinheim, Germany
Ethyl butyrylacetate	Sigma-Aldrich, Steinheim, Germany
(*S*)- and (*R*)-2-Heptanol	Sigma-Aldrich, Steinheim, Germany
Heptanoyl chloride	Sigma-Aldrich, Steinheim, Germany
3-Hepten-2-one	Alfa Aesar, Karlsruhe, Germany
n-Hexane (AnalaR Normapur)	VWR, Darmstadt, Germany
n-Hexane (HiPerSolv Chromanorm)	VWR, Darmstadt, Germany
Hexanoyl chloride	Sigma-Aldrich, Steinheim, Germany
4-Hexen-3-one	Sigma-Aldrich, Steinheim, Germany
Hydrochloric acid (25%, puriss, p.a.)	Sigma-Aldrich, Steinheim, Germany
Lithium aluminum hydride	Sigma-Aldrich, Steinheim, Germany

Magnesium sulfate (anhydrous)	Sigma-Aldrich, Steinheim, Germany
Methanol	Sigma-Aldrich, Steinheim, Germany
(*R*)-(-)-2-methoxy-2-(1-naphthyl) propionic acid	TCI Europe, Zwijndrecht, Belgium
(*S*)-(+)-2-methoxy-2-(1-naphthyl) propionic acid	TCI Europe, Zwijndrecht, Belgium
(*R*)-(-)-2-methoxy-2-phenylacetic acid	Sigma-Aldrich, Steinheim, Germany
(*S*)-(+)-2-methoxy-2-phenylacetic acid	Alfa Aesar, Karlsruhe, Germany
2-Octen-4-one	TCI Europe, Zwijndrecht, Belgium
Oxalyl chloride	Sigma-Aldrich, Steinheim, Germany
3-Penten-2-one	Sigma-Aldrich, Steinheim, Germany
(*R*)-(-)-2-Phenylpropionic acid	TCI Europe, Zwijndrecht, Belgium
Potassium dihydrogen phosphate	Riedel-de Haën, Seelze, Germany
di-Potassium hydrogen phosphate trihydrate	Merck, Darmstadt, Germany
S-Potassium thioacetate	TCI Europe, Zwijndrecht, Belgium
iso-Propanol (HiPerSolv Chromanorm)	VWR, Darmstadt, Germany
Pyridine (anhydrous, 99.8%)	Sigma-Aldrich, Steinheim, Germany
Silica Gel (NormaSil 60, 40-63 µm)	VWR, Darmstadt, Germany
Sodium chloride (technical)	VWR International, Leuven, Belgium
Sodium hydrogen carbonate	Sigma-Aldrich, Steinheim, Germany
Sodium hydroxide (≥97%, pellets)	Sigma-Aldrich, Steinheim, Germany
Sodium sulfate (anhydrous)	VWR, Darmstadt, Germany
Sulfuric acid (95-98%, extra pure)	Merck, Darmstadt, Germany
Thioacetic acid	Merck Schuchardt OHG, Hohenbrunn, Germany
p-Toluenesulfonyl chloride	Sigma-Aldrich, Steinheim, Germany
Toluol (anhydrous, 99.8%)	Sigma-Aldrich, Steinheim, Germany

3.1.2. Enzymes

The following lipases were purchased from Sigma-Aldrich, Steinheim, Germany

1. *Candida antarctica* lipase B (CAL-B)
≥5,000 U/g, recombinant, expressed in *Aspergillus niger*, adsorbed on a macroporous acrylic resin

2. Lipase from porcine pancreas (PPL)
Type II, 30-90 U/mg

3. Lipase from wheat germ (WGL)
Type I, lyophilized powder, 5-15 U/mg protein

4. Lipase from *Aspergillus niger* (ANL)
Powder (fine), ~200 U/g

5. Esterase from hog liver (PLE (imm.))
immobilized on Eupergit® C, 257 U/g

6. Esterase from hog Liver (PLE)
lyophilized powder, 131 U/g

The following lipase was purchased from Sigma Chemical Co., Japan

7. Candida Rugosa Lipase (CRL)
835 U/mg solid, 1.440 U/mg Prot. (Biuret)

3.2. Syntheses

3.2.1. Methyl 3-oxooctanoate and Methyl 3-oxononanoate

Both esters were synthesized according to Oikawa *et al.* (1978), starting with 69.4 mmol Meldrum's acid in 70 mL CH_2Cl_2. After addition of 138.8 mmol (2.0eq.) pyridine and 76.3 mmol (1.1eq.) hexanoyl chloride (for C9) or heptanoyl chloride (for C10) dropwise, the reaction mixture was stirred for 1 h under ice cooling and for another hour at room temperature (RT) under argon. Afterwards, it was washed with

(10%) HCl (3x20 mL) and H_2O (2x20 mL), dried over anhydrous sodium sulfate, and the solvent was removed using a rotary evaporator. The crude product was mixed with 10 mL of MeOH and was stirred for 2 h under reflux, followed by evaporation of the solvent and column chromatography on silica gel with a mixture of *n*-hexane/Et_2O (6+1, v/v). Three reaction batches were combined, respectively.

Methyl 3-oxooctanoate: yield: 78.2%, purity: 76.1% (by GC); Linear retention indices (LRI) determined by GC: 1761 (RTX-WAX); GC-MS (m/z, rel. %): 43 (100), 116 (55), 99 (52), 71 (33), 101 (32), 59 (30), 74 (29), 55 (22), 84 (20), 172 (M^+,1).

Methyl 3-oxononanoate: yield: 73.0%, purity: 79.6% (by GC); LRI: 1887 (RTX-WAX); GC-MS (m/z, rel. %): 43 (100), 116 (75), 113 (45), 74 (32), 59 (31), 101 (27), 55 (27), 84 (26), 186 (M^+,2).

3.2.2. 2-Hepten-4-one, 2-Nonen-4-one, and 2-Decen-4-one

The alkenones were synthesized as described by Naef *et al*. (2008). In a round bottom flask, 3.5 g NaOH were mixed with 80 mL H_2O and 78.2 mmol of the respective ester was added dropwise under ice cooling. After stirring the reaction mixture at RT overnight, 166 mL saturated $(NH_4)_2SO_4$ was added, the reaction mixture was cooled down with an ice bath, and ~40 mL of diluted H_2SO_4 was added dropwise (pH~2). The mixture was extracted with Et_2O (2x100 mL), washed with brine (1x50 mL), and dried over anhydrous $MgSO_4$. After filtration, the solvent was removed at 30 °C (max) under reduced pressure. The solid residue (3-oxo-hexanoic acid, 3-oxo-octanoic acid, and 3-oxo-nonanoic acid) was immediately used for the next reaction step. In a Schlenk flask, flame-dried under argon, 5.3 mL acetaldehyde and 10 mL pyridine were mixed under ice cooling, the respective 3-oxo-alkanoic acid was added in 2-3 mL pyridine, and the flask was rinsed with 3-5 mL pyridine. After 30 min, the ice cooling was removed and the mixture was stirred at RT overnight. The reaction mixture was heated to 90 °C for 15 min, cooled down, and diluted with 30 mL H_2O. The mixture was extracted with Et_2O (2x100 mL), then washed with 2N H_2SO_4 (5x40 mL), saturated $NaHCO_3$ (1x40 mL), and brine (1x40 mL) to pH 7, dried over anhydrous Na_2SO_4; after filtration it was concentrated under vacuum.

2-Hepten-4-one: yield: 44.5%, purity: 57.4% (by GC); GC-MS (m/z, rel.%): 69 (100), 41 (74), 97 (53), 39 (31), 84 (19), 43 (13), 27 (9), 55 (4), 112 (M+, 0.5). Mass spectrometric data were in accordance with those previously reported (Naef *et al.*, 2008).

2-Nonen-4-one and 2-decen-4-one were purified by distillation under vacuum:

2-Nonen-4-one: boiling point: 78-80 °C (11 mbar), yield: 56.0%, purity: 84.7% (by GC); LRI: 1485 (DB-WAX), 1101 (DB-1); GC-MS (*m/z*, rel.%): 69 (100), 84 (44), 41 (26), 39 (11), 43 (7), 97 (5), 125 (M^+, 8); ^{1}H-NMR (500 MHz, $CDCl_3$): δ 6.77 (dq, *J* = 15.8, 6.8 Hz, 1H, H-2), 6.05 (m, dq, *J* = 15.7, 1.7 Hz, 1H, H-3), 2.44 (m, 2H, H-5), 1.82 (dd, *J* = 6.9, 1.8 Hz, 3H, H-1), 1.53 (dt, *J* = 14.8, 7.5 Hz, 2H, H-6), 1.30-1.18 (m, 4H, H-8, H-7), 0.82 (t, *J* = 7.1 Hz, 3H, H-9); ^{13}C-NMR (126 MHz, $CDCl_3$): δ 199.77 (C-4), 141.32 (C-2), 130.94 (C-3), 38.96 (C-5), 30.49 (C-7), 22.98 (C-6), 21.48 (C-8), 17.22 (C-1), 12.93 (C-9).

2-Decen-4-one: boiling point: 83-85 °C (5 mbar), yield: 18.9%, purity: 76.2% (by GC); LRI: 1578 (DB-WAX), 1203 (DB-1), GC-MS (*m/z*, rel.%): 69 (100), 84 (57), 41 (25), 43 (47), 41 (7), 97 (7), 139 (6), 154 (M^+, 2); ^{1}H-NMR (500 MHz, $CDCl_3$): δ 6.77 (dq, *J* = 15.7, 6.8 Hz, 1H, H-2), 6.05 (dq, *J* = 15.8, 1.7 Hz, 1H, H-3), 2.44 (m, 2H, H-5), 1.82 (dd, *J* = 6.8, 1.7 Hz, 3H, H-1), 1.53 (m, 2H, H-6), 1.27-1.16 (m, 6H, H-7, H-8, H-9), 0.80 (m, 3H, H-10); ^{13}C-NMR (126 MHz, $CDCl_3$): δ 199.83 (C-4), 141.32 (C-2), 130.93 (C-3), 39.03 (C-5), 30.61 (C-8), 27.98 (C-7), 23.25 (C-6), 21.50 (C-9), 17.23 (C-1), 13.03 (C-10).

3.2.3. Acetylthioalkanones

2-Acetylthio-4-alkanones **6**-**10**, 4-acetylthio-2-pentanone **13**, and 4-acetylthio-2-heptanone **14** were synthesized by Michael-type addition of thioacetic acid (1.1eq.) to the respective alkenones (10-20 mmol) as previously described by Wakabayashi *et al*. (2011 and 2015). The mixture was stirred at 0 °C for 1 h and then at RT for 20 h (C5-C8). For C9 and C10, the method described by Naef *et al*. (2008) was used; to this end, the alkenones and thioacetic acid were heated at 100 °C for 4 h. The remaining thioacetic acid was removed at a rotary evaporator at 60 °C under vacuum. Some of the crude products were purified by column chromatography on silica gel by elution

with a mixture of *n*-hexane/Et_2O (3:1, v/v) for **13**, and (4:1, v/v) for **6** and **7**; the obtained fractions were checked by TLC (ALUGRAM® SIL G/UV_{254}, Macherey-Nagel, Germany), visualization was achieved by spraying with 10% sulfuric acid and subsequent heating until dryness.

2-Acetylthio-4-hexanone **6**: yield: 107.1%, purity: 92.4% (GC); LRI: 1822 (RTX-WAX), 1225 (DB-1), GC-MS (*m/z*, rel.%): 43 (100), 99 (71), 57 (65), 29 (22), 75 (12), 41 (10), 69 (10), 103 (8); ^{1}H-NMR (500 MHz, $CDCl_3$): *δ* 3.85 (m, 1H, H-2), 2.72 (dd, *J* = 16.9, 5.5 Hz, 1H, H-3'), 2.57 (dd, *J* = 16.9, 7.8 Hz, 1H, H-3), 2.36 (q, *J* = 7.8, 7.2 Hz, 2H, H-5), 2.22 (s, 3H, COC$\underline{H}_3$), 1.25 (d, *J* = 7.0 Hz, 3H, H-1), 0.98 (t, *J* = 7.3 Hz, 3H, H-6); ^{13}C-NMR (126 MHz, $CDCl_3$): *δ* 207.58 (C-4), 194.49 (C-7), 47.34 (C-3), 35.19 (C-5), 33.69 (C-2), 29.60 (C-8), 19.64 (C-1), 6.59 (C-6).

2-Acetylthio-4-heptanone **7**: yield: 89.6%, purity: 95.5% (by GC); linear retention index (LRI): 1918 (DB-WAX), 1315 (DB-1); GC-MS (m/z, rel.%): 43 (100), 113 (72), 71 (66), 41 (18), 75 (15), 145 (10), 69 (10), 103 (7), 39 (7), 27 (7), 188 (M^+, 0.2); ^{1}H-NMR (500 MHz, $CDCl_3$): *δ* 3.85 (m, 1H, H-2), 2.71 (dd, *J* = 16.9, 5.5 Hz, 1H, H-3'), 2.55 (dd, *J* = 16.9, 7.8 Hz, 1H, H-3), 2.31 (m, 2H, H-5), 2.22 (s, 3H, COC$\underline{H}_3$), 1.53 (m, 2H, H-6), 1.25 (d, *J* = 7.0 Hz, 3H, H-1), 0.84 (t, *J* = 7.4 Hz, 3H, H-7); ^{13}C-NMR (126 MHz, CDCl3): *δ* 207.21 (C-4), 194.56 (C-8), 47.74 (C-3), 43.94 (C-5), 33.67 (C-2), 29.62 (C-9), 19.63 (C-1), 16.10 (C-6), 12.66 (C-7).

2-Acetylthio-4-octanone **8**: yield: 97.1%, purity: 96.0% (by GC); LRI: 1989 (RTX - WAX), 1411 (DB-1), GC-MS (*m/z*, rel.%): 43 (100), 99 (72), 57 (65), 29 (22), 75 (12), 69 (10), 41 (10), 103 (8), 131 (6), 174 (M^+, 0.2); ^{1}H-NMR (500 MHz, $CDCl_3$): *δ* 3.84 (m, 1H, H-2), 2.72 (dd, *J* = 16.9, 5.4 Hz, 1H, H-3'), 2.56 (dd, *J* = 16.9, 7.8 Hz, 1H, H-3), 2.33 (m, 2H, H-5), 2.22 (s, 3H, COC$\underline{H}_3$), 1.48 (m, 2H, H-6), 1.25 (d, *J* = 7.0 Hz, 3H, H-1), 1.24 (m, 2H, H-7), 0.83 (t, *J* = 7.3 Hz, 3H, H-8); ^{13}C-NMR (126 MHz, $CDCl_3$): *δ* 207.25 (C-4), 194.46 (C-9), 47.68 (C-3), 41.76 (C-5), 33.66 (C-2), 29.60 (C-10), 24.72 (C-6), 21.25 (C-7), 19.62 (C-1), 12.84 (C-8).

2-Acetylthio-4-nonanone **9**: yield: 115.1%, purity: 88.0% (by GC); LRI: 2093 (RTX - WAX), 1511 (DB-1); GC-MS (*m/z*, rel.%): 43 (100), 99 (85), 141 (77), 71 (43), 41 (18), 69 (20), 75 (15), 84 (14) 55 (10); ^{1}H-NMR (500 MHz, $CDCl_3$): *δ* 3.84 (m, 1H, H-2), 2.72 (dd, *J* = 16.9, 5.5 Hz, 1H, H-3'), 2.56 (dd, *J* = 16.9, 7.9 Hz, 1H, H-3), 2.32 (m, 2H, H-5), 2.21 (s, 3H, COC$\underline{H}_3$), 1.50 (m, 2H, H-6), 1.25 (d, *J* = 7.0 Hz, 3H, H-1), 1.28-1.15

(m, 4H, H-8, H-7), 0.81 (t, *J* = 7.2 Hz, 3H, H-9); ^{13}C-NMR (126 MHz, $CDCl_3$): *δ* 207.23 (C-4), 194.41 (C-10), 47.67 (C-3), 42.00 (C-5), 33.67 (C-2), 30.30 (C-7), 29.58 (C-11), 22.32 (C-6), 21.43 (C-8), 19.63 (C-1), 12.91 (C-9).

2-Acetylthio-4-decanone **10**: yield: 116.6%, purity: 89.1% (by GC); LRI: 2198 (RTX - WAX), 1613 (DB-1); GC-MS (*m/z*, rel.%): 43 (100), 155 (76), 113 (74), 85 (26), 84 (17), 69 (17), 41 (17), 57 (13), 75 (11), 55 (9); ^{1}H-NMR (500 MHz, $CDCl_3$): *δ* 3.85 (m, 1H, H-2), 2.71 (dd, *J* = 16.9, 5.4 Hz, 1H, H-3'), 2.55 (dd, *J* = 16.9, 7.8 Hz, 1H, H-3), 2.32 (m, 2H, H-5), 2.22 (s, 3H, $COCH_3$), 1.49 (m, 2H, H-6), 1.25 (d, *J* = 7.0 Hz, 3H, H-1), 1.26-1.15 (m, 6H, H-9, H-7, H-8), 0.80 (m, 3H, H-10); ^{13}C-NMR (126 MHz, $CDCl_3$): *δ* 207.35 (C-4), 194.56 (C-11), 47.70 (C-3), 42.08 (C-5), 33.68 (C-2), 30.55 (C-8), 29.61 (C-12), 27.80 (C-7), 22.60 (C-6), 21.46 (C-9), 19.62 (C-1), 13.02 (C-10).

4-Acetylthio-2-pentanone **13**: yield: 94.5%, purity: 91.0% (by GC).

4-Acetylthio-2-heptanone **14**: yield: 102.3%, purity: 94.5% (by GC).

3.2.4. Mercaptoalkanones

15 mL of methanol (MeOH) acidified with 2.5 mL of 2N sulfuric acid (H_2SO_4, pH 1-2) was added to the acetylthioalkanone, and the mixture was stirred for 24 h at 83 °C under reflux. After cooling to RT and addition of 70 mL of Et_2O, the organic phase was washed with water (3x20 mL), dried over Na_2SO_4, and the solvent was evaporated. The crude product was purified by column chromatography on silica gel by elution with a mixture of *n*-hexane/Et_2O (4:1, v/v) for **1**, (7:1, v/v) for **3**, and (8:1, v/v) for **4** and **5**; the obtained fractions were checked by TLC (ALUGRAM® SIL G/UV_{254}, Macherey-Nagel, Germany), visualization was achieved by spraying with 10% sulfuric acid and subsequent heating until dryness.

.

2-Mercapto-4-hexanone **1**: yield: 46.7%, purity: 92.1% (by GC); LRI: 1471 (RTX-WAX), 982 (DB-1); GC-MS (*m/z*, rel.%): 57 (100), 29 (60), 41 (45), 61 (41), 75 (40), 99 (35), 43 (22), 132 (19), 39 (17), 114 (16), 174 (M^+, 8); ^{1}H-NMR (500 MHz, $CDCl_3$): *δ* 3.36 (dp, *J* = 13.4, 6.8 Hz, 1H, H-2), 2.70-2.57 (m, 2H, H-3), 2.36 (q, *J* = 7.3 Hz, 2H, H-5),

1.75 (d, *J* = 6.4 Hz, 1H, SH), 1.27 (d, *J* = 6.8 Hz, 3H, H-1), 1.00 (t, *J* = 7.3 Hz, 3H, H-6); ^{13}C-NMR (126 MHz, $CDCl_3$): *δ* 208.24 (C-4), 52.09 (C-3), 35.62 (C-5), 29.08 (C-2), 23.80 (C-1), 6.56 (C-6).

2-Mercapto-4-heptanone **2**: yield: 79.3%, purity: 91.6% (by GC); LRI: 1568 (DB-WAX), 1076 (DB-1); GC-MS (*m/z*, rel.%): 71 (100), 43 (97), 75 (50), 41 (50), 61 (46), 113 (38), 128 (22), 39 (17), 27 (15), 146 (M+, 28); ^{1}H-NMR (500 MHz, $CDCl_3$): *δ* 3.44 (m, 1H, H-2), 2.71 (qd, *J* = 17.2, 6.8 Hz, 2H, H-3), 2.39 (t, *J* = 17.3, 2H, H-5), 1.85 (d, *J* = 6.4, 1H, SH), 1.62 (m, 2H, H-6), 1.34 (d, *J* = 6.8, 3H, H-1), 0.93 (t, *J* = 7.4, 3H, H-6); ^{13}C-NMR (126 MHz, $CDCl_3$): *δ* 207.82 (C-4), 52.47 (C-3), 44.34 (C-5), 29.00 (C-2), 23.79 (C-1), 16.05 (C-6), 12.69 (C-7).
Chromatographic, mass spectrometric and NMR data were in accordance with those previously reported (Naef *et al.*, 2008).

2-Mercapto-4-octanone **3**: yield: 54.2%, purity: 95.7% (by GC); LRI: 1649 (RTX-WAX), 1176 (DB-1); GC-MS (*m/z*, rel.%): 85 (100), 57 (99), 75 (67), 41 (58), 61 (53), 127 (37), 29 (36), 58 (23), 160 (M^+, 16); ^{1}H-NMR (500 MHz, $CDCl_3$): *δ* 3.35 (m, 1H, H-2), 2.66 (dd, *J* = 17.2, 7.7 Hz, 1H, H-3'), 2.59 (dd, *J* = 17.2, 5.9 Hz, 1H, H-3), 2.33 (m, 2H, H-5), 1.50 (m, 2H, H-6), 1.26 (d, *J* = 7.0 Hz, 3H, H-1), 1.29-1.21 (m, 4H, H-8, H-7), 0.84 (t, *J* = 7.4 Hz, 3H, H-8); ^{13}C-NMR (126 MHz, $CDCl_3$): *δ* 207.90 (C-4), 52.45 (C-3), 42.18 (C-5), 29.02 (C-2), 24.68 (C-6), 23.77 (C-1), 21.28 (C-7), 12.84 (C-8).

2-Mercapto-4-nonanone **4**: yield: 89.8%, purity: 73.0% (by GC); LRI: 1755 (RTX-WAX), 1279 (DB-1); GC-MS (*m/z*, rel.%): 43 (100), 99 (72), 141 (62), 71 (36), 69 (17), 41 (15), 75 (12), 84 (12), 29 (8), 103 (8) 174 (M^+, 4); ^{1}H-NMR (500 MHz, $CDCl_3$): *δ* 3.35 (m, 1H, H-2), 2.66 (dd, *J* = 17.2, 7.7 Hz, 1H, H-3'), 2.59 (dd, *J* = 17.2, 6.0 Hz, 1H, H-3), 2.32 (m, 2H, H-5), 1.51 (m, 2H, H-6), 1.26 (d, *J* = 6.9 Hz, 3H, H-1), 1.30-1.16 (m, 4H, H-8, H-7), 0.82 (t, *J* = 7.1 Hz, 3H, H-9); ^{13}C-NMR (126 MHz, $CDCl_3$): *δ* 207.91 (C-4), 52.46 (C-3), 42.43 (C-5), 30.32 (C-7), 29.02 (C-2), 23.77 (C-1), 22.28 (C-6), 21.43 (C-8), 12.91 (C-9).

2-Mercapto-4-decanone **5**: yield: 41.8%, purity: 93.1% (by (GC); LRI: 1861 (RTX-WAX), 1383 (DB-1); GC-MS (*m/z*, rel.%): 43 (100), 113 (58), 85 (51), 61 (50), 75 (50), 41 (42), 155 (40), 57 (25), 55 (24), 103 (21) 188 (M^+, 2); ^{1}H-NMR (500 MHz, $CDCl_3$): *δ* 3.35 (m, 1H, H-2), 2.66 (dd, *J* = 17.2, 7.7 Hz, 1H, H-3'), 2.59 (dd, *J* = 17.2, 5.9 Hz, 1H, H-3), 2.32 (m, 2H, H-5), 1.50 (m, 2H, H-6), 1.26 (d, *J* = 7.0 Hz, 3H, H-1), 1.28-1.17 (m,

6H, H-9, H-8, H-7), 0.80 (m, 3H, H-10); ^{13}C-NMR (126 MHz, $CDCl_3$): δ 207.94 (C-4), 52.46 (C-3), 42.48 (C-5), 30.56 (C-8), 29.02 (C-2), 27.83 (C-7), 23.77 (C-1), 22.56 (C-6), 21.46 (C-9), 13.02 (C-10).

4-Mercapto-2-pentanone **11**: yield: 54.0%, purity: 96.7% (by GC).

4-Mercapto-2-heptanone **12**: yield: 62.8%, purity: 97.0% (by GC).

3.2.5. (*R*)-2-Heptanethiol

The synthesis was performed according to Simian *et al.* (2004) starting from *p*-toluenesulfonyl chloride (1.1eq.) and (*S*)-2-heptanol (3 mmol). The resulting 2-(*p*-toluenesulfonyl)heptane (yield: 96.1%) was used for the synthesis of 2-(acetylthio)heptane without further purification. The reaction of 2-(*p*-toluenesulfonyl)heptane (5.3 mmol) and potassium thioacetate (13.3 mmol, 2.5eq.) yielded 2-(acetylthio)heptane (66.0%; purity: 58.5% (by GC)). The reduction of this intermediate (0.92 mmol) with lithium aluminum hydride (4.5eq.) in dry Et_2O resulted in (*R*)-2-heptanethiol: yield: 83.7%, purity: 80.9% (by GC); LRI: 1147 on DB WAX; GC-MS (m/z, rel.%): 57 (100), 56 (71), 41 (69), 61 (58), 43 (43), 70 (40), 69 (40), 98 (37), 55 (34), 132 (M^+, 45); ^{1}H-NMR (500 MHz, $CDCl_3$): δ 2.86 (dq, J = 7.6, 6.3 Hz, 1H, H-2), 1.54-1.42 (m, 2H, H-3), 1.41 (d, J = 6.0, 1H, SH), 1.40-1.27 (m, 2H, H-4), 1.26 (d, J = 6.7, 3H, H-1), 1.25-1.16 (m, 4H, H-6, H-5), 0.82 (t, J = 7.1, 3H, H-7); ^{13}C-NMR (126 MHz, $CDCl_3$): δ 39.87 (C-3), 34.61 (C-2), 30.50 (C-5), 26.11 (C-4), 24.60 (C-1), 21.56 (C-6), 13.03 (C-7).
Chromatographic, mass spectrometric and NMR data were in accordance with those previously reported (Sakoda and Hayashi, 2002).

3.3. Lipase-catalyzed kinetic resolutions

3.3.1. Parameters

3.3.1.1. Response factors (R_f)

In order to determine the response factors, the purities of the products (1 µL/mL Et_2O) as well as of the substrates (1 µL/mL Et_2O) were determined by triplicate GC/FID analysis (GC/FID I).

Subsequently, it was determined if the response factors were constant in the working range of the experiments. Therefore, stock solutions (1 mg/mL Et_2O) of the products (mercaptoalkanones) and of the substrates (acetylthioalkanones) were prepared and diluted to 25%, 50% und 75% solutions with Et_2O. Each concentration stage was analyzed in triplicate using GC system I, and the R_f-values were calculated using the obtained peak areas and the following equation 1:

$$R_f = \frac{n_p \cdot A_s}{n_s \cdot A_p} \qquad \text{(equation 1)}$$

n_p: amount of substance [µmol], taking into account the purity
n_s: amount of substance [µmol], taking into account the purity
A_p: mean peak area of the product
A_s: mean peak area of the substrate

3.3.1.2. Conversion Rates (c)

The conversion rates at time t were determined using two different methods.

The first calculation of the conversion rate was based on the ratios of the peak areas of product and substrate, taking into account the previously determined response factors and using GC/FID system I.

$$c\,[\%] = \frac{A_s \cdot R_f}{A_s + A_p \cdot R_f} \cdot 100 \qquad \text{(equation 2)}$$

A_P: peak area of product
A_S: peak area of substrate
R_f: response factor

The second calculation was based on the enantiomeric excesses of product and substrate (chapter 3.3.1.3) according to Chen *et al.* (1982).

$$c_{ee}\,[\%] = \frac{ee_s}{ee_s + ee_p} \cdot 100 \qquad \text{(equation 3)}$$

ee_p: enantiomeric excess of product
ee_s: enantiomeric excess of substrate

3.3.1.3. Enantiomeric Excess (ee)

The enantiomeric excess specifies the percentage of one enantiomer within a mixture. For ee = 100%, an enantiopure compound is present and for ee = 0%, both enantiomers are present in the same ratio (racemate) (Chen *et al.*, 1982; Ghanem and Aboul-Enein, 2005). The enantiomeric excess ee was calculated via the peak areas of the respective enantiomers, determined via GC/FID system II and III.

$$ee\,[\%] = \frac{A_1 - A_2}{A_1 + A_2} \cdot 100 \qquad \text{(equation 4)}$$

A_1 peak area of the enantiomer with higher concentration
A_2 peak area of the enantiomer with lower concentration

3.3.1.4. Enantioselectivity (E)

The enantioselectivity reflects the quality of an enzyme-catalyzed kinetic resolution and describes the degree of selectivity of an enzyme to distinguish between two enantiomers. That means, the higher the E-value the more selective is the enzyme for the respective reaction. A value of more than 20 means that there is a clear preference for one of the enantiomers and the employed conversion is useful (Bornscheuer and Kazlauskas, 2006). Enantioselectivity E is an intrinsic property of an enzyme and represents its enantioselective properties for the conversion of a substrate using the same conditions (Straathof and Jongejan, 1997). Chen *et al.* (1982) developed two methods for the calculation of the enantioselectivity E including the terms conversion rate and enantiomeric excesses. Requirements for the validity for both methods are (i)

the irreversibility of the reaction, i.e. one substrate is converted to exactly one product, and (ii) no product inhibition.

Method 1: Calculation of E via c and ee_S

$$E = \frac{\ln[(1-c)\cdot(1-ee_s)]}{\ln[(1-c)\cdot(1+ee_s)]} \qquad \text{(equation 5)}$$

This equation is particularly suitable when the remaining substrate is enantiopure (Chen *et al.*, 1982; Straathof and Jongejan, 1997).

Method 2: Calculation of E via c and ee_p

$$E = \frac{\ln[1-c\cdot(1+ee_p)]}{\ln[1-c\cdot(1-ee_p)]} \qquad \text{(equation 6)}$$

This method should be used when the product is the target compound (Straathof and Jongejan, 1997).

Method 3: Calculation of E via ee_s and ee_p

Rakels *et al.* (1993) developed an equation for determining the enantioselectivity in which only the enantiomeric excesses of product and substrate are considered:

$$E = \frac{\ln[(1-ee_s)/(1+\frac{ee_s}{ee_p})]}{\ln[(1+ee_s)/(1+\frac{ee_s}{ee_p})]} \qquad \text{(equation 7)}$$

3.3.2. Enzyme Screening via Enzyme-Catalyzed Hydrolysis of Acetylthioalkanones

In a vial with a Teflon stir bar, 85 µmol of the respective substrate (**14**: 16.8 mg, **6**: 17.7 mg, **7**: 16.5 mg, **8**: 17.2 mg, **9**: 23.5 mg, **10**: 23.5 mg) were mixed with 1 mL potassium phosphate buffer (KH_2PO_4/K_2HPO_4, 50 mM, pH 7.4). With addition of the respective lipase or esterase (each 20 mg CAL-B, PPL, ANL, WGL, CRL, PLE, and PLE (imm.) the enzyme-catalyzed thioester hydrolysis was started. The mixture was stirred continuously at RT.

At defined time points after the addition, 100 µL of the sample was withdrawn and extracted with 1 mL CH_2Cl_2 for 1 min with a vortexer. The organic phase was dried with anhydrous Na_2SO_4 and the vial was washed with 1 mL CH_2Cl_2.
An aliquot of the extract was subjected to GC analyses with DB-WAX as achiral stationary phase and with MEGA-DEX DET-Beta (2-mercapto- and 2-acetylthio-4-alkanones) and CycloSil B (4-mercapto- and 4-acetylthio-2-alkanones) for chiral analysis.

3.3.3. Preparation of Enantiomerically Enriched 4-Mercapto-2-pentanone, 4-Mercapto-2-heptanone, and 2-Mercapto-4-heptanone

The preparation of enantiomerically enriched **11** and **2** by enzyme-catalyzed hydrolysis of the respective acetylthioalkanones **13** and **7** was carried out as follows: The acetylthioalkanone (425 mg) was mixed with 25 mL of 50 mM potassium phosphate buffer (KH_2PO_4/K_2HPO_4, pH 7.4), CAL-B (500 mg) was added, and the mixture was stirred magnetically with a Teflon stir bar at RT. After defined reaction times, the mixture was filtered and extracted with Et_2O (3x15 mL). The combined organic layers were dried with anhydrous Na_2SO_4, filtered, and the solvent was removed under reduced pressure. The enantiomerically enriched mercaptoalkanone resulting from the hydrolysis of the acetylthioalkanone (enantiomer E1) was separated from the remaining substrate via column chromatography on silica gel by elution with a mixture of *n*-hexane/Et_2O (3:1, v/v) for **11** and (4:1, v/v) for **2**; the obtained fractions were checked by TLC (ALUGRAM® SIL G/UV_{254}, Macherey-Nagel, Germany), visualization was achieved by spraying with 10% sulfuric acid and subsequent heating until dryness. To obtain the opposite enantiomer of the mercaptoalkanone (enantiomer E2), the remaining acetylthioalkanone substrate was transesterified with 10 mL acidified methanol (pH 1-2) under reflux for 24 h. The reaction mixture was cooled to RT, diluted with 30 mL of Et_2O, and washed with water (3x10 mL). After drying with anhydrous Na_2SO_4, the solvent was removed under reduced pressure to yield the mercaptoalkanone enantiomer.

The preparation of enantiomerically enriched **12** by enzyme-catalyzed kinetic resolution was carried out as follows: 4-acetylthio-2-heptanone **14** (425 mg) was mixed with 25 mL of 50 mM potassium phosphate buffer (KH_2PO_4/K_2HPO_4, pH 7.4), either

PPL or ANL (500 mg) was added, and the mixture was stirred magnetically with a Teflon stir bar at RT. After defined reaction times, the mixture was filtered and extracted with Et_2O (3x15 mL). The reaction mixture with PPL was additionally centrifuged (20,000 rpm, 5 min) before filtration. The combined organic layers were dried with anhydrous Na_2SO_4, filtered, and the solvent was removed under reduced pressure. After column chromatography on silica gel by elution with a mixture of *n*-hexane/Et_2O (4:1, v/v), the enantiomers were obtained by transesterification of the remaining substrate with 10 mL acidified methanol (pH 1-2) under reflux for 24 h. The reaction mixture was cooled to RT, diluted with 30 mL of Et_2O and washed with water (3x10 mL). After drying with anhydrous Na_2SO_4, the solvent was removed under reduced pressure to yield both enantiomers (**12**-E2-PPL and **12**-E2-ANL).
In Table 3, the employed enzymes, reaction times, conversion rates, enantiomeric excesses, purities, and yields are presented.

3.3.4. Preparation of Enantiomerically Enriched 2-Mercapto-4-alkanones

The preparation of enantiomerically enriched mercaptoalkanones **1**, **3**-**5** by enzyme-catalyzed hydrolyses of the respective acetylthioalkanones **6**, **8**-**10** was carried out as follows: The acetylthioalkanones were mixed with 50 mM potassium phosphate buffer (pH 7.4), CAL-B was added, and the mixture was stirred magnetically with a Teflon stir bar at RT. After defined reaction times, the mixture was filtered and extracted with Et_2O (3x15 mL). The combined organic layers were dried with anhydrous Na_2SO_4, filtered, and the solvent was removed under reduced pressure. The (*R*)-mercaptoalkanones resulting from the hydrolysis of the acetylthioalkanones were separated from the remaining substrates via column chromatography on silica gel by elution with a mixture of *n*-hexane/Et_2O (4+1, v/v) for **1**, (7+1, v/v) for **3**, and (8+1, v/v) for **4** and **5**; the obtained fractions were checked by TLC. To obtain the (*S*)-enantiomer of the mercaptoalkanones, the remaining (*S*)-acetylthioalkanone substrates were transesterified with 10 mL acidified methanol (pH 1-2) under reflux for 24 h. The reaction mixture was cooled to RT, diluted with 30 mL of Et_2O, and washed with water (3x10 mL). After drying with anhydrous Na_2SO_4, the solvent was removed under reduced pressure to yield the mercaptoalkanone enantiomers.

In Table 4, the employed enzymes, reaction times, conversion rates, enantiomeric excesses, purities, and yields are presented.

Table 3. Preparation of mercaptoalkanone enantiomers via lipase-catalyzed hydrolysis of acetylthioalkanones.

starting compound[a]	obtained enantiomer[b]	configuration[c], optical rotation	lipase[d]	reaction time [h]	conversion[e] [%]	ee[f] [%]	purity[e] [%]	yield[g] [%]
13	**11**-E1	(*R*)-(-)	CAL-B	1	18	91.2	98.3	17.9
	11-E2	(*S*)-(+)	CAL-B	8	60	92.6	95.2	5.4
14	**12**-E2	(*R*)[h]	PPL	8	86	92.5	96.0	0.9
	12-E2	(*S*)-(+)	ANL	16	83	84.3	98.0	3.1
7	**2**-E1	(*R*)-(-)	CAL-B	0.5	44	94.0	93.0	9.5
	2-E2	(*S*)-(+)	CAL-B	4	61	88.3	96.8	4.8

[a] 425 mg
[b] Numbering refers to the enantiomers obtained either as direct hydrolysis product (E1) or via the remaining substrate (E2)
[c] configurations determined via VCD (Kiske *et al*., 2016), and ^{1}H NMR analysis of HTA and MPA thioesters; for optical rotations see Materials and Methods
[d] 500 mg
[e] determined via GC (DBWAX)
[f] enantiomeric excess, determined via GC (chiral stationary phases)
[g] molar yields
[h] optical rotation not determined due to low yield

Table 4. Preparation of 2-mercapto-4-alkanone enantiomers via lipase-catalyzed hydrolysis of the respective 2-acetylthio-4-alkanones.

starting compound	obtained enantiomer[a]	configuration[b], optical rotation	amount[c] [g]	lipase CAL-B [g]	volume of buffer [mL]	reaction time [h]	conversion rate[d] [%]	ee[e] [%]	purity[d] [%]	yield[f] [%]
6	**1**-E1	(*R*)-(-)	0.866	1.00	50	0.5	33	92.9	96.8	11.0
	1-E2	(*S*)-(+)	0.689	0.8	40	2	50	84.4	98.3	12.6
8	**3**-E1	(*R*)-(-)	1.947	2.21	110	0.5	33	92.9	98	11.9
	3-E2	(*S*)-(+)	1.36	1.61	95	2	46	88.6	97.3	5.3
9	**4**-E1	(*R*)-(-)	1.029	1.21	60	1	62	91.7	95.6	23.3
	4-E2	(*S*)-(+)	2.130	2.51	150	4	46	94.2	97.8	12.4
10	**5**-E1	(*R*)-(-)	2.132	2.52	150	1	42	94.6	97.1	22.4
	5-E2	(*S*)-(+)	1.068	1.31	70	6	48	93.1	96.7	6.4

[a] Configurations determined via VCD (Kiske *et al*., 2019) and ^{1}H-NMR analysis of HTA and MPA thioesters; for optical rotations see Materials and Methods
[b] Determined via GC (DBWAX)
[c] Enantiomeric excess, determined via GC (MEGA-DEX DET-Beta)
[d] Molar yields

3.4. Formation of Diastereoisomers with Chiral Auxiliaries

3.4.1. (*S*)- and (*R*)-M*α*NP-Thioesters and Esters (15-26)

A solution of DCC (2.0eq.) and DMAP (1.0eq.) in dry CH_2Cl_2 was added to a solution of (*S*)- or (*R*)-M*α*NP (1.0eq.) and the respective mercaptoalkanone, 2-heptanethiol or 2-heptanol (0.0868 mmol) in dry CH_2Cl_2. The mixture was stirred at RT for 20 h. The reaction was quenched with 0.2 mL of H_2O. After stirring for another hour, 1 mL of dry CH_2Cl_2 and anhydrous Na_2SO_4 were added; the solution was filtered and dried under a N_2-stream. The residue was dissolved in 5 mL EtOAc, dried with anhydrous Na_2SO_4 and evaporated at a max. temperature of 28 °C. The residue was separated by semi-preparative HPLC.

(*S*)-M*α*NP thioesters of:

4-mercapto-2-pentanone **11**: Peak I, **15**: 8.5 mg, yield: 29.6%; Peak II, **16**: 7.1 mg, yield: 24.7%, ^{13}C-NMR (126 MHz, $CDCl_3$): 19.47 (C-5), 21.41 (C-8), 29.06 (C-1), 32.95 (C-4), 48.83 (C-3), 49.62 (C-9), 86.38 (C-7), 123.58, 124.70, 124.76, 125.33, 126.12, 127.77, 129.03, 130.32, 133.16, 133.58 (Naphthyl) 202.79 (S-CO-C, C-6), 204.96 (C-2).

4-mercapto-2-heptanone **12**: Peak I, **17**: 5.0 mg, yield: 16.0%; Peak II, **18**: 11.7 mg, yield: 37.7%, ^{13}C-NMR (126 MHz, $CDCl_3$): 12.66 (C-7), 19.13 (C-6), 21.40 (C-10), 29.02 (C-1), 35.28 (C-5), 37.68 (C-4), 47.91 (C-3), 49.61 (C-11), 86.45 (C-9), 123.57, 124.70, 124.85, 125.23, 126.09, 127.75, 129.00, 130.31, 133.16, 133.64 (Naphthyl), 202.96 (S-CO-C, C-8), 205.15 (C-2).

2-mercapto-4-heptanone **2**: Peak I, **19**: 7.0 mg, yield: 22.5%; Peak II, **20**: 9.8 mg, yield: 30.3%.

^{1}H-NMR data are presented in Table 8 (cf. 4.2.2.1.).

2-heptanol: Peak I, **23**: 9.6 mg, yield: 35.1%; Peak II, **24**: 11.8 mg, yield: 43.2%.

(*R*)-2-heptanethiol **25**: 3.4 mg, yield: 11.9%; ^{13}C-NMR (126 MHz, $CDCl_3$): 13.12 (C-7), 20.11 (C-6), 21.53 (C-10), 25.61 (C-1), 28.68 (C-4), 30.51 (C-5), 37.68 (C-3), 59.61 (C-11), 86.46 (C-9), 123.55, 124.65, 124.96, 125.21, 126.03, 127.68, 128.89, 130.36, 133.15, 133.92 (Naphthyl), 203.11 (S-CO-C, C-8).

(*R*)-M*α*NP thioesters of:

(*R*)-2-mercapto-4-heptanone **21**: 11 mg, yield: 36.8%, ^{13}C-NMR (126 MHz, $CDCl_3$): 12.65 (C-7), 16.06 (C-6), 19.54 (C-1), 21.42 (C-10), 33.06 (C-2), 43.84 (C-5), 47.84 (C-3), 49.62 (C-11), 86.38 (C-9), 123.58, 124.69, 124.79, 125.31, 126.11, 127.77, 129.01, 130.33, 133.16, 133.62 (Naphthyl), 202.76 (S-CO-C, C8), 207.22 (C-4).

(*R*)-2-heptanol **22**: 17.5 mg, yield: 64.2%, ^{13}C-NMR (126 MHz, $CDCl_3$): 12.85 (C-7), 18.69 (C-1), 20.53 (C-10), 21.20 (C-5), 23.04 (C-4), 30.13 (C-6), 34.31 (C-3), 49.80 (C-11), 70.93 (C-2), 80.34 (C-9), 123.53, 124.32, 124.63, 124.69, 125.34, 127.54, 128.31, 130.47, 132.98, 134.08 (Naphthyl), 172.79 (O-CO-C, C-8).

(*R*)-2-heptanethiol **26**: 13.4 mg, yield: 46.8%.

^{1}H-NMR data are presented in the Appendix (cf. 8., Tables 24-26).

3.4.2. (*S*)-M*α*NP-Thioesters (53-60)

A solution of DCC (2.0eq.) and DMAP (1.0eq.) in dry CH_2Cl_2 was added to a solution of (*S*)-M*α*NP (1.0eq.) and the respective enantiomerically enriched mercaptoalkanone (0.0868 mmol) in dry CH_2Cl_2. The mixture was stirred at RT for 20 h. The reaction mixture was filtered through a syringe filter (0.45 µm) and dried under a N_2-stream. The residue was separated by semi-preparative HPLC.

(*S*)-M*α*NP thioesters:
53 of (*R*)-**1**: 3.6 mg, yield: 23.1%, ^{13}C-NMR (126 MHz, $CDCl_3$): 6.54 (C-6), 19.15 (C-1), 21.45 (C-CH_3, C-9), 33.17 (C-2), 34.97 (C-5), 47.74 (C-3), 49.61 (-O-CH_3, C-10), 86.39 (C_q, C-8), 123.61, 124.71, 124.81, 125.29, 126.13, 127.80, 129.02, 130.34, 133.19, 133.67 (Naphthyl) 202.94 (S-CO-C, C-7), 207.72 (C-4); **54** of (*S*)-**1**: 4.6 mg, yield: 23.3%.
55 of (*R*)-**3**: 4.8 mg, yield: 29.5%, ^{13}C-NMR (126 MHz, $CDCl_3$): 12.81 (C-8), 19.10 (C-1), 21.21 (C-7), 21.45 (C-CH_3, C-11), 24.65 (C-6), 33.12 (C-2), 41.57 (C-5), 48.06 (C-3), 49.61 (-O-CH_3, C-12), 86.39 (C_q, C-10), 123.61, 124.70, 124.81, 125.29, 126.12, 127.80, 129.01, 130.35, 133.19, 133.68 (Naphthyl), 202.92 (S-CO-C, C-8), 207.41 (C-4); **56** of (*S*)-**3**: 5.5 mg, yield: 27.9%.

57 of (*R*)-**4**: 7.7 mg, yield: 40.4%, ^{13}C-NMR (126 MHz, $CDCl_3$): 12.87 (C-9), 19.11 (C-1), 21.39 (C-6), 21.45 (C-$\underline{C}H_3$, C-12), 22.25 (C-8), 30.24 (C-7), 33.12 (C-2), 41.82 (C-5), 48.06 (C-3), 49.61 (-O-$\underline{C}H_3$, C-13), 86.38 (C_q, C-11), 123.61, 124.70, 124.81, 125.29, 126.13, 127.80, 129.01, 130.35, 133.19, 133.68 (Naphthyl), 202.91 (S-$\underline{C}$O-C, C-8), 207.44 (C-4); **58** of (*S*)-**4**: 8.0 mg, yield: 43.4%.

59 of (*R*)-**5**: 8.4 mg, yield: 31.4%, ^{13}C-NMR (126 MHz, $CDCl_3$): 13.00 (C-10), 19.10 (C-1), 21.43 (C-9), 21.45 (C-$\underline{C}H_3$, C-13), 22.53 (C-6), 27.76 (C-7), 30.53 (C-8), 33.12 (C-2), 41.87 (C-5), 48.06 (C-3), 49.61 (-O-$\underline{C}H_3$, C-14), 86.38 (C_q, C-12), 123.61, 124.70, 124.82, 125.29, 126.13, 127.80, 129.01, 130.35, 133.19, 133.68 (Naphthyl), 202.91 (S-$\underline{C}$O-C, C-11), 207.44 (C-4); **60** of (*S*)-**5**: 7.8 mg, yield: 29.6%.

^{1}H-NMR data are presented in Table 14 (cf. 4.4.3.).

3.4.3. (*R*)-HTA-Thioesters (27-32)

In a 50 mL round bottom flask equipped with a drying tube filled with calcium chloride, (*R*)-HTA (1.67 mmol) and 1.1 mL oxalyl chloride were stirred at RT. After 10 min, the excess oxalyl chloride was removed by rotary evaporation, the residue was mixed with toluene (3x3 mL), and the solvent was evaporated. The mixture was suspended in 2 mL dry $CHCl_3$ and 0.6 mmol of the respective mercaptoalkanone enantiomer dissolved in 3 mL of dry $CHCl_3$ was added dropwise. The glassware was rinsed with 3 mL of dry $CHCl_3$. The reaction mixture was heated at 55 °C under reflux and the conversion was checked by GC. After 48-72 h, the sample was cooled down and diluted with 20 mL of water. The mixture was extracted with Et_2O (3x15 mL), the organic phase was washed with water (2x10 mL), dried with anhydrous Na_2SO_4 and evaporated. The product was purified by semi-preparative HPLC:

(*R*)-HTA thioester:

27 of **11**-E1: 84.2 mg, yield: 65.5%, ^{13}C-NMR (126 MHz, $CDCl_3$): 19.34 (C-5), 29.11 (C-1), 33.62 (C-4), 48.89 (C-3), 54.22 (C-7), 126.42, 126.86, 127.65, 138.68 (Phenyl), 199.78 (S-$\underline{C}$O-C, C-6), 204.87 (C-2); **28** of **11**-E2: 98.2 mg, yield: 70.9%.

29 of **12**-E2-PPL: 74.6 mg, yield: 75.0%, ^{13}C-NMR (126 MHz, $CDCl_3$): 12.70 (C-7), 17.43 (C-10), 19.25 (C-6), 29.05 (C-1), 35.13 (C-5), 38.44 (C-4), 47.69 (C-3), 53.25 (C-9), 126.37, 126.84, 127.62, 138.75 (Phenyl), 199.96 (S-CO-C, C-8), 205.13 (C-2); **30** of **12**-E2-ANL: 50.3 mg, yield: 50.0%.

31 of **2**-E1: 40.2 mg, yield: 32.6%, ^{13}C-NMR (126 MHz, $CDCl_3$): 12.66 (C-7), 16.07 (C-6), 17.34 (C-10), 19.42 (C-1), 33.74 (C-2), 43.91 (C-5), 47.85 (C-3), 53.17 (C-9), 126.39, 126.85, 127.63, 138.71 (Phenyl), 199.78 (S-CO-C, C-8), 207.17 (C-4); **32** of **2**-E2: 30.5 mg, yield: 28.9%.

^{1}H-NMR data are presented in Table 9 (cf. 4.2.2.3.).

3.4.4. (*R*)-HTA-Thioesters (37-44)

The thioesters were synthesized as described in the previous chapter (3.4.3), using (*R*)-HTA (1.09 mmol), 0.72 mL oxalyl chloride, and 0.36 mmol of the respective mercaptoalkanone enantiomer. After 72 h, the sample was worked up and the product was purified by semi-preparative HPLC:

(*R*)-HTA thioester:

37 of (*R*)-**1**: 84.3 mg, yield: 88.9%, ^{13}C-NMR (126 MHz, $CDCl_3$): 6.54 (C-6), 17.33 (C-9), 19.42 (C-1), 33.72 (C-2), 35.14 (C-5), 47.50 (C-3), 53.15 (C-8), 126.39, 126.85, 127.62, 139.69 (Phenyl), 199.77 (S-CO-C, C-7), 207.65 (C4); **38** of (*S*)-**1**: 64.2 mg, yield: 66.7%.

39 of (*R*)-**3**: 89.1 mg, yield: 86.1%; ^{13}C-NMR (126 MHz, $CDCl_3$): 12.82 (C-8), 17.34 (C-11), 19.42 (C-1), 21.21 (C-7), 24.65 (C-6), 33.69 (C-2), 41.71 (C-5), 47.81 (C-3), 53.15 (C-10), 126.39, 126.86, 127.63, 138.72 (Phenyl), 199.96 (S-CO-C, C-9), 207.34 (C-4); **40** of (*S*)-**3**: 55.5 mg, yield: 52.8%.

41 of (*R*)-**4**: 101.8 mg, yield: 91.7%, ^{13}C-NMR (126 MHz, $CDCl_3$): 12.89 (C-9), 17.35 (C-12), 19.41 (C-1), 21.39 (C-8), 22.25 (C-6), 30.25 (C-7), 33.69 (C-2), 41.96 (C-5), 47.81 (C-3), 53.15 (C-11), 126.38, 126.85, 127.62, 138.71 (Phenyl), 199.75 (S-CO-C, C-10), 207.34 (C-4); **42** of (*S*)-**4**: 74.5 mg, yield: 66.7%.

43 of (*R*)-**5**: 92.1 mg, yield: 80.6%, ^{13}C-NMR (126 MHz, $CDCl_3$): 13.02 (C-10), 17.35 (C-13), 19.41 (C-1), 21.44 (C-9), 22.53 (C-6), 27.76 (C-7), 30.53 (C-8), 33.69 (C-2), 42.01 (C-5), 47.81 (C-3), 53.15 (C-12), 126.38, 126.85, 128623, 138.71 (Phenyl), 199.71 (S-CO-C, C-11), 207.36 (C-4); **44** of (*S*)-**5**: 56.8 mg, yield: 50.0%.

^{1}H-NMR data are presented in Table 13 (cf. 4.4.3.).

3.4.5. (*S*)- and (*R*)-MPA-Thioesters (34-36)

The derivatization was performed according to Porto *et al*. (2014) using 0.0868 mmol (1.0eq.) of the thiol or mercaptoalkanone, 0.1042 mmol (1.2eq.) of the respective (*R*)- and (*S*)-MPA, 0.1736 mmol (2.0eq.) of DCC and DMAP (5 mg) in 1 mL of dry CH_2Cl_2. The reaction mixtures were stirred for 2 h under RT. After work up, purification was achieved by semi-preparative HPLC.

(*R*)-MPA thioester **34** of (*R*)-2-heptanethiol: 26.7 mg, yield: 109.6%, ^{13}C-NMR (126 MHz, $CDCl_3$): 12.95 (C-7), 20.23 (C-1), 21.45 (C-4), 25.52 (C-6), 30.45 (C-5), 35.49 (C-3), 37.53 (C-2), 56.96 (C-10), 87.97 (C-9), 125.95, 127.55, 127.59, 135.39 (Naphthyl), 199.45 (S-CO-C, C-8); (*S*)-MPA thioester **33** of (*R*)-2-heptanethiol: 17.0 mg, yield: 69.8%.

(*R*)-MPA thioester **36** of (*R*)-**2**: 14.3 mg, yield: 56.0%, ^{13}C-NMR (126 MHz, $CDCl_3$): 12.65 (C-7), 16.09 (C-6), 19.39 (C-1), 32.76 (C-2), 43.91 (C-5), 47.90 (C-3), 56.99 (C-10), 87.77 (C-9), 125.92, 127.60, 127.69, 135.10 (Phenyl), 199.15 (S-CO-C, C-8), 207.13 (C-4); (*S*)-MPA thioester **35** of (*R*)-**2**: 7.7 mg, yield: 30.1%.

^{1}H-NMR data are provided in the Appendix (cf. 8., Tables 22 and 23).

3.4.6. (*S*)- and (*R*)-MPA-Thioesters (45-52)

The thioesters were synthesized as described in the previous chapter (cf. 3.4.5), using 0.1736 mmol (1.0eq.) of the (*R*)-mercaptoalkanone, 0.2083 mmol (1.2eq.) of the respective (*R*)- and (*S*)-MPA, 0.2083 mmol (1.2eq.) of DCC, and DMAP (5 mg) in 1 mL

of dry CH_2Cl_2. The reaction mixtures were stirred for 2 h under RT. After work up, purification was achieved by semi-preparative HPLC.

(*R*)-MPA thioester **45** of (*R*)-**1**: 7.0 mg, yield: 14.4%, ^{13}C-NMR (126 MHz, $CDCl_3$): 6.61 (C-6), 19.43 (C-1), 32.82 (C-2), 35.20 (C-5), 47.55 (C-3), 56.99 (C-9), 87.77 (C-8), 125.93, 127.62, 127.70, 135.11 (Phenyl), 199.17 (S-CO-C, C-7), 207.55 (C-4); (*S*)-MPA thioester **46** of (*R*)-**1**: 14.5 mg, yield: 29.8%.

(*R*)-MPA thioester **47** of (*R*)-**3**: 7.0 mg, yield: 13.2%, ^{13}C-NMR (126 MHz, $CDCl_3$): 12.83 (C-8), 19.40 (C-1), 21.24 (C-7), 24.70 (C-6), 32.77 (C-2), 41.75 (C-5), 47.86 (C-3), 56.98 (C-11), 87.76 (C-10), 125.92, 127.60, 127.68, 135.10 (Phenyl), 199.14 (S-CO-C, C-9), 207.23 (C-4); (*S*)-MPA thioester **48** of (*R*)-**3**: 14.5 mg, yield: 27.1%.

(*R*)-MPA thioester **49** of (*R*)-**4**: 7.7 mg, yield: 13.8%, ^{13}C-NMR (126 MHz, $CDCl_3$): 12.90 (C-9), 19.40 (C-1), 21.41 (C-8), 22.30 (C-6), 30.29 (C-7), 32.77 (C-2), 42.01 (C-5), 47.87 (C-3), 56.99 (C-12), 87.77 (C-11), 125.92, 127.60, 127.69, 135.10 (Phenyl), 199.14 (S-CO-C, C-10), 207.25 (C-4); (*S*)-MPA thioester **50** of (*R*)-**4**: 13.9 mg, yield: 24.8%.

(*R*)-MPA thioester **51** of (*R*)-**5** 20.8 mg, yield: 35.6%, ^{13}C-NMR (126 MHz, $CDCl_3$): 13.02 (C-10), 19.40 (C-1), 21.45 (C-9), 22.58 (C-6), 27.79 (C-7), 30.54 (C-8), 32.77 (C-2), 42.05 (C-5), 47.87 (C-3), 56.99 (C-13), 87.77 (C-12), 125.93, 127.61, 127.69, 135.12 (Phenyl), 199.15 (S-CO-C, C-11), 207.26 (C-4); (*S*)-MPA thioester **52** of (*R*)-**5**: 14.3 mg, yield: 24.5%.

^{1}H-NMR data are provided in the Appendix (cf. 8., Tables 27-30).

3.5. Analyses

3.5.1. Capillary Gas Chromatography (GC)

3.5.1.1. Gas Chromatography/Flame Ionization Detector (GC/FID)

Achiral analyses were performed on the following GC systems:

GC/FID I:

Instrument:	HP5890 A (Hewlett Packard INC, Waldbronn, Germany)
Column:	DB-Wax (J&W Scientific, Waldbronn, Germany); 30 m x 0.25 mm i.d.; 0.5 µm film thickness
Temperature program:	40 °C/5 min//4 °C/min//240 °C/30 min
Injector:	Split/splitless (split ratio of 1:10), 230 °C
Detector:	300 °C
Carrier gas:	H_2 (150 kPa)

GC/FID II:

Instrument:	HP5890 A (Hewlett Packard INC)
Column:	Rtx®-Wax (Restek, Bad Homburg, Germany); 30 m x 0.25 mm i.d.; 0.5 µm film thickness
Temperature program:	40 °C/5 min//4 °C/min//240 °C/30 min
Injector:	Split/splitless (split ratio of 1:10), 215 °C
Detector:	300 °C
Carrier gas:	H_2 (150 kPa)

GC/FID III:

Instrument:	Agilent 6890 N (Agilent Technologies, Waldbronn, Germany)
Column:	DB-1 (J&W Scientific); 30 m x 0.25 mm i.d.; 1.0 µm film thickness
Temperature program:	60 °C/5 min//5 °C/min//250 °C/5 min
Injector:	Split/splitless (split ratio of 1:22), 230 °C

Detector:	300 °C
Carrier gas:	H_2 (72 kPa)
Makeup gas:	N_2 (25 mL/min)

Linear retention indices (LRI) were calculated using the following equation. *n*-Alkane standard solutions (C8-C20 and C21-C40) were used as references (van den Dool and Kratz, 1963).

$$LRI = \left[C + \frac{Rt - Rt_n}{Rt_{n+1} - Rt_n}\right] \cdot 100 \qquad \text{(equation 8)}$$

Rt: retention time of the unknown compound
Rt_n: retention time of the n-alkane eluting before the unknown compound
Rt_{n+1}: retention time of the n-alkane eluting after the unknown compound
C: number of carbon atoms of the n-alkane eluting before the unknown compound

Enantioselective analyses of 2-acetylthio-4-alkanones, 2-mercapto-4-alkanones, 4-acetylthio-2-alkanones, and 4-mercapto-2-alkanones were performed on the following GC-systems:

<u>GC/FID IV:</u>

Instrument:	HRGC 5160 Mega Series (Carlo Erba Instruments, Milano, Italy)
Column:	CycloSil-B: 30% heptakis(2,3-di-*O*-methyl-6-*O*-*tert*-butyl dimethylsilyl)-*β*-cyclodextrin in DB-1701, (J&W Scientific); 30 m x 0.25 mm i.d.; 0.25 µm film thickness
Temperature program:	75 °C/0 min//2 °C/min//180 °C/10 min
Injector:	Split/splitless (split ratio of 1:10), 215 °C
Detector:	350 °C
Carrier gas:	H_2 (75 kPa)

GC/FID V:

Instrument:	HRGC 5160 Mega Series (Carlo Erba Strumentazione, Milano, Italy)
Column:	MEGA-DEX DET Beta: 2,3-diethyl *tert*-butylsilyl-*β*-cyclodextrin (Mega s.n.c., Legnano, Italy); 25 m x 0.25 mm i.d.; 0.25 µm film thicknessµm film thickness
Temperature program:	80 °C/0 min//1.5 °C/min//115 °C/0 min//2 °C/min// 180 °C/10 min
Injector:	Split/splitless (split ratio of 1:10), 215 °C
Detector:	350 °C
Carrier gas:	H_2 (75 kPa)

GC/FID VI:

Instrument:	Agilent 6890 N (Agilent Technologies)
Column:	MEGA-DEX DET Beta: 2,3-diethyl *tert*-butylsilyl-*β*-cyclodextrin (Mega s.n.c., Legnano, Italy); 25 m x 0.25 mm i.d.; 0.25 µm film thickness
Temperature programs:	
for C6-C8	80 °C/0 min//1 °C/min//120 °C/0 min//4 °C/min// 180 °C/5 min
for C9-C10	95 °C/0 min//0.5 °C/min//125 °C/0 min//4 °Cmin// 180 °C/5 min
Injector:	Split/splitless (split ratio of 1:10), 230 °C
Detector:	300 °C
Carrier gas:	H_2 (75 kPa)
Makeup gas:	N_2 (25 mL/min)

GC/FID VII:

Instrument:	Agilent 6890 N (Agilent Technologies)
Column:	CycloSil-B: 30% heptakis(2,3-di-*O*-methyl-6-*O*-*tert*-butyl dimethylsilyl)-*β*-cyclodextrin in DB-1701, (J&W Scientific); 30 m x 0.25 mm i.d.; 0.25 µm film thickness
Temperature program:	75 °C/0 min//0,5 °C/min//120 °C/0 min//2 °C/min// 180 °C/5 min
Injector:	Split/splitless (split ratio of 1:10), 230 °C
Detector:	300 °C
Carrier gas:	H_2 (75 kPa)
Makeup gas:	N_2 (25 mL/min)

3.5.1.2. Gas Chromatography-Mass Spectrometry (GC-MS)

The following GC-MS conditions were used:

Instrument:	GC 8000^{TOP} gas chromatograph (CE Instruments, Hindley Green, United Kingdom)
Detector:	Fisons MD8000^{TOP} mass spectrometer (Fisons Instruments, Manchester, United Kingdom)
Column:	DB-Waxetr (J&W Scientific); 30 m x 0.25 mm i.d.; 0.5 µm film thickness
Temperature program:	40 °C/5 min//4 °C/min//240 °C/25 min
Injector:	Split/splitless (split ratio of 1:50), 220 °C
Carrier gas:	He (75 kPa)
Ionization mode:	Electron impact (EI), ionization energy: 70 eV
MS temperature:	240 °C (interface); 200 °C (ion source)
Scan mode:	*m/z* 30-250

Data acquisition was done via Xcalibur software, version 1.4 (Thermo Fisher Scientific, Dreieich, Germany).

3.5.1.3. Gas Chromatography/Olfactometry (GC/O)

Sensory evaluations were performed by four panelists (females 21-36 years old). Panelists 1 and 4 had no prior experience with GC/O assessments whereas panelists 2 and 3 were experienced.

Odor thresholds in air were determined according to the procedure described by UIlrich and Grosch (1987) using (*E*)-2-decenal with the reported odor threshold of 2.7 ng/L in air as internal standard. Known amounts of the internal standard, of the 2-mercapto- and 2-acetylthio-4-alkanones (**1**-**10**), as well as 4-mercapto- and 4-acetylthio-2-pentanone (**11** and **13**) were dissolved in Et_2O and diluted stepwise (1+1, (v/v)). Stock solutions were freshly prepared for each panelist. The aliquots were analyzed by GC/O until no odor was perceivable. The panelists considered a concentration level only as odor threshold if it was the lowest dilution step at which the odor was consistently perceived in three consecutive GC/O-runs. Flavor dilution (FD) factors of the internal standard and of the target compounds were obtained by aroma extract dilution analysis (AEDA). FD factors were determined according to equation 9 with n as the number of 1+1 dilutions (Grosch, 1993).

$$FD = 2^n \qquad \text{(equation 9)}$$

Using the FD factors, the odor thresholds Ox (ng/L in air) of the respective substances were calculated as follows:

$$O_x = \frac{O_s \cdot C_x \cdot FD_s}{C_s \cdot FD_x} \qquad \text{(equation 10)}$$

Os: odor threshold of the internal standard (*E*)-2-decenal, 2.7 ng/L in air
Cx: concentration of the respective substance
Cs: concentration of the internal standard
FDx: flavor dilution factor of the respective substance
FDs: flavor dilution factor of the internal standard

The odor qualities were determined at one dilution step above the odor threshold. Sensory evaluations were performed on the following GC system:

GC/O:

Instrument:	Trace GC Ultra (Thermo Fisher)
Injector:	Cold on-column (35 °C), samples were applied onto a deactivated pre-column (30 cm x 0.5 mm i.d, BGB Analytik AG, Rheinfelden, Germany)
Detector:	250 °C, FID
Sniffing Port:	200 °C
Carrier gas:	H_2 (75 kPa)
Makeup gas:	N_2 (25 mL/min)

The effluent was split 1:1 via a press-fit Y-splitter and 30 cm x 0.25 mm i.d. deactivated fused silica capillaries (BGB Analytik AG, Rheinfelden, Germany) among sniffing port and FID.

For achiral sensory analyses the conditions were as follows:

GC/O I:

Column:	DB-Wax (J&W Scientific); 60 m x 0.25 mm i.d.; 0.5 µm film thickness
Temperature programs:	
SH-alkanones:	35 °C/0min//30 °C/min//80 °C/10 min//2 °C/min// 240 °C/5 min
AcS-alkanones:	35 °C/0min//30 °C/min//100 °C/5 min//4 °C/min// 240 °C/5 min

For chiral sensory analyses the conditions were as follows:

GC/O II:

Column:	MEGA-DEX DET Beta: 2,3-diethyl *tert*-butylsilyl-*β*-cyclodextrin (Mega s.n.c., Legnano, Italy); 25 m x 0.25 mm i.d.; 0.25 µm film thickness
Temperature program:	
C6-C8:	35 °C/0min//30 °C/min//85 °C/0 min//1 °C/min// 120 °C/0 min//5 °C/min//180 °C/4 min
C9-C10:	35 °C/0min//30 °C/min//95 °C/0 min//0.5 °C/min// 125 °C/0 min//5 °C/min//180 °C/4 min

For chiral sensory analyses of **11** and **13**, the conditions were as follows:

GC/O III:

Column:	CycloSil-B: 30% heptakis(2,3-di-*O*-methyl-6-*O*-*tert*-butyl dimethylsilyl)-*β*-cyclodextrin in DB-1701, (J&W Scientific); 30 m x 0.25 mm i.d.; 0.25 µm film thickness
Temperature program:	35 °C/0min//30 °C/min//80 °C/10 min//2 °C/min// 240 °C/5 min

3.5.2. High Performance Liquid Chromatography (HPLC)

Semi-preparative separations of the diastereoisomers of (*R*)-HTA, (*S*)- and (*R*)-MPA, and (*S*)- and (*R*)-M*α*NP thioesters and esters were carried out under the following conditions:

Instrument:	UltiMate 3000 series (Dionex, Germering, Germany)
Column:	Nucleosil 50-5 column (CS Chromatography, Langerwehe, Germany); 250 x 8 mm ID
Temperature:	30 °C
Mode:	isocratic elution
Detector:	3100 wavelength detector set at 254 nm

The following conditions were used for the diastereoisomers **15**-**36** (cf. 4.2.):

(*S*)-M*α*NP thioesters **15** and **16** (R_S: 1.66, *α*: 1.15) and **17** and **18** (R_S: 1.41, *α*: 1.18): hexane/isopropanol (96/4, v/v) with 2 mL/min; (*S*)-M*α*NP thioesters **19** and **20** (R_S: 2.94, *α*: 1.19), and (*R*)-/(*S*)-M*α*NP esters **22** and **23**: hexane/ethylacetate (20/1, v/v) with 3.5 mL/min; (*R*)-HTA thioesters **27**-**32**, (*R*)-/(*S*)-MPA thioesters **25**, **26**, **33**, and **34**, and (*R*)-/(*S*)-M*α*NP thioesters **19**, **21**, **35**, and **36**: hexane/ethylacetate (90/10, v/v) with 2.5 mL/min.

The following conditions were used for the diastereoisomers **37**-**60** (cf. 4.4.):

HTA-thioesters **37**-**42** and MPA-thioesters **45** and **46**: Hex/EtOAc (90/10, v/v) with 3 mL/min; HTA-thioesters **43** and **44**: Hex/EtOAc (85/15, v/v) with 3 mL/min; MPA-thioesters **47** and **48** Hex/EtOAc 92/8 with 3.5 mL/min; MPA-thioesters **49** and **50** Hex/EtOAc 95/5 with 3.5 mL/min; MPA-thioesters **51** and **52**: Hex/EtOAc 96/4 with 4.0 mL/min, M*α*NP-thioesters **53** and **54**: Hex/EtOAc 10/1 with 4.0 mL/min; M*α*NP-thioesters **55** and **56**: Hex/EtOAc 20/1 with 4.0 mL/min; M*α*NP-thioesters **57**-**60**: Hex/EtOAc 25/1 with 4.0 mL/min.

3.5.3. Nuclear Magnetic Resonance Spectroscopy (NMR)

$CDCl_3$ was used as solvent. ^{1}H-NMR and ^{13}C-NMR spectra were recorded at 500 MHz and 126 MHz, respectively with Avance500 spectrometers (Bruker, Billerica, MA, USA). ^{1}H-detected experiments were done with an inverse ^{1}H/^{13}C probehead. Direct ^{13}C-measurements were performed with a QNP ^{13}C/^{31}P/^{29}Si/^{19}F/^{1}H cryoprobe. The experiments were done in full automation using standard parameter sets of the TOPSPIN 3.0 software package (Bruker). ^{13}C-NMR spectra were recorded in proton-decoupled mode. The spectra were recorded at 27 °C. All signals were assigned by proton-proton and proton-carbon correlation experiments (e.g. COSY, HSQC, and HMBC). Data processing was typically done with the MestreNova software (Mestrelab Research, Santiago de Compostela, Spain).

3.5.4. Determination of Optical Rotations

Optical rotations were measured on a Polartronic-E polarimeter (Schmidt & Haensch, Berlin, Germany) fitted with a measuring cell (path length 1 dm) and a sodium lamp (wavelength 589 nm). Samples were diluted in ethanol and the measurements were performed at a temperature of 24 °C.
The specific rotation was calculated according to equation 11.

$$[\alpha]_D = \frac{\alpha}{c \cdot l} \cdot 100 \qquad \text{(equation 11)}$$

$[\alpha]_D$: specific rotation
α: optical rotation
c: concentration [g/100 mL]
l: path length [dm]

(*S*)-2-Mercapto-4-hexanone (*S*)-**1**: $[\alpha]_D$ +59.4, concentration (c): 3.25 g/100 mL, GC purity (p): 98.3%, enantiomeric excess (ee): 84.4%; (*S*)-2-acetylthio-4-hexanone (*S*)-**6**: $[\alpha]_D$ -11.6, c: 2.22, p: 97., ee: 99.6; (*R*)-2-mercapto-4-hexanone (*R*)-**1**: $[\alpha]_D$ -55.3, c: 2.18, p: 96.8, ee: 92.9.

(*S*)-2-Mercapto-4-heptanone (*S*)-**2**: $[\alpha]_D$ +51.4, c: 2.05, p: 98.6, ee: 94.0; (*S*)-2-acetylthio-4-heptanone (*S*)-**7**: $[\alpha]_D$ -7.4, c: 1.95, p: 94.7, ee: 97.7 (*R*)-2-mercapto-4-heptanone (*R*)-**2**: $[\alpha]_D$ -48.1, c: 1.61, p: 90.8, ee: 94.2.

(*S*)-2-Mercapto-4-octanone (*S*)-**3**: $[\alpha]_D$ +55.9, c: 1.96, p: 97.3, ee: 88.6; (*S*)-2-acetylthio-4-octanone (*S*)-**8**: $[\alpha]_D$ -16.5, c: 1.52, p: 96.7, ee: 99.6; (*R*)-2-mercapto-4-octanone (*R*)-**3**: $[\alpha]_D$ -25.0, c: 0.86, p: 90.7, ee: 92.9.

(*S*)-2-Mercapto-4-nonanone (*S*)-**4**: $[\alpha]_D$ +50.6, c: 1.49, p: 97.8, ee: 94.2; (*S*)-2-acetylthio-4-nonanone (*S*)-**9**: $[\alpha]_D$ -18.4, c: 1.07, p: 91.2, ee: 96.4; (*R*)-2-mercapto-4-nonanone (*R*)-**4**: $[\alpha]_D$ -47.1, c: 1.46, p: 95.6, ee: 91.7.

(*S*)-2-Mercapto-4-decanone (*S*)-**5**: $[\alpha]_D$ +45.0, c: 1.48, p: 96.7, ee: 93.1; (*S*)-2-acetylthio-4-decanone (*S*)-**10**: $[\alpha]_D$ -18.4, c: 1.44, p: 95.0, ee: 97.9; (*R*)-2-mercapto-4-decanone (*R*)-**5**: $[\alpha]_D$ -42.1, c: 1.23, p: 84.3, ee: 94.6.

(*S*)-4-Mercapto-2-pentanone (*S*)-**11**: $[\alpha]_D$ +51.7, c: 1.10, p: 97.9, ee: 98.3; (*S*)-4-acetylthio-2-pentanone (*S*)-**13**: $[\alpha]_D$ -15.9, c: 2.10, p: 98.3, ee: 99.0; (*R*)-4-mercapto-2-pentanone (*R*)-**11**: $[\alpha]_D$ -63.6, c: 1.89, p: 94.1, ee: 87.7.

(*S*)-4-Mercapto-2-heptanone (*S*)-**12**: $[\alpha]_D$ +22.7, c: 1.48, p: 73.0, ee: 89.3; (*S*)-4-acetylthio-2-heptanone (*S*)-**14**: $[\alpha]_D$ -27.1, c: 2.08, p: 96.5, ee: 94.0.

4. RESULTS AND DISCUSSION

4.1. Lipase-Catalyzed Kinetic Resolutions of 2-Acetylthio-4-heptanone and 4-Acetylthio-2-heptanone

4.1.1. Synthesis and GC Separation

Acetylthioheptanones **7** and **14** were synthesized by Michael-type addition of thioacetic acid to 2-hepten-4-one and 3-hepten-2-one, respectively. To obtain the mercaptoalkanones, the respective acetylthioalkanones were refluxed with methanol/sulfuric acid. The identities of the compounds were confirmed by GC-MS and NMR spectroscopy.

Using diethyl *tert*-butylsilyl-*β*-cyclodextrin as chiral stationary phase, the enantiomers of 2-mercapto-4-heptanone **2** as well as of 2-acetylthio-4-heptanone **7** could be separated for the first time (Figure 9). This allowed the determination of the enantiomeric excess of product (ee_P) and remaining substrate (ee_S) using chiral GC as well as the determination of conversion rates (c and c_{ee}) and enantioselectivities (E). 4-Acetylthio- and 4-mercapto-2-heptanone (**14** and **12**) were separated using 30% heptakis(2,3-di-*O*-methyl-6-*O*-*tert*-butyl dimethylsilyl)-*β*-cyclodextrin in DB-1701 as chiral stationary phase as described by Wakabayashi *et al*. (2011; 2015).

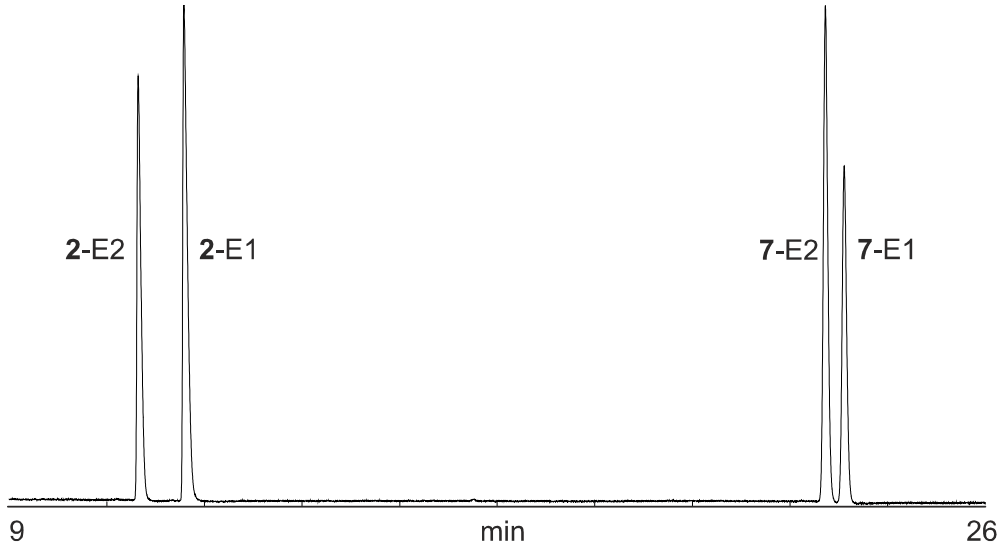

Figure 9: GC separation of the enantiomers of 2-mercapto-4-heptanone **2** and 2-acetylthio-4-heptanone **7**; for conditions, see Material and Methods (cf. 3.5.1.1., GC/FID V).

4.1.2. Enzyme Screening and Optimization of Reaction Conditions

As a first step, response factors were determined (for the calculation of the conversion rates using the achiral approach) in order to counterbalance the differences of the FID signals of substrate and product. Mercaptoalkanones generally show lower FID signals and therefore, lower response factors than the acetylthioalkanones. The additional carbon atoms of the acetyl-group cause the higher FID signals.
To this end, equation 1 (cf. 3.3.1.1.) and GC/FID system I were used. The resulting R_f-values are 1.15 for 2-acetylthio-/2-mercapto-4-heptanone and 1.07 for 4-acetylthio-/4-mercapto-2-heptanone.

Three commercially available lipases were investigated with respect to their suitability for the kinetic resolution of both racemic acetylthioalkanones. For testing, thioesters **7** and **14** were reacted with CAL-B, PPL, and WGL within a time span of 24 h. Aliquots were analyzed at specific times by means of achiral (GC/FID I) and chiral GC/FID (GC/FID IV for **12** and V for **2**) with respect to conversion rates (c) using equation 3 (cf. 3.1.1.2.), enantiomeric excesses (ee) using equation 4, and enantioselectivities (E) using equation 7 (cf. 3.1.1.4). Three batches for each enzyme were analyzed and the mean values are given in Table 5. The results of the different calculations for c and E for compound **7** are given in the Appendix (cf. 8, Table 32).

Table 5: Conversion rates (c_{ee}), enantiomeric excesses of substrates (ee_S) and respective products (ee_P) as well as enantioselectivities (E) in the course of the enzyme-catalyzed kinetic resolutions of 2-acetylthio-4-heptanone **7** and 4-acetylthio-2-heptanone **14**.

7	**CAL-B**				**PPL**				**WGL**			
time [h]	c_{ee} [%]	ee_S [%]	ee_P [%]	E	c_{ee} [%]	ee_S [%]	ee_P [%]	E	c_{ee} [%]	ee_S [%]	ee_P [%]	E
0.5	39.6	61.4	93.7	58	47.7	28.7	31.4	2	27.7	10.5	27.5	2
0.75	46.7	80.1	91.3	54	57.1	35.8	26.9	2	34.2	12.9	24.8	2
1	49.5	88.0	89.8	44	61.3	37.8	23.9	2	42.2	15.4	21.1	2
2	54.7	97.7	81.0	42	74.1	49.1	17.1	2	58.2	18.2	13.1	2
4	60.0	100	66.6	43	83.6	59.8	11.7	2	73.3	17.7	6.4	1
8	67.9	100	47.3	n.d.[a]	90.0	67.3	7.4	2	90.1	14.9	1.7	1
24	84.0	100	19.1	n.d.[a]	95.4	68.8	3.3	2	97.1	4.4	0.2	1
14												
time [h]	c_{ee} [%]	ee_S [%]	ee_P [%]	E	c_{ee} [%]	ee_S [%]	ee_P [%]	E	c_{ee} [%]	ee_S [%]	ee_P [%]	E
1	n.d.[a]	7.7	n.d.[a]	n.d.[a]	50.5	39.8	39	3	60.4	12.3	8.1	1
2	n.d.[a]	6.9	n.d.[a]	n.d.[a]	67.3	64.1	31.1	3	69.0	14.3	6.4	1
4	5.9	6.3	100	n.d.[a]	79.4	82.1	21.4	3	81.1	17.3	4	1
8	7.1	5.2	68.6	5.7	86.8	89	13.5	3	93.6	28.2	1.9	1
24	3.3	2.4	70.9	6	90.7	85	8.5	2	98.7	34.3	0.4	1

[a] not determinable

Considering the enantiomeric excesses and enantioselectivities determined for the kinetic resolution of **7**, it becomes apparent that PPL and WGL were not suitable for the preparation of enantiopure 2-mercapto-4-heptanone. The enantioselectivity of both lipases was only 2 and the ee values were not high enough. On the other hand, CAL-B turned out to be appropriate for the hydrolysis of **7** (E=58), the highest ee_P (93.7%) was obtained after 0.5 h and the highest ee_S (100%) after 4 h. Thus, both enantiomers can be obtained with this lipase.

As can be seen from Table 5, the conversion rates reached high values up to 98.7% (hydrolysis of **14** with WGL), except for the conversion of **14** with CAL-B (<10%). Here, the hydrolysis started between 2 and 4 h and seemed to decrease again after 8 h. This can be explained by the ratios of ee_S and ee_P and the underlying equation for c_{ee}. Comparing this value with the conversion rate determined via the achiral approach (cf. Appendix, Table 36), a slight increase from 0.2% (1 h) to 4.3% (24 h) was observed.

For obtaining the direct hydrolysis product (E1) of **12**, none of the three lipases was an ideal candidate as their applications only resulted in low enantioselectivities (1-3) and low ee_P-values. Reaching 89.0% ee_S after 8 h, the conversion with PPL was appropriate for obtaining one enriched enantiomer (E2) of 4-mercapto-2-heptanone. As PPL is not able to create the opposite enantiomer (E1) of **12**, further tests were performed using the lipases CRL and ANL as well as two esterases from hog liver, one as lyophilized powder (PLE) and the other one immobilized on Eupergit® (PLE imm.). The results are presented in Table 6.

PLE (imm.) already yielded an almost total conversion after 2 h. Therefore, conversion rates and enantiomeric excesses were determined at additional time points (15, 30, 45, 60, and 120 min). The conversion was found to be 95.1% after 15 min with an ee_S of 66.0% and 98.7% after 30 min with an ee_S of 100%. Due to the high conversion rate, PLE (imm.) was not considered for the preparation of optically pure **12**.

CRL and PLE were also not considered due to poor correlations between conversion rates and enantiomeric excesses. For example, PLE revealed an ee_P of 100% after 4 h but c_{ee} was only at 12.4%. For CRL, the highest ee_S (100%) value was found at a high c_{ee} (98.3%). For ANL, the optimal reaction time seemed to be between 8 and 24 h, therefore, additional time points (14, 16, 18, 20, and 22 h) were examined with respect to conversion rates and enantiomeric excesses. The results are given in Table 7.

As can be seen from Table 7, the enantiomeric excess of the substrate increased whereas the ee_P decreased; the enantioselectivity was not high (E=3). The conversion

was high and reached 76.8% and 72%, respectively, already after 8 h. It was important to achieve an ee_S of 90% which was the case at 16 h. At this time point, ee_S was 92.3% with a c_{ee} of 88.2% and c of 83.1%. For the preparation of the second enantiomer of 4-mercapto-2-heptanone **14** was reacted with ANL for 16 h.

Table 6. Conversion rates (c_{ee}), enantiomeric excesses of substrates (ee_S) and respective products (ee_P) as well as enantioselectivities (E) in the course of the enzyme-catalyzed kinetic resolution of 4-acetylthio-2-heptanone **14** to 4-mercapto-2-heptanone **12**.

	CRL				**ANL**				**PLE**				**PLE imm.**			
time [h]	c_{ee} [%]	ee_S [%]	ee_P [%]	E	c_{ee} [%]	ee_S [%]	ee_P [%]	E	c_{ee} [%]	ee_S [%]	ee_P [%]	E	c_{ee} [%]	ee_S [%]	ee_P [%]	E
2	32.0	22.5	47.8	3.5	33.3	27.7	55.5	4.6	4.4	4.6	100	n.d.[a]	99.6	46.8	0.2	1.2
4	59.4	52.2	35.6	3.4	48.1	45.5	49.2	4.5	12.4	14.2	100	n.d.[a]	100	n.d.[a]	0	n.d.[a]
8	83.5	84.6	16.7	3.1	65.3	67.7	35.9	4	25.9	30.1	86.1	18	100	n.d.[a]	0.5	n.d.[a]
24	98.3	100	1.8	n.d.[a]	87.4	90.7	13	3.1	43.4	62.4	81.5	18.5	100	n.d.[a]	0.4	n.d.[a]

[a] not determinable

Table 7. Conversion rates (c_{ee}), enantiomeric excesses (ee_S) and (ee_P), and enantioselectivities (E) in the course of the enzyme-catalyzed kinetic resolution of 4-acetylthio-2-heptanone **14** to 4-mercapto-2-heptanone **12** using ANL.

	ANL				
time [h]	c_{ee} [%]	c [%]	ee_s [%]	ee_p [%]	E
8	76.8	72.8	75.8	22.9	3
14	85.3	80.8	89.7	15.4	3
16	88.2	83.1	92.3	12.3	3
18	90.9	85.7	94.4	9.5	3
20	93.2	87.7	95.7	6.9	3
22	95.3	89.0	96.8	4.8	3
24	96.9	90.5	97.3	3.2	3

4.2. Determination of the Absolute Configurations of Chiral *β*-Mercapto-alkanones Using ^{1}H-NMR Anisotropy Methods

4.2.1. ^{1}H-NMR Anisotropy Method Using (*S*)-M*α*NP as Chiral Auxiliary

Wakabayashi *et al.* (2011) previously deduced the configurations of 4-mercapto-2-alkanones based on the ^{1}H-NMR anisotropy method in combination with lipase-catalyzed kinetic resolutions of the respective 4-acetylthio-2-alkanones. The diastereoisomeric derivatives resulting from reaction of the mercaptoalkanones with (*S*)-2-methoxy-2-(1-naphthyl)propionic acid ((*S*)-MαNP) were separated via HPLC, and the configurations were assigned by applying the sector rule as established for secondary alcohols (Harada *et al.*, 2000; Kasai *et al.*, 2004; Taji *et al.*, 2002). Based on these results, structure-odor relationships for the enantiomers of 4-mercapto-2-alkanones and 4-acetylthio-2-alkanones have been investigated (Wakabayashi *et al.*, 2015). Nörenberg *et al*. (2013) also made use of this approach to study the impact of the stereochemistry on the odor thresholds and the odor properties of 4-mercapto-2-heptanol and its acetyl derivatives.

Vibrational circular dichroism (VCD) has been successfully applied for the determination of the absolute configurations of 2-substituted 3(2*H*)-furanones and 5-substituted 2(5*H*)-furanones (Emura *et al.*, 2009; Nakahashi *et al.*, 2011). A preliminary test of the suitability of this technique to determine the configurations of the enantiomers of 2-mercapto-4-heptanone indicated that the results were not in agreement with those obtained by applying the assignment via (*S*)-MαNP derivatives as reported by Wakabayashi *et al*. (2011). Therefore, the assignments of the configurations of selected representatives of *β*-mercaptoalkanones (Figure 10) were reinvestigated. By applying the ^{1}H-NMR anisotropy method using (*S*)-MαNP as chiral auxiliary, the results should be compared to those of VCD measurements.

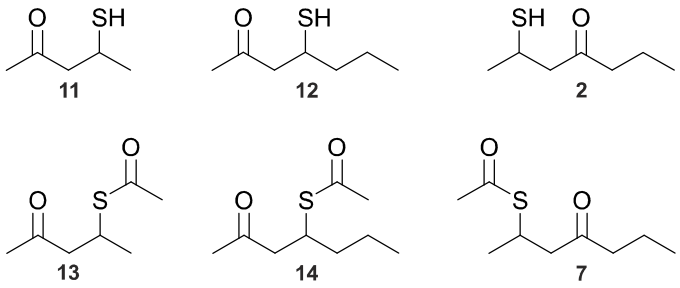

Figure 10. Structures of investigated mercaptoalkanones **2**, **11**, **12** and the respective acetylthioalkanones **7**, **13**, **14**.

The racemic mercaptoalkanones **11**, **12**, and **2** were reacted with (*S*)-M*α*NP. The resulting diastereoisomeric thioesters were separated and isolated by semi-preparative HPLC using a silica gel column. In Figure 11, the separation of the (*S*)-M*α*NP thioesters of 4-mercapto-2-pentanone **11** is exemplarily shown.

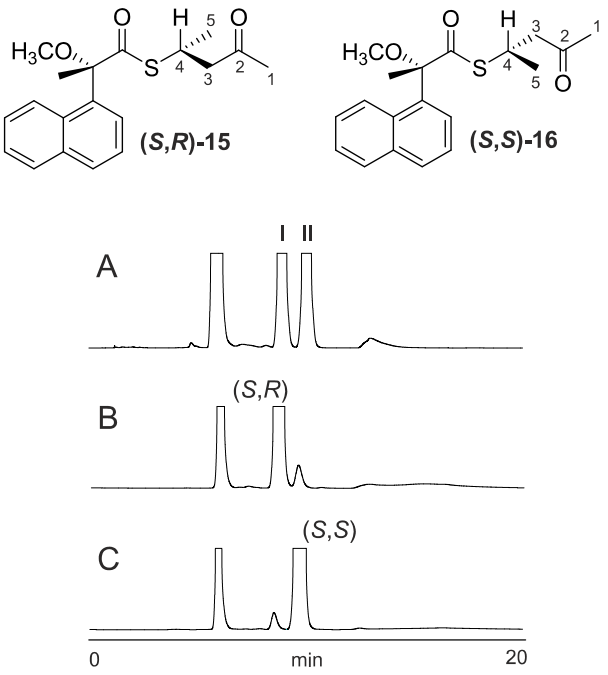

Figure 11: (A) HPLC separation of (*S*)-M*α*NP thioesters of racemic 4-mercapto-2-pentanone **11**; (B) HPLC separation of (*S*)-M*α*NP thioester (*S*,*R*)-**15** of (*R*)-(-)-4-mercapto-2-pentanone; (C) HPLC separation of (*S*)-M*α*NP thioester (*S*,*S*)-**16** of (*S*)-(+)-4-mercapto-2-pentanone.

The collected diastereoisomeric thioesters (LC-peak I, **15** and II, **16**, respectively) were subjected to NMR analysis (Table 8). As previously described for secondary alcohols (Kasai *et al.*, 2004; Taji *et al.*, 2002), the sector rule was applied for the determination of the absolute configurations. According to this rule, the (*S*)-M*α*NP ester group is fixed in the down/front side and the methine proton of the secondary alcohol in the down/rear side, as shown in Figure 12. Protons with a negative Δ*δ* are arranged on the left side and protons with a positive Δ*δ* on the right side.

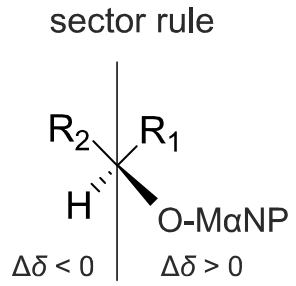

Δδ = δ(Peak II) - δ(Peak I)

Figure 12. Sector rule developed for the determination of the absolute configurations of secondary alcohols with (*S*)-M*α*NP as chiral derivatizing agent (Kasai *et al.*, 2004; Wakabayashi *et al.*, 2011).

As a result, the absolute configuration of the compound eluted as LC-peak I is given by Δ*δ* = *δ* (second peak) – *δ* (first peak). By using this rule (Figure 12) for the (*S*)-M*α*NP thioesters of **11**, the Δ*δ* value for H-5 is arranged on the left side due to its negative value (-0.01), whereas the Δ*δ* values of H-1 and H-3 are arranged on the right side as they are positive (0.04 for both). Consequently, the C-4 atom (bearing the SH-group) of the first eluting compound (LC-peak I, **15**) is suggested to have (*S*)-configuration. The (*S*)-M*α*NP thioesters of the mercaptoalkanone **13** showed the same result. For the first eluting fraction (LC-peak I, **19**) of **2**, (*S*)-configuration was also deduced at the C-2 position.

Table 8. ^{1}H-NMR data and Δδ values of (*S*)-MαNP thioesters of 4-mercapto-2-pentanone **11**, 4-mercapto-2-heptanone, **12**, and 2-mercapto-4-heptanone **2**.

	4-mercapto-2-pentanone **11**			4-mercapto-2-heptanone **12**			2-mercapto-4-heptanone **2**		
H	LC-Peak I[a] **15**	LC-Peak II[a] **16**	Δδ	LC-Peak I[a] **17**	LC-Peak II[a] **18**	Δδ	LC-Peak I[b] **19**	LC-Peak II[b] **20**	Δδ
1	1.99 (s)	2.03 (s)	0.04	1.97 (s)	2.03 (s)	0.06	1.24 (d, 7.0)	1.22 (d, 6.8)	-0.02
2							3.79 (m)	3.83 (m)	0.04
3	2.66 (dd, 16.7, 4.9)	2.70 (dd, 16.6, 5.4)	0.04	2.61 (d, 2.1)	2.66 (dd, 16.5, 6.4)	0.05	2.64 (dd, 16.6, 4.9)	2.68 (m)	0.04
3'	2.52 (dd, 16.6, 8.5)	2.52 (dd, 16.6, 8.1)	0	2.60 (d, 3.1)	2.59 (dd, 18.8, 7.0)	-0.01	2.49 (dd, 16.6, 8.6)	2.49 (dd, 16.5, 8.2)	0
4	3.79 (m)	3.79 (m)	0	3.75 (m)	3.75 (m)	0			
5	1.24 (d, 6.9)	1.23 (d, 6.9)	-0	1.51 (m)	1.50 (m)	-0.01	2.22 (td, 7.3, 3.0)	2.27 (td, 7.2, 1.5)	0.05
6				1.33 (m)	1.35 (m)	0.02	1.46 (q, 7.4)	1.49 (q, 7.4)	0.03
6’				1.26 (m)	1.25 (m)	-0.01			
7				0.8 (t, 7.3)	0.77 (t, 7.3)	-0.03	0.77 (t, 7.4)	0.81 (m)	0.04

[a] eluent: hexane/isopropanol 96/4 (v/v)

[b] eluent: hexane/ethyl acetate 20/1 (v/v)

The next step was the preparation of mercaptoalkanone enantiomers. To obtain enantiomerically enriched mercaptoalkanones, lipase-catalyzed kinetic resolutions were applied to the respective racemic acetylthioalkanones. The use of the lipase CAL-B as biocatalyst resulted in the opposite enantiomers of **11** and **2** as hydrolysis products (enantiomers E1) and remaining substrates (enantiomers E2), respectively. This was confirmed by GC analysis using chiral stationary phases. The reaction sequence of the lipase-catalyzed kinetic resolutions of racemic acetylthioalkanones is exemplarily shown for 4-acetylthio-2-pentanone **13** in Figure 13.

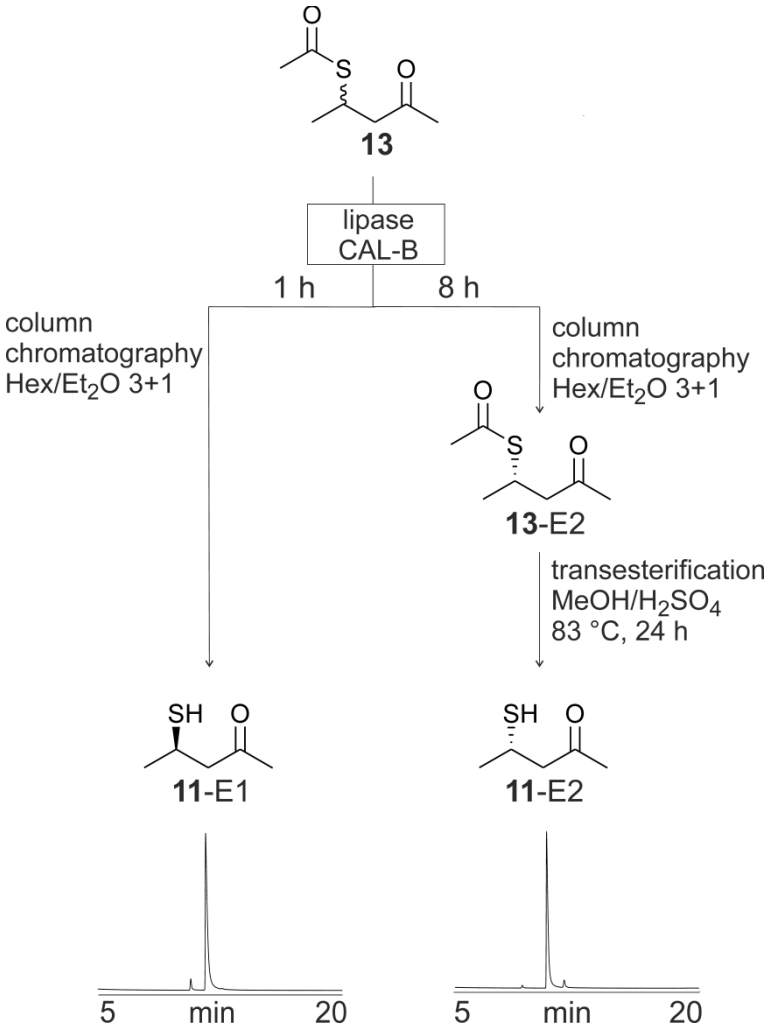

Figure 13. Preparation of the enantiomers of 4-mercapto-2-pentanone **11**-E1 and **11**-E2 via kinetic resolution of 4-acetylthio-2-pentanone **13** catalyzed by CAL-B.

A lipase suitable for the production of one of the enantiomers of 4-mercapto-2-heptanone **12** in sufficiently high optical purity as hydrolysis product of the respective thioacetate **14** was not commercially available. Therefore, the remaining unreacted

substrates obtained after kinetic resolution of 4-acetylthio-2-heptanone **14**, using lipases from *Aspergillus niger* (**12**-E2-ANL) and porcine pancreas (**12**-E2-PPL), respectively, as biocatalysts, were refluxed with MeOH/H_2SO_4 in order to yield the two opposite enantiomers of **12** (cf. 3.3.2, Table 3).

The enantiomers of the *β*-mercaptoalkanones obtained by the described procedures were then reacted with (*S*)-M*α*NP. The absolute configurations of the enantiomers were derived based on a comparison of the order of elution of the racemic (*S*)-M*α*NP thioesters (Figure 11A) and of the enantiomerically enriched **11**, **12**, and **2**. The configurations of enantiomers **11**-E1, **12**-E2-PPL, and **2**-E1 were tentatively assigned as (*S*) and those of **11**-E2, **12**-E2-ANL, and **2**-E2 as (*R*).

The assignment of the absolute configurations by applying VCD spectroscopy resulted in opposite configurations of **11**, **12**, and **2** (Kiske *et al*., 2016). Therefore, additional chiral auxiliaries were applied, as described in the following sections.

4.2.2. ^{1}H-NMR Spectroscopy Using (*R*)-HTA as Chiral Auxiliary

At first, a method based on ^{1}H-NMR spectroscopic behavior of diastereoisomeric hydratropic acid thioesters (Helmchen and Schmierer, 1976) was applied as alternative to determine the absolute configurations of the mercaptoalkanones. The differences in chemical shifts of constitutionally equivalent protons in diastereoisomeric derivatives form the basis of this method. To this end, the different mercaptoalkanone enantiomers obtained via lipase-catalyzed hydrolysis of **7**, **13**, and **14** were derivatized with (*R*)-hydratropic acid chloride. The resulting ^{1}H-NMR spectra of (*R*)-HTA thioesters **27** and **28** are exemplarily shown in Figures 14 A and B, respectively.

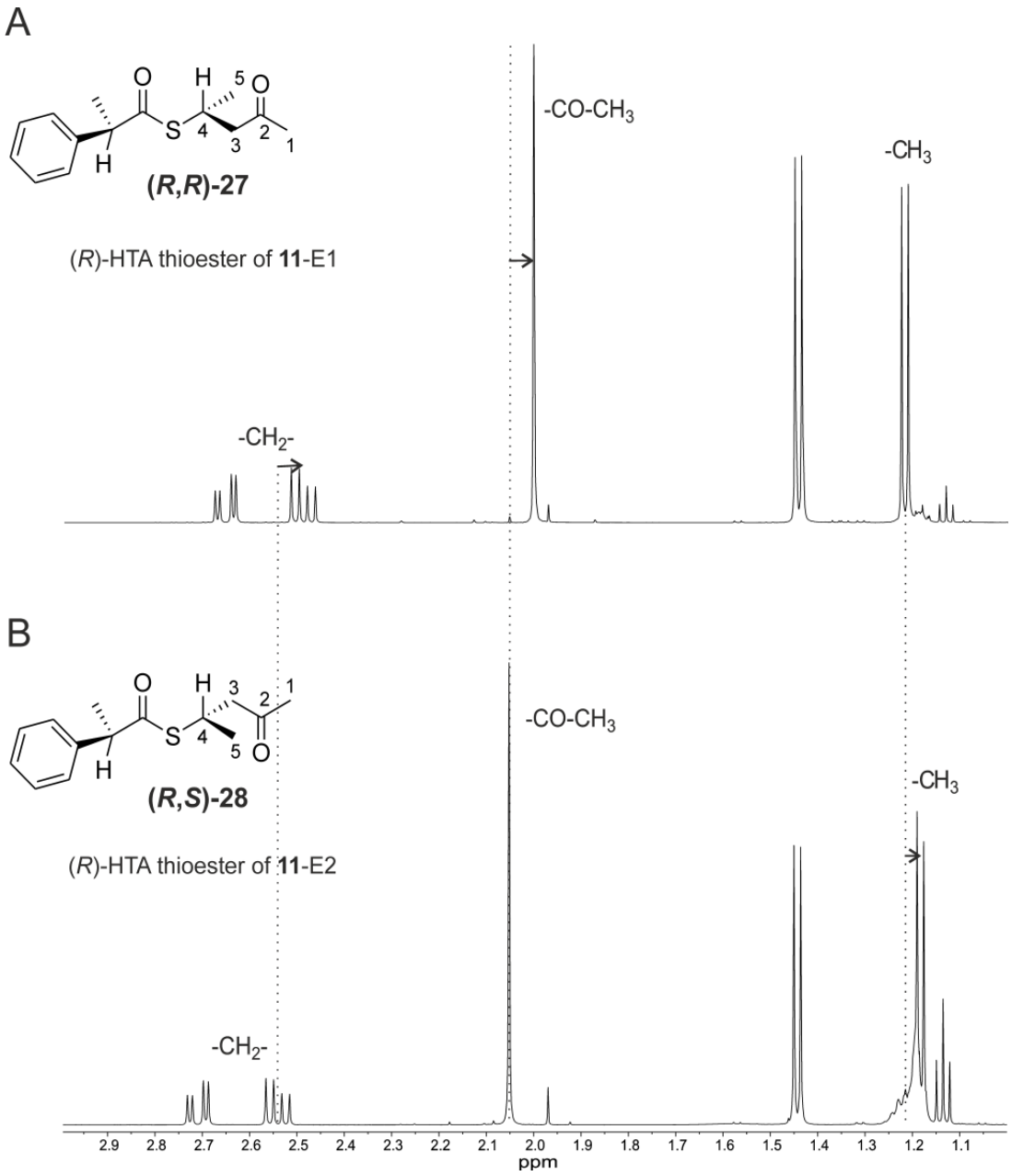

Figure 14. (A) ^{1}H-NMR spectrum of the (*R*)-hydratropic acid thioester **27** of **11**-E1 (corresponds to diastereoisomer (*R*,*R*)); (B) ^{1}H-NMR spectrum of the (*R*)-hydratropic acid thioester **28** of **11**-E2 (corresponds to diastereoisomer (*R*,*S*)).

When comparing the equivalent protons of both diastereoisomers, i.e. of the terminal CH_3-groups and the CH_2-group, characteristic shifts can be observed. For (*R*)-HTA thioester **28** of **11**-E2, the protons of the terminal methyl group at C-5 position show a relative upfield shift compared to the equivalent protons of (*R*)-HTA thioester **27** of **11**-E1. Conversely, the protons of the CH_2-group and of the other terminal methyl group (C-1 position) of (*R*)-HTA thioester **28** undergo a downfield shift compared to the equivalent protons of (*R*)-HTA thioester **27**. The observed shifting effects are ascribed

to cisoid arrangements of the acid's phenyl ring and the alkyl substituent bearing the oxo group and the methyl substituent, respectively, in the depicted constellations of (*R*)-HTA thioesters **27** and **28**. The absolute configuration of **11** can be deduced, since the absolute configuration of the hydratropic acid used as chiral auxiliary is known. Therefore, (*R*)-HTA thioester **27** of **11**-E1 is assigned as (*R*,*R*) while (*R*)-HTA thioester **28** of **11**-E2 is assigned as (*R*,*S*). ^{1}H-NMR data of (*R*)-HTA thioesters **27**-**32** of the enantiomers of **11**, **12**, and **2** are shown in Table 9.

Table 9. ^{1}H-NMR data of (*R*)-HTA thioesters of the enantiomers of 4-mercapto-2-pentanone **11**, 4-mercapto-2-heptanone **12**, and 2-mercapto-4-heptanone **2**.

	4-mercapto-2-pentanone **11**			4-mercapto-2-heptanone **12**			2-mercapto-4-heptanone **2**		
	(*R*)-HTA thioester of								
H	**11**-E1 (*R*,*R*)-**27**	**11**-E2 (*R*,*S*)-**28**	Δ*δ*	**12**-E2-PPL (*R*,*R*)-**29**	**12**-E2-ANL (*R*,*S*)-**30**	Δ*δ*	**2**-E1 (*R*,*R*)-**31**	**2**-E2 (*R*,*S*)-**32**	Δ*δ*
1	2.00 (s)	2.05 (s)	0.05	1.98 (s)	2.05 (s)	0.07	1.22 (d, 7.0)	1.18 (d, 7.0)	-0.04
2							3.81 (m)	3.81 (m)	0
3	2.65 (dd, 16.9, 4.8)	2.71 (dd, 16.9, 5.3)	0.06	2.62 (dd, 16.9, 5.6)	2.68 (dd, 16.8, 6.1)	0.06	2.62 (dd, 16.8, 4.9)	2.68 (dd, 16.7, 5.3)	0.06
3'	2.49 (dd, 16.9, 8.4)	2.54 (dd, 16.9, 8.1)	0.05	2.55 (dd, 16.9, 7.4)	2.62 (dd, 16.8, 7.1)	0.07	2.46 (dd, 16.7, 8.4)	2.51 (dd, 16.8, 8.1)	0.05
4	3.79 (m)	3.78 (m)	-0.01	3.77 (m)	3.76 (m)	-0.01			
5	1.22 (d, 7.0)	1.18 (d, 7.0)	-0.04	1.50 (m)	1.45 (m)	-0.05	2.23 (td, 7.2, 3.5)	2.28 (t, 7.3)	0.05
5'				1.46 (m)	1.45 (m)	-0.01			
6				1.30 (m)	1.21 (m)	-0.09	1.47 (m)	1.51 (dt, 14.7, 7.4)	0.04
6'				1.23 (m)	1.17 (m)	-0.06			
7				0.81 (td, 7.1, 1.9)	0.76 (t, 7.3)	-0.05	0.79 (t, 7.4)	0.82 (t, 7.4)	0.03

Considering the data of **12**, the same result is found. The terminal methyl group at C-7 position and the protons of both methylene bridges (C-5 and C-6 position) of the (*R*)-HTA thioester **30** of **12**-E2-ANL show an upfield shift. In contrast, the protons of the methylene bridge at C-3 position and the terminal methyl group at C-1 position of the (*R*)-HTA thioester **30** undergo a downfield shift. For **2**, the protons of the terminal methyl group at C-1 position of (*R*)-HTA thioester **32** of **2**-E2 undergo an upfield shift compared to the protons of (*R*)-HTA thioester **31** of **2**-E1. At the same time, the protons at positions C-3, C-5, C-6, and C-7 of (*R*)-HTA thioester **32** show a downfield shift. Based on these findings, the absolute configurations of **11**-E1, **12**-E2-PPL, and **2**-E1 can be confirmed as (*R*) and for **11**-E2, **12**-E2-ANL, and **2**-E2 as (*S*). These configurations of the *β*-mercaptoalkanones assigned via ^{1}H-NMR spectroscopy of their (*R*)-HTA thioesters were in agreement with the results obtained by VCD spectroscopy (Kiske *et al*., 2016).

4.2.3. ^{1}H-NMR Spectroscopy Using (*S*)- and (*R*)-MPA as Chiral Auxiliary

The application of the chiral auxiliary 2-methoxy-2-phenylacetic acid (MPA) was used for a final confirmation. MPA has been shown to be suitable for the assignment of the absolute configurations of chiral thiols (Porto *et al.*, 2014; Porto *et al.*, 2007). The (*R*)- and (*S*)-MPA thioesters **36** and **35** were obtained after derivatization of the enantiomer **2**-E1 (assigned as (*R*), cf. 4.2.1.2.); their determined $\Delta\delta^{RS}$ signs are presented in Figure 15. The (*R*)-configuration of the *β*-mercaptoalkanone was confirmed by the spatial arrangement of the L_1/L_2 side chains which was in accordance to the model developed by Porto *et al*. (2007). By using the (*R*)-2-heptanethiol for the preparation of (*R*)- and (*S*)-MPA thioesters **34** and **33**, the $\Delta\delta^{RS}$ signs illustrated that the presence of the additional carbonyl group at C-4 position did not affect the suitability of this model for the assignment of the configurations (Figure 15).

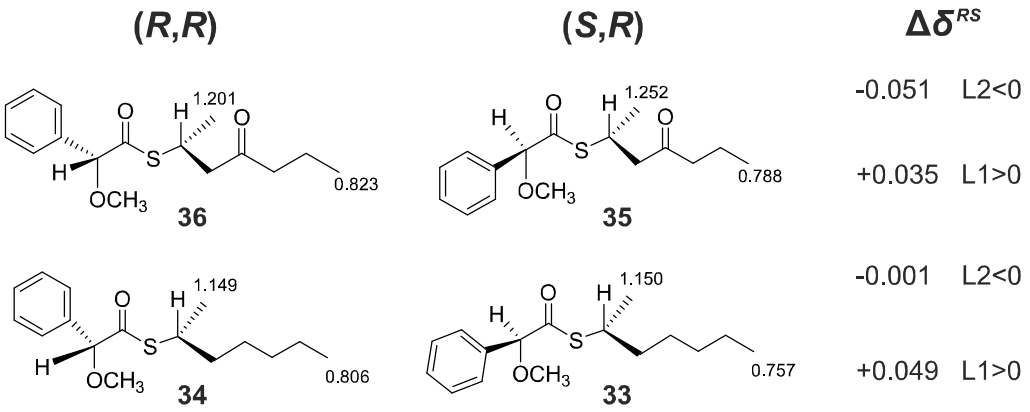

Figure 15. Structures of (*R*)- and (*S*)-MPA thioesters **36** and **35** of **2**-E1 and **34** and **33** of (*R*)-2-heptanethiol with δ values (ppm) and $\Delta\delta^{RS}$ values (ppm). L1 (front side) and L2 (rear side) correspond to the side chains at the asymmetric centers of the mercaptoalkanone and the thiol moieties, respectively.

The use of (*R*)- and (*S*)-MαNP as derivatizing reagent for the syntheses of thioesters **21** and **19** of **2**-E1 and **26** and **25** of (*R*)-2-heptanethiol revealed the same findings. Considering the signs of the $\Delta\delta^{RS}$ values, the application of the model established by Porto *et al*. (2007) results in (*R*)-configuration of the mercaptoalkanone as well as of the thiol (Figure 16). In contrast, the obtained (*R*)- and (*S*)-MαNP esters **22** and **23** of (*R*)-2-heptanol showed opposite $\Delta\delta^{RS}$ signs compared to those of the thioesters.

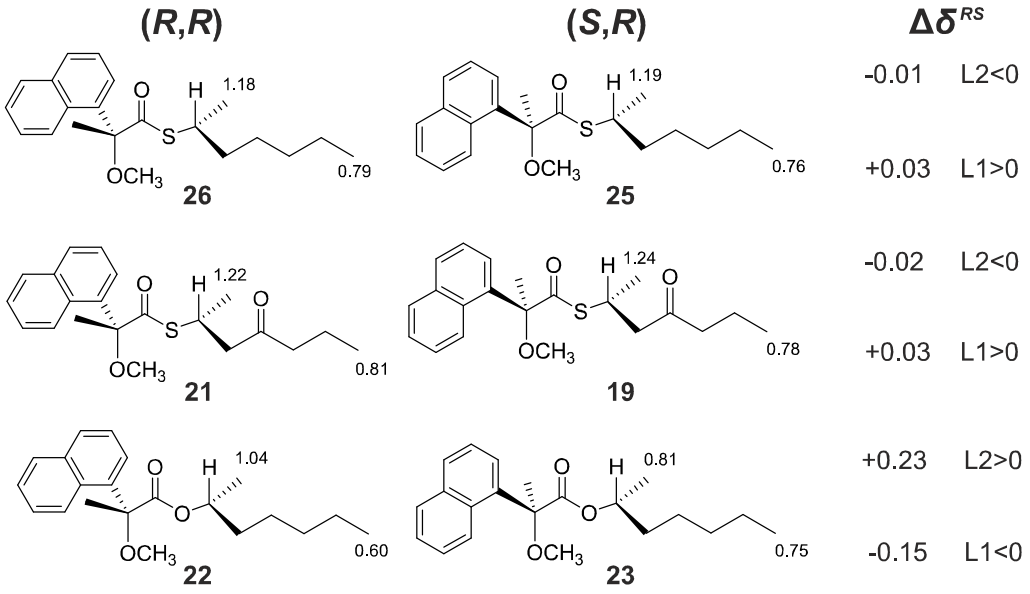

Figure 16. Structures of (*R*)- and (*S*)-MαNP thioesters **26** and **25** of (*R*)-2-heptanethiol, **21** and **19** of **2**-E1, and (*R*)- and (*S*)-MαNP esters **22** and **23** of (*R*)-2-heptanol with δ values (ppm) and $\Delta\delta^{RS}$ values (ppm). L1 (front side) and L2 (rear side) correspond to the side chains at the asymmetric centers of the thiol, mercaptoalkanone and alcohol moieties, respectively.

The occurrence of different predominant conformers could explain this phenomenon. The prerequisite for the determination of the absolute configurations of chiral secondary alcohols by the use of M*α*NP as chiral auxilliary is the existence of stable and preferred conformers of the M*α*NP esters. Conformational analysis of these esters revealed a *syn*-periplanar arrangement of the oxygen atom of the methoxy group to the ester's carbonyl oxygen atom, which is also *syn*-periplanar to the methine proton of the alcohol moiety (Figure 17A) (Kasai *et al.*, 2007). The *syn*-periplanar conformation also applies for MPA esters (Figure 17B). In contrast, regarding the arrangement of the methoxy group to the carbonyl oxygen for MPA thioesters, the *anti*-periplanar conformation is predominant (Figure 17D) (Porto *et al.*, 2007). For other arylmethoxyacetic acid thioesters, the higher stability of the *anti*-periplanar conformation has also been proven (Porto *et al.*, 2014). Therefore, a preferred *anti*-periplanar conformation of methoxy and carbonyl oxygen can be assumed also for M*α*NP thioesters (Figure 17C).

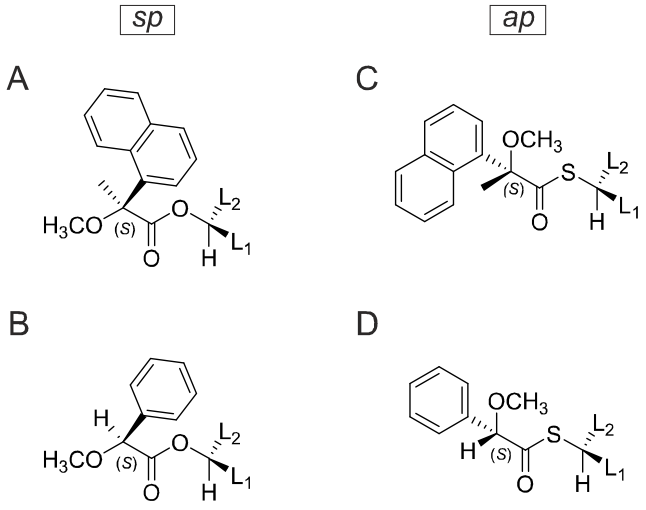

Figure 17. Predominant *syn*-periplanar (*sp*) and *anti*-periplanar (*ap*) conformers of (A and C) (*S*)-M*α*NP; and (B and D) (*S*)-MPA esters and thioesters, respectively.

Consequently, M*α*NP esters and M*α*NP thioesters show diverging anisotropy effects, as the side chains in proximity to the plane of the naphthalene moiety are different. Therefore, the sector rule as established for secondary alcohols (cf. 4.2.1.1., Figure 12) has to be changed for the application of M*α*NP as chiral auxilliary for the assignment of the configurations of *β*-mercaptoalkanones (Figure 18).

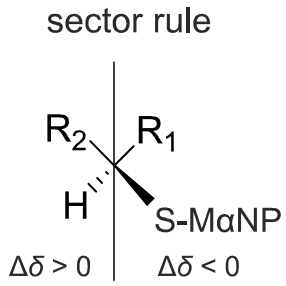

Δδ = δ(Peak II) - δ(Peak I)

Figure 18. Sector rule used for the determination of the absolute configurations of chiral *β*-mercaptoalkanones with (*S*)-M*α*NP as chiral derivatizing agent based on the results elaborated in this study.

Contrary to the sector rule established for secondary alcohols, the absolute configurations of *β*-mercaptoalkanones can be deduced when setting the protons with a positive Δ*δ* on the left side and the protons with a negative Δ*δ* on the right side.

As a consequence, absolute configurations previously assigned for mercapto-alkanones and their respective acetylthioalkanones on the basis of the secondary alcohol's sector rule have to be revised (Wakabayashi *et al*., 2011; Nörenberg *et al*., 2013; Wakabayashi *et al*., 2015).

4.3. Lipase-Catalyzed Kinetic Resolutions of 2-Acetylthio-4-alkanones (Chain Lengths C6 and C8-C10)

4.3.1. Enzyme Screening and Optimization of Reaction Conditions

Response factors were determined for the calculation of the conversion rates using the achiral approach as described in chapter 4.1.1. Equation 1 (cf. 3.3.1.1.) and GC/FID systems I (for C6, C8) and II (for C9, C10) were used; the resulting R_f- values are listed in Table 10.

Table 10. GC response factors of 2-acetylthio-4-alkanones (chain lengths C6-C10).

compound	response factor R_f
2-acetylthio-4-hexanone	1.22
2-acetylthio-4-heptanone	1.15
2-acetylthio-4-octanone	1.03
2-acetylthio-4-nonanone	1.08
2-acetylthio-4-decanone	1.0

The mercaptoalkanones generally show lower FID signals and therefore, lower response factors than the acetylthioalkanones. The higher FID signals are caused by the additional carbon atoms of the acetyl-group. It can be seen that the response factors decrease with increasing chain length due to the decreasing influence of the additional acetyl group on the molecular weight within longer chain lengths. 2-Acetylthio-4-alkanones with chain lengths C8 to C10 are quite similar and there is hardly any difference in the R_f values.

For the enzyme screening, three commercially available lipases were investigated regarding their suitability for kinetic resolutions of racemic 2-acetylthio-4-alkanones. 2-Acetylthio-4-alkanones **6** and **8**-**10** were reacted with CAL-B, PPL, and WGL within a time span of 24 h. Aliquots were analyzed at specific time points by means of chiral and achiral GC/FID with respect to conversion rates (c) using equation 3 (cf. 3.1.1.2.) and enantioselectivities (E) using equation 7 (cf. 3.1.1.4.). Three batches for each enzyme were analyzed and the mean values are given in Table 11. The results of the different calculations for c and E are given in the Appendix (cf. 8, Tables 31, 33-35).

Table 11. Conversion rates (c_{ee}), enantiomeric excesses of substrates (ee_S) and respective products (ee_P) as well as enantioselectivities (E) in the course of the enzyme-catalyzed kinetic resolutions of 2-acetylthio-4-alkanones (chain lengths C6-C10).

C6	**CAL-B**				**PPL**				**WGL**			
time [h]	c_{ee} [%]	ee_S [%]	ee_P [%]	E	c_{ee} [%]	ee_S [%]	ee_P [%]	E	c_{ee} [%]	ee_S [%]	ee_P [%]	E
0.5	32.6	49.9	93.6	50	44.7	43.2	53.1	5	27.5	4.8	12.6	1
0.75	42.3	70.3	91.7	49	53.2	55.9	49.2	5	37.7	5.6	9.3	1
1	46.7	84.1	89.4	48	57.4	62.8	46.6	5	47.4	5.9	6.6	1
2	54.5	98.4	80.4	43	68.0	80.0	37.5	5	71.9	4.7	1.8	1
4	60.2	99.8	63.7	28	78.2	93.4	26.1	5	19.3	0.3	1.0	1
8	69.6	100	41.9	n.d.[a]	87.1	98.1	14.6	4	86.1	9.4	1.5	1
24	89.2	100	10.9	n.d.[a]	95.4	99.5	4.8	3	90.1	12.0	1.2	1
C8												
0.5	35.4	50.0	90.9	35	27.3	5.0	13.2	1	11.6	2.5	18.9	2
0.75	42.6	66.6	89.7	37	35.8	5.1	9.1	1	16.2	3.2	16.7	1
1	47.3	79.1	88.1	38	43.6	4.8	6.3	1	19.8	3.9	15.6	1
2	53.7	94.2	81.1	34	67.8	2.9	1.5	1	29.9	5.5	13.0	1
4	58.2	95.8	68.7	20	30.0	1.0	1.7	1	43.4	7.7	10.0	1
8	66.5	100	50.5	n.d.[a]	66.1	6.9	3.5	1	60.6	9.7	6.3	1
24	84.1	100	19.0	n.d.[a]	83.6	17.6	3.5	1	85.9	7.1	1.2	1
C9												
0.5	33.7	48.8	95.6	71	--[b]	--[b]	--[b]	--[b]	--[b]	--[b]	--[b]	--[b]
0.75	38.9	60.5	94.7	67	--[b]	--[b]	--[b]	--[b]	--[b]	--[b]	--[b]	--[b]
1	44.1	75.2	95.0	89	2.0	0.2	10.5	1	21.7	6.0	21.7	2
1.5	48.2	86.8	93.0	78	--[b]	--[b]	--[b]	--[b]	--[b]	--[b]	--[b]	--[b]
2	50.7	94.4	91.6	82	3.0	0.5	15.2	1	36.5	11.1	19.2	2
4	54.2	99.2	84.0	62	4.9	1.0	20.4	2	50.9	15.4	14.8	2
8	57.9	99.8	72.6	42	6.8	2.1	29.2	2	60.8	16.0	10.2	1
24	67.1	99.9	49.0	19	10.7	4.8	39.7	2	79.4	15.4	4.0	1

Table 11. continued.

C10	**CAL-B**				**PPL**				**WGL**			
time [h]	c_{ee} [%]	ee_S [%]	ee_P [%]	E	c_{ee} [%]	ee_S [%]	ee_P [%]	E	c_{ee} [%]	ee_S [%]	ee_P [%]	E
0.5	10.7	29.6	82.8	20	-- [b]	-- [b]	-- [b]	-- [b]	-- [b]	-- [b]	-- [b]	-- [b]
0.75	35.2	52.0	94.3	57	-- [b]	-- [b]	-- [b]	-- [b]	-- [b]	-- [b]	-- [b]	-- [b]
1	37.9	58.8	95.5	79	7.6	1.0	12.9	1	8.4	2.0	17.2	1
1.5	44.2	73.5	91.9	52	-- [b]	-- [b]	-- [b]	-- [b]	-- [b]	-- [b]	-- [b]	-- [b]
2	43.4	73.8	94.5	78	18.1	2.4	10.6	1	14.2	2.0	9.0	1
4	50.7	92.8	90.1	65	23.1	3.2	10.6	1	18.7	1.4	5.3	1
6	52.8	93.5	83.5	38	-- [b]	-- [b]	-- [b]	-- [b]	-- [b]	-- [b]	-- [b]	-- [b]
8	54.3	98.6	82.9	52	31.0	4.5	10.1	1	0.2	0.7	3.6	1
24	63.4	99.7	57.6	21	37.9	6.3	10.3	1	54.0	8.1	7.1	1

[a] not determinable

[b] not determined at that time point

The conversion rates reached high values up to 97%, except for the hydrolyses of C9 (11%) and C10 (38%) using PPL, and of C10 (54%) using WGL. In general, conversion rates were higher for the shorter chain length C6, slightly decreased for the longer chain C8 but decreased stronger for C9 and C10. The time courses of the hydrolyses of 2-acetylthio-4-alkanones of the different chain lengths (including C7 from chapter 4.1.2.) are exemplarily shown for CAL-B catalyzed reactions in Figure 19.

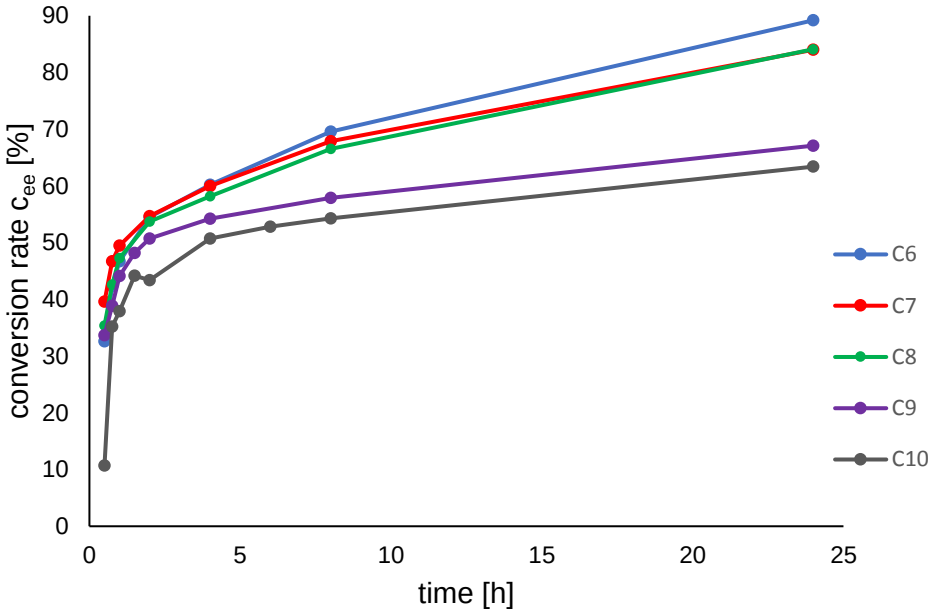

Figure 19. Conversion rates (c_{ee}) in the course of the CAL-B catalyzed hydrolyses of 2-acetylthio-4-alkanones (C6-C10) to the respective 2-mercapto-4-alkanones.

As can be seen from Figure 19, a conversion of 50% was reached within 2 h, except for C10. The overall fast conversion of the substrates shows that the lipase in the used reaction medium (potassium phosphate buffer) possesses a high activity.

Regarding the enantiomeric excesses and enantioselectivities, it becomes apparent that PPL and WGL are not suitable for the preparation of enantiopure compounds. Enantioselectivities for WGL were only 1 or 2, and ee values were too low for enantio-enriched preparation. The hydrolysis with PPL showed the highest enantioselectivity (E=5) for thioester **6** and reached an ee_S >90% after 4 h, but the conversion rate at that time point was too low for an acceptable yield. For the substrates with longer chain lengths, the enantioselectivity was as low as for WGL.

Quite different results were obtained with the lipase from *Candida antarctica* B. Enantioselectivities reached values from 19 (C9, 24 h) up to 89 (C9, 1 h). Regarding

the enantiomeric excesses, the ee_S values increased during the hydrolysis whereas ee_P values decreased. For C6 and C8, the highest ee_P values (>90%) were reached after 30 min with conversion rates of 32.6 and 35.4%, respectively, afterwards ee_P decreased. For C9, ee_P showed values above 90% within the first 2 h, and for C10 ee_P increased at the beginning (0.5-1 h) to a maximum of 95.5% with a conversion rate of 37.9% and decreased from 2 h on. The ee_S values reached over 90% for C6, C8, and C9 after 2 h and for C10 after 4 h.

In Figure 20, the ee_S and ee_P values in dependency of time are presented for the lipase-catalyzed hydrolyses of the homologous series of 2-acetylthio-4-alkanones (C6-C10).

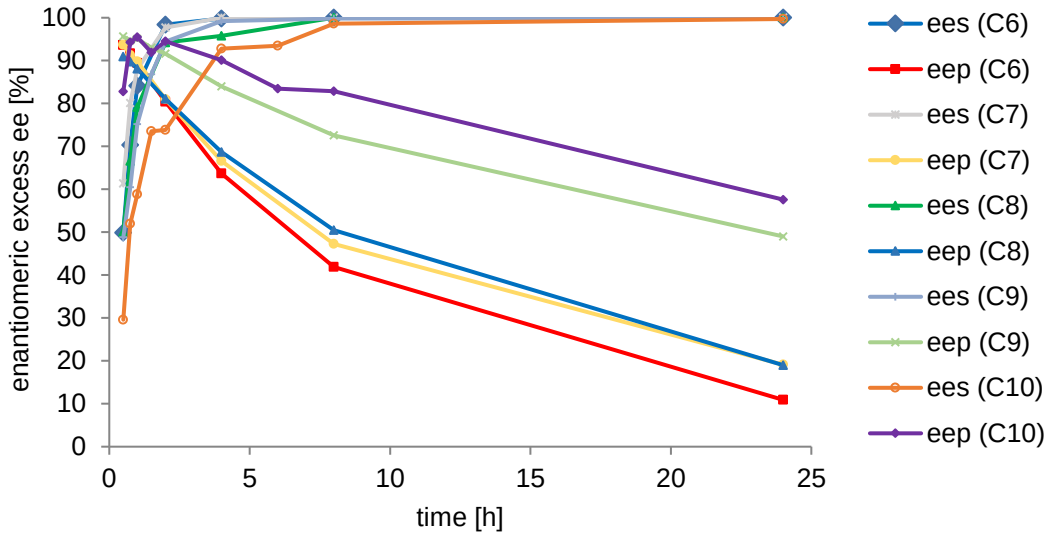

Figure 20. Enantiomeric excesses of substrates (ee_S) and products (ee_P) in the course of the CAL-B catalyzed hydrolyses of 2-acetylthio-4-alkanones (C6-C10) to the respective 2-mercapto-4-alkanones.

The curves of the ee_S values were quite similar within the homologous series, only the values of C10 were slightly different between 2 and 8 h. For the ee_P values, major differences were observed between compounds C9/C10 and C6-C8.

4.3.2. Influence of Chain Length and Position of the Functional Group on the Enantioselectivity of Lipase-Catalyzed Kinetic Resolutions of 2-Acetylthio-4-alkanones

Regarding the enantioselectivities of the lipase-catalyzed hydrolyses, there were only very small differences for PPL and WGL. Both lipases were non-selective with E-values of 1-5.

In contrast, CAL-B showed a high selectivity towards 2-acetylthio-4-alkanones. Regarding the influence of the chain length on the enantioselectivity, an increase with growing chain length was observed. Including the 4-acetylthio-2-pentanone investigated by Wakabayashi *et al.* (2015), the correlation between enantioselectivity and chain length is depicted in Figure 21. It shows a moderate increase of the enantioselectivity from C5 (E=34) to C6 (E=50) and a small increase from C6 to C7 (E=58). C8 showed the same enantioselectivity as C6 whereas a higher increase was observed for C9 (E=89) and C10 (E=79).

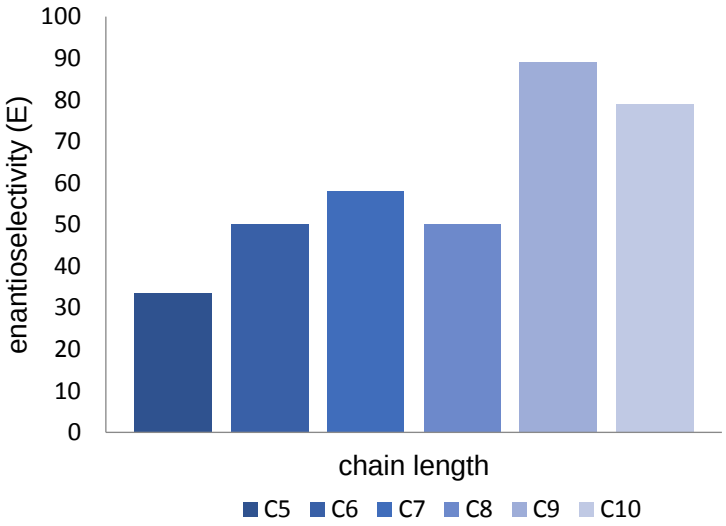

Figure 21. Observed enantioselectivities (E) of CAL-B-catalyzed hydrolyses of 2-acetylthio-4-alkanones depending on the chain lengths.

The influence of the position of the functional group was also examined using 2-acetylthio-4-heptanone **7** and 4-acetylthio-2-heptanone **14**. For both lipases PPL and WGL, the difference of the enantioselectivities were only marginal, E=2 for **7** and E=3/E=1 for **14**, i.e. the lipases are non-selective for both positional isomers. Conversely, the conversion of both isomers using CAL-B as lipase showed a significant

difference for the enantioselectivity (as well as for the conversion rate; cf. 4.1.2.2.; Table 5). Whilst C5 as common isomer for both homologous series showed an E of 34, 4-acetylthio-2-heptanone exhibited an enantioselectivity of 6. Therefore, CAL-B is not selective for 4-acetylthio-2-alkanones. The situation is different for the positional isomer 2-acetylthio-4-heptanone; the lipase CAL-B showed sufficient enantioselectivity (E=58).

As outlined in section 2.4.1.4., the enantioselectivity is dependent on the different binding properties of the enantiomers to the enzyme. The better a substrate can bind to the catalytic triad of the enzyme's active site, the lower is the required activation energy and the more rapidly the respective enantiomer can be converted. That means, the higher the difference of the size of the substituents at the chiral center is, the better is the binding to the active site and the higher is the enantioselectivity (Ghanem and Aboul-Enein, 2005; Kazlauskas *et al.*, 1991; Kovac *et al.*, 2000).

If the Kazlauskas-rule (cf. 2.4.1.4., Figure 8) is applied to both positional isomers, the following facts can be stated: (i) with elongation of the carbon chain length the difference of the substituent's size decreases for 4-acetylthio-2-alkanones. Therefore, no preferred enantiomer can be determined for the lipase-catalyzed hydrolysis which resulted in very low enantioselectivity. One substituent becomes bigger only for chain lengths C9 or C10. (ii) The difference of the substituent's size increases with elongation of the carbon chain length of 2-acetylthio-4-alkanones, resulting in a medium-sized/small substituent and a large substituent. According to the Kazlauskas-rule, the (*R*)-enantiomer would be the preferred compound. This could be confirmed for 2-acetylthio-4-heptanone for which the (*R*)-enantiomer was the faster reacting one. As the (*R*)-enantiomer is the direct hydrolysis product, it can be assumed that this rule can be applied to the homologous series of 2-acetylthio-4-alkanones and 2-mercapto-4-alkanones, respectively (Figure 22).

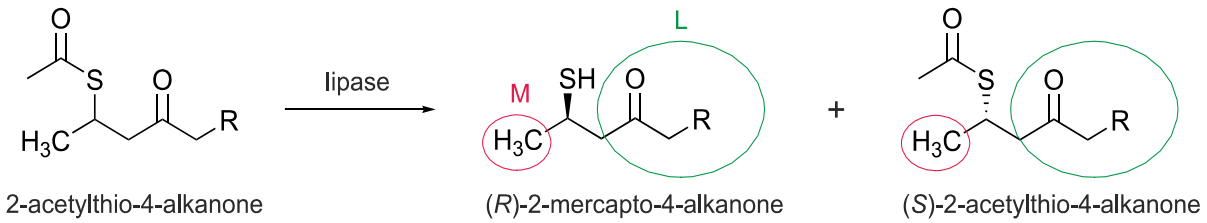

Figure 22. Application of the Kazlauskas-rule to the kinetic resolutions of 2-acetylthio-4-alkanones to 2-mercapto-4-alkanones (C6: R=CH_3, C7: R=CH_2CH_3, C8: R=$(CH_2)_2CH_3$, C9: R=$(CH_2)_3CH_3$, C10: R=$(CH_2)_4CH_3$) using CAL-B as biocatalyst; M: medium-sized/small substituent; L: large substituent

4.3.3. Optimal Reaction Conditions

Micro-sized pretests showed that CAL-B is the most suitable enzyme for the lipase-catalyzed preparation of enantio-enriched 2-mercapto-4-alkanones (chain lengths C6-C10). The reaction conditions shown in Table 12 were used to obtain the respective enantiomers for polarimetric measurements as well as for determinations of their configurations.

Table 12. Reaction conditions for the preparation of enantio-enriched 2-acetylthio-4-alkanones (**6**-**10**) and 2-mercapto-4-alkanones (**1**-**5**) of the chain lengths C6-C10.

comp.[a]	**6**		**7**		**8**		**9**		**10**	
lipase[b]	CAL-B		CAL-B		CAL-B		CAL-B		CAL-B	
	substrate	product	substrate	product	substrate	product	substrate	product	substrate	product
	6-E2	**1**-E1	**7**-E2	**2**-E1	**8**-E2	**3**-E1	**9**-E2	**4**-E1	**10**-E2	**5**-E1
time [h]	2	0.5	4	0.5	2	0.5	4	1	6	1
c_{ee} [%]	54.5	34.6	60.0	39.6	53.7	35.4	54.2	44.1	52.8	37.9
ee [%]	98.4	93.6	100	93.7	94.2	90.9	99.2	95.0	93.5	95.5
E	43	50	n.d.[c]	58	34	35	64	89	43	82

[a] compound: 85 µmol
[b] 20 mg
[c] not determinable

The preparation of the hydrolysis product (E1) within 30 min for chain lengths C6-C8 and within 1 h for chain lengths C9 and C10 (Figure 23A-E, upper chromatogram) led to good ee values (90.9-95.5%) and conversion rates (34.6-44.1%). To obtain the opposite enantiomer (E2), the remaining enantio-enriched substrates C6 and C8 were transformed for 2 h, C7 and C9 for 4 h, and C10 for 6 h (Figure 23A-E, lower chromatogram). Conversion rates ranged between 52.8 and 60% and ee values between 93.5 and 100%.

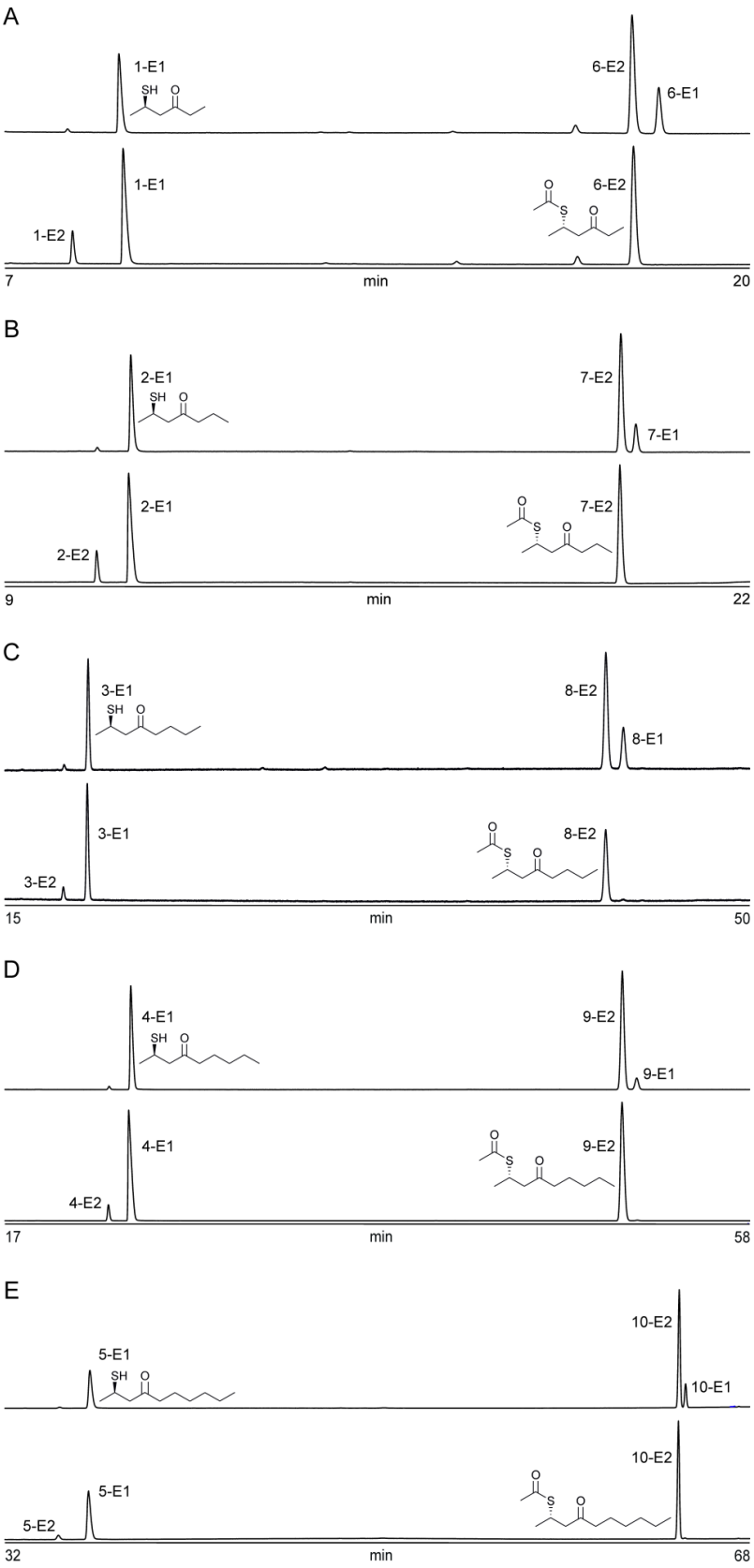

Figure 23. Capillary gas chromatographic separations of the enantiomers of 2-mercapto-4-alkanones and 2-acetylthio-4-alkanones (C6-C10) after enzyme-catalyzed kinetic resolutions with CAL-B, using GC system VI. A: 2-Mercapto- and 2-acetylthio-4-hexanone after 0.5 and 2 h; B: 2-mercapto- and 2-acetylthio-4-heptanone after 0.5 and 4 h; C: 2-mercapto- and 2-acetylthio-4-octanone after 0.5 and 2 h; D: 2-mercapto- and 2-acetylthio-4-nonanone after 1 and 4 h; E: 2-mercapto- and 2-acetylthio-4-decanone after 1 and 6 h.

4.4. Assignment of the Configurations and Assessment of the Sensory Properties of the Enantiomers of a Homologous Series of 2-Mercapto-4-alkanones

4.4.1. Synthesis and GC Separation

As described for 2-mercapto-4-heptanone **2** in chapter 4.2. and by Naef *et al.* (2008), 2-mercapto-4-alkanones with carbon chain lengths C6 and C8-C10 (**1** and **3**-**5**, Figure 24) were synthesized by Michael-type addition of thioacetic acid to the respective alkenones. Subsequently, the formed 2-acetylthio-4-alkanones (**6** and **8**-**10**, Figure 24) were treated with methanol/sulfuric acid.

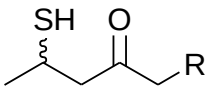

1-5

1 R= methyl
2 R= ethyl
3 R= *n*-propyl
4 R= *n*-butyl
5 R= *n*-pentyl

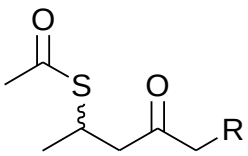

6-10

6 R= methyl
7 R= ethyl
8 R= *n*-propyl
9 R= *n*-butyl
10 R= *n*-pentyl

Figure 24. Structures of investigated 2-mercapto-4-alkanones **1**-**5** and the respective 2-acetylthio-4-alkanones **6**-**10**.

By applying the chiral stationary phase diethyl *tert*-butylsilyl-*β*-cyclodextrin, the enantiomers of the homologous series of 2-mercapto-4-alkanones (Figure 24A) and 2-acetylthio-4-alkanones (Figure 24B) could be separated via GC (Figure 25).

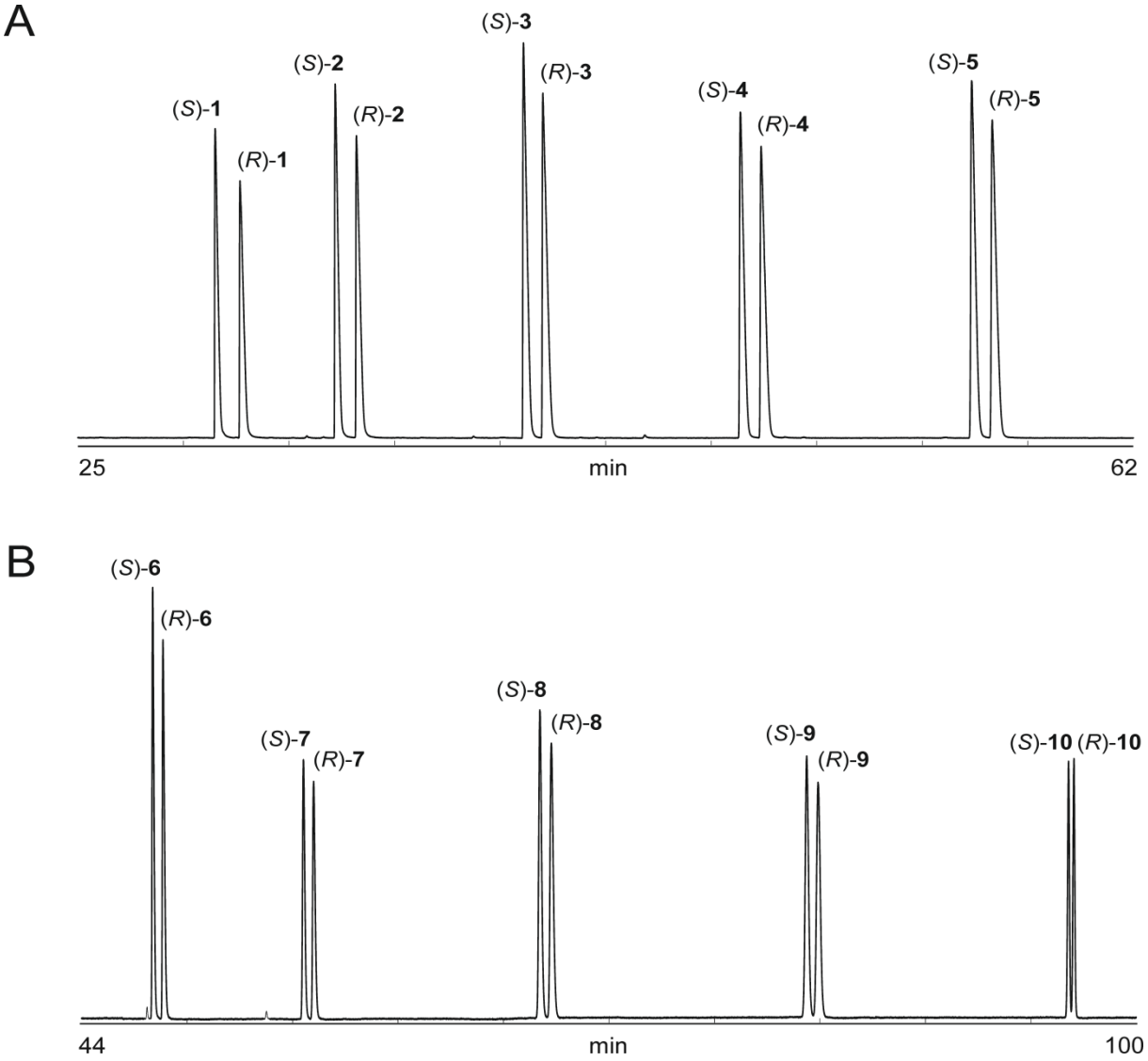

Figure 25. Capillary gas chromatographic separation of the enantiomers of (A) 2-mercapto-4-alkanones **1**-**5** and (B) 2-acetylthio-4-alkanones **6**-**10**.

4.4.2. Determination of the Absolute Configurations

To obtain enantiomerically enriched 2-mercapto-4-alkanones, lipase-catalyzed kinetic resolutions of the respective racemic 2-acetylthio-4-alkanones were performed by using CAL-B as biocatalyst. As an example, the applied approach is outlined in Figure 26 for 2-mercapto-4-octanone **3**. A compilation of yields and optical purities of the 2-mercapto-4-alkanone enantiomers obtained by this procedure is given in Table 4 (cf 3.3.4.).

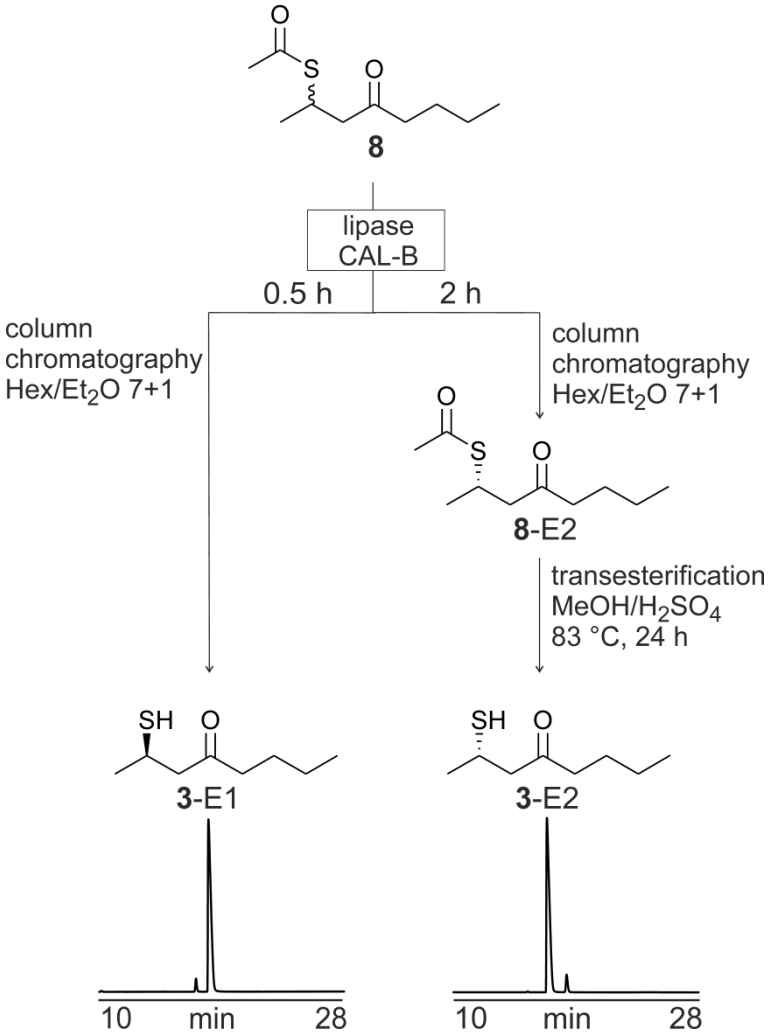

Figure 26. Preparation of the enantiomers of 2-mercapto-4-octanone **3**-E1 and **3**-E2 via kinetic resolution of 2-acetylthio-4-octanone **8** catalyzed by CAL-B.

Based on the procedures described for 2-mercapto-4-heptanone in chapter 4.2., i.e. ^{1}H-NMR analyses of diastereoisomeric thioesters using different chiral derivatizing reagents, the absolute configurations and the orders of elution of the 2-mercapto-4-alkanone and the corresponding 2-acetylthio-4-alkanone enantiomers (chain lengths C6 and C8-C10) were determined.

The enantiomers of 2-mercapto-4-alkanones obtained via lipase-catalyzed hydrolysis of the respective 2-acetylthio-4-alkanones were reacted with (*R*)-hydratropic acid chloride, according to the procedure described by Helmchen and Schmierer (1976). Figures 27 A and B show exemplarily the ^{1}H-NMR spectra of (*R*)-HTA thioesters **37** and **38** of (*R*)-**1**, and (*S*)-**1**, respectively.

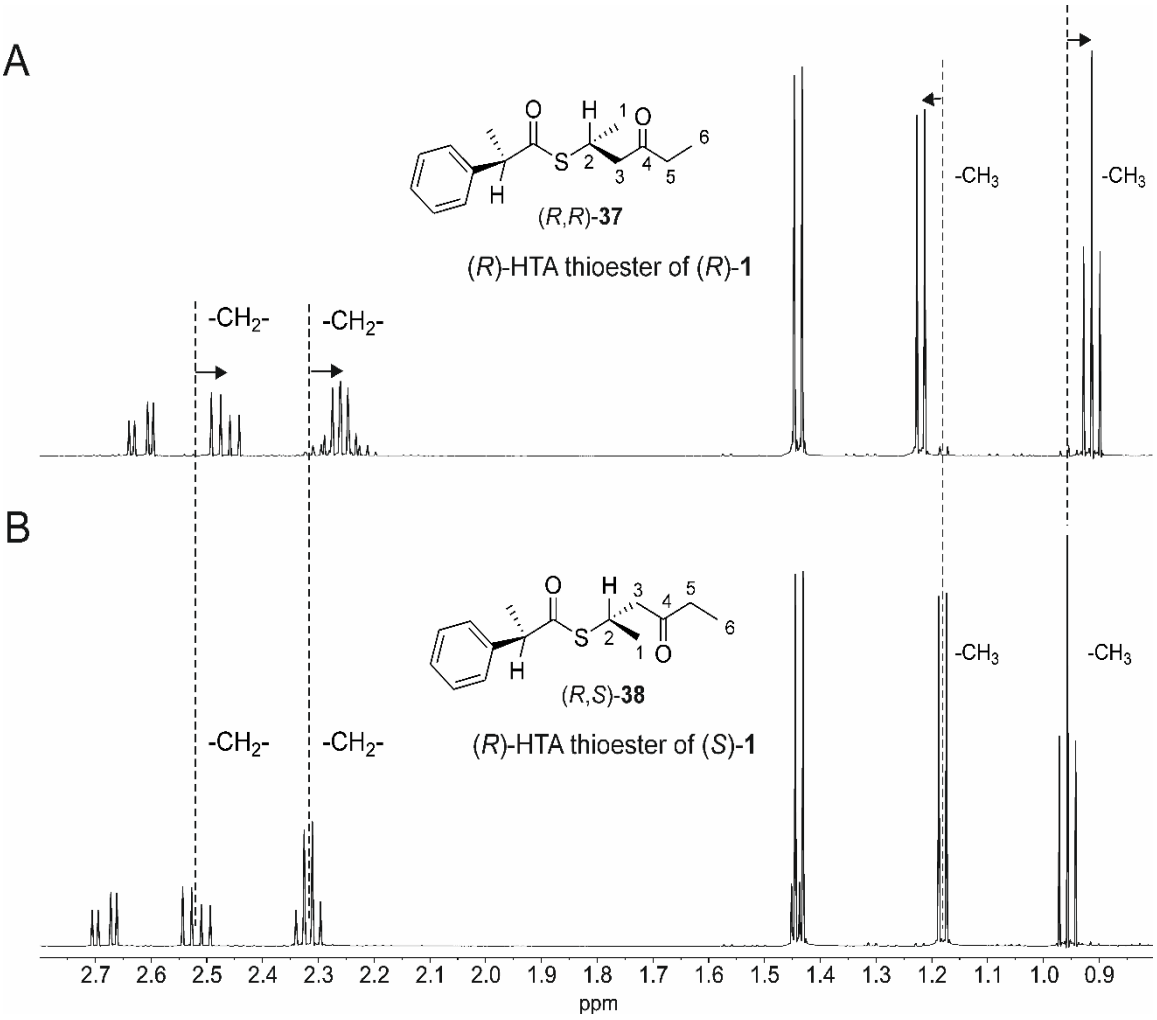

Figure 27. ^{1}H-NMR spectra of (*R*)-hydratropic acid thioesters (A) (*R*,*R*)-**37** of (*R*)-**1** and (B) (*R*,*S*)-**38** of (*S*)-**1**.

For (*R*)-HTA thioester **37**, the protons of the terminal C-6 methyl group as well as of both methylene bridges (C-3 and C-5) underwent upfield shifts in comparison with the equivalent protons of (*R*)-HTA thioester **38**. In contrast, the protons of the terminal C-1 methyl group of **37** showed a downfield shift compared to the equivalent protons of **38**. These shifting effects are ascribed to the cisoid arrangements of the acid's phenyl ring and the alkyl substituent bearing the oxo group and the methyl substituent, respectively, in the depicted constellations of (*R*)-HTA thioesters **37** and **38**. Consequently, the (*R*)-HTA thioester **37** was assigned as (*R*,*R*) whereas the (*R*)-HTA thioester **38** was assigned as (*R*,*S*). Table 13 shows the ^{1}H-NMR data of (*R*)-HTA thioesters **37**-**44** of the enantiomers of **1** and **3**-**5**.

Table 13. ^{1}H-NMR data of (*R*)-HTA thioesters of the enantiomers of 2-mercapto-4-hexanone **1**, 2-mercapto-4-octanone **3**, 2-mercapto-4-nonanone **4**, and 2-mercapto-4-decanone **5**.

	2-mercapto-4-hexanone **1**			2-mercapto-4-octanone **3**			2-mercapto-4-nonanone **4**			2-mercapto-4-decanone **5**		
	(*R*)-HTA thioester											
	1-E1	**1**-E2		**3**-E1	**3**-E2		**4**-E1	**4**-E2		**5**-E1	**5**-E2	
H	(*R*,*R*)-**37**	(*R*,*S*)-**38**	Δ*δ*	(*R*,*R*)-**39**	(*R*,*S*)-**40**	Δ*δ*	(*R*,*R*)-**41**	(*R*,*S*)-**42**	Δ*δ*	(*R*,*R*)-**43**	(*R*,*S*)-**44**	Δ*δ*
1	1.22 (d, 7.0)	1.18 (d, 7.0)	-0.04	1.22 (s)	1.18 (s)	-0.04	1.22 (d, 7.0)	1.18 (d, 7.0)	-0.04	1.22 (d, 6.9)	1.18 (d,7.0)	-0.04
2	3.81 (m)	3.80 (m)	-0.01	3.80 (m)	3.80 (m)	0	3.80 (m)	3.80 (m)	0	3.81 (m)	3.80 (m)	-0.01
3	2.62 (dd, 16.7, 5.0)	2.68 (dd, 16.7, 5.4)	0.06	2.62 (dd, 16.7, 5.0)	2.68 (dd, 16.7, 5.3)	0.06	2.62 (dd, 16.7, 4.9)	2.68 (dd, 16.7, 5.3)	0.06	2.62 (dd, 16.7, 4.9)	2.68 (dd, 16.7, 5.4)	0.06
3'	2.47 (dd, 16.6, 8.3)	2.52 (dd, 16.7, 8.1)	0.05	2.46 (dd, 16.7, 3.3)	2.51 (dd, 16.7, 8.0)	0.05	2.46 (dd, 16.8, 8.3)	2.51 (dd, 16.7, 8.1)	0.05	2.46 (dd, 16.8, 8.3)	2.51 (dd, 16.7, 8.1)	0.05
5	2.26 (m)	2.32 (q, 7.4)	0.08	2.24 (td, 7.3, 3.6)	2.29 (dd, 7.9, 7.0)	0.05	2.23 (td, 7.3, 3.7)	2.29 (m)	0.06	2.24 (td, 7.3, 3.7)	2.29 (m)	0.05
6	0.91 (t, 7.3)	0.96 (t, 7.3)	0.05	1.41 (m)	1.46 (m)	0.05	1.43 (m)	1.46 (m)	0.03	1.42 (m)	1.47 (m)	0.05
7				1.18 (t, 7.3)	1.22 (m)	0.04	1.14 (m)	1.15 (m)	0.01	1.17 (m)	1.20 (m)	0.03
8				0.80 (t, 7.3)	0.82 (t, 7.3)	0.02	1.19 (m)	1.22 (m)	0.03	1.17 (m)	1.20 (m)	0.03
9							0.80 (t, 7.2)	0.81 (t, 7.1)	0.01	1.17 (m)	1.20 (m)	0.03
10										0.80 (t, 7.1)	0.81 (t, 7.0)	0.01

2-Methoxy-2-phenylacetic acid (MPA) was applied as second chiral auxiliary, since it has been shown to be suitable for the assignment of the absolute configurations of chiral thiols by Porto *et al*. (2007, 2014). The consistency within the homologous series of the determined $\Delta\delta^{RS}$ signs of the MPA-thioesters obtained after derivatization of the (*R*)-enantiomers of **1** and **3**-**5** with (*R*)- and (*S*)-MPA, is shown in Figure 28. In accordance with Porto *et al*. (2007), the (*R*)-configuration of the 2-mercapto-4-alkanones is confirmed by the spatial arrangement of the L1/L2 side chains.

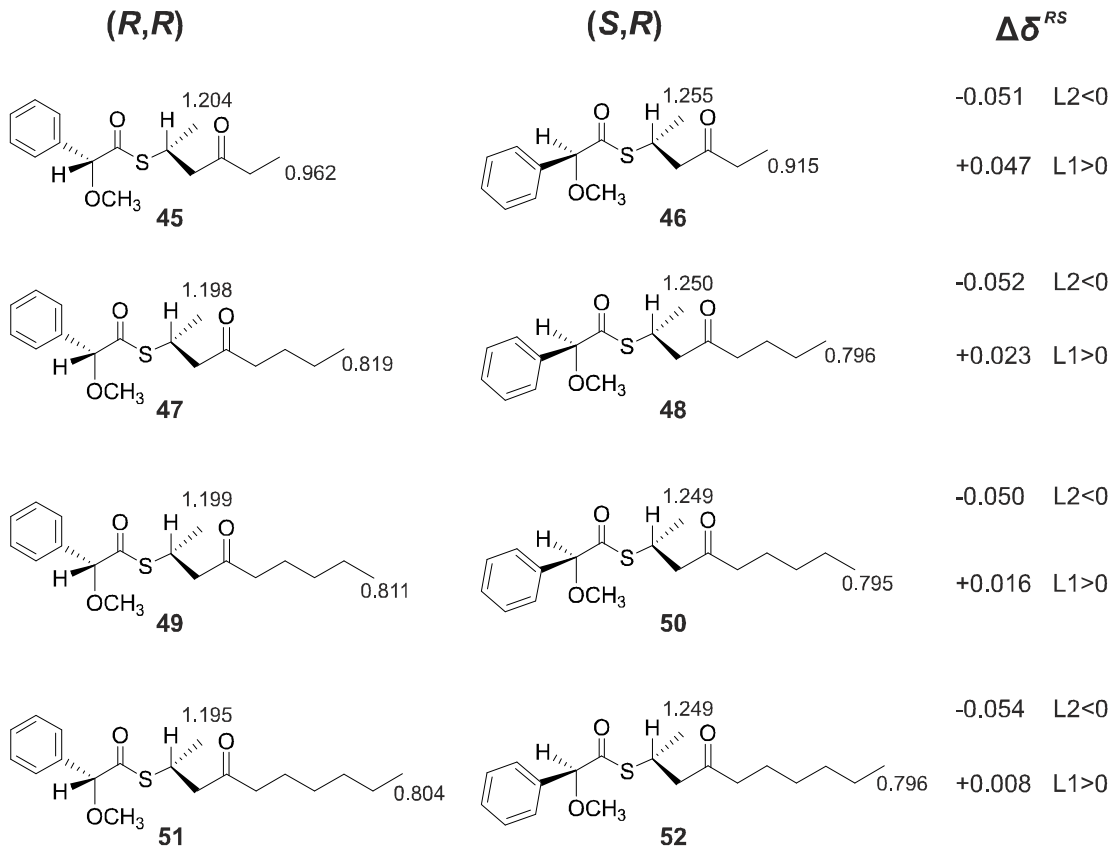

Figure 28. Structures of (*R*)- and (*S*)-MPA thioesters **45** and **46** of (*R*)-**1**, **47** and **48** of (*R*)-**3**, **49** and **50** of (*R*)-**4**, and **51** and **52** of (*R*)-**5** with δ values (ppm) and $\Delta\delta^{RS}$ values (ppm). L1 (front side) and L2 (rear side) correspond to the side chains at the asymmetric centers of the mercaptoalkanone moieties.

Finally, (*S*)-M*α*NP was used for the derivatization of the (*R*)- and (*S*)-enantiomers obtained after lipase-catalyzed kinetic resolution. The (*S*)-M*α*NP-thioesters were analyzed by ^{1}H-NMR spectroscopy after purification by semi-preparative HPLC (Table 14). The application of the revised sector rule for *β*-mercapto-alkanones and thiols (cf. 4.2.2.4.) to the (*S*)-M*α*NP thioesters **53** and **54** of mercaptoalkanone **1** revealed

positive Δ*δ* values for H-3, H-5, and H-6 (0.04, 0.04, and 0.03, respectively) and a negative Δ*δ* value for H-1 (-0.01). Therefore, H-3, H-5, and H-6 are arranged on the left side and H-1 is arranged on the right side. The resulting configuration at the C-2 position of the first eluting compound (corresponding to LC-peak I, **53**) is (*R*). For the (*S*)-M*α*NP thioesters **55**-**60** of mercaptoalkanones **3**-**5** the same results were found.

Based on the concordant results obtained by the described NMR analyses and the additional VCD experiments (Kiske *et al.*, 2019), the GC-order of elution of the enantiomers of 2-mercapto-4-alkanones (**1** and **3**-**5**) and of 2-acetylthio-4-alkanones (**6** and **8**-**10**) on the used chiral stationary phase diethyl *tert*-butylsilyl-*β*-cyclodextrin is (*S*) before (*R*), (Figure 25 A and B).

Table 14. ^{1}H-NMR data of (*S*)-M*α*NP thioesters of the enantiomers of 2-mercapto-4-hexanone **1**, 2-mercapto-4-octanone **3**, 2-mercapto-4-nonanone **4**, and 2-mercapto-4-decanone **5**.

	2-mercapto-4-hexanone **1**			2-mercapto-4-octanone **3**			2-mercapto-4-nonanone **4**			2-mercapto-4-decanone **5**		
	(*S*)-M*α*NP thioester											
	LC Peak I[a]	LC Peak II[a]		LC Peak I[a]	LC Peak II[a]		LC Peak I[b]	LC Peak II[b]		LC Peak I[b]	LC Peak II[b]	
H	(*S*,*R*)-**53**	(*S*,*S*)-**54**	Δ*δ*	(*S*,*R*)-**55**	(*S*,*S*)-**56**	Δ*δ*	(*S*,*R*)-**57**	(*S*,*S*)-**58**	Δ*δ*	(*S*,*R*)-**59**	(*S*,*S*)-**60**	Δ*δ*
1	1.24 (d, 7.0)	1.23 (d, 7.9)	-0.01	1.23 (d, 7.0)	1.22 (d, 7.0)	-0.01	1.23 (d, 6.9)	1.22 (d, 7.0)	-0.01	1.23 (d, 7.0)	1.22 (d, 6.9)	-0.01
2	3.80 (m)	3.81 (m)	-0.01	3.80 (m)	3.79 (m)	-0.01	3.79 (m)	3.80 (m)	0.1	3.79 (m)	3.80 (m)	0.01
3	2.64 (dd, 16.6, 5.0)	2.68 (dd, 16.5, 5.6)	0.04	2.64 (dd, 18.5, 5.1)	2.68 (dd, 16.6, 5.5)	0.04	2.64 (dd, 16.6, 4.8)	2.68 (dd, 16.6, 5.2)	0.04	2.64 (dd, 16.6, 4.9)	2.68 (dd, 16.6, 5.5)	0.04
3'	2.51 (dd, 16.5, 8.5)	2.50 (dd, 15.6, 8.1)	-0.01	2.49 (dd, 16.6, 8.5)	2.49 (dd, 16.5, 8.2)	0	2.49 (dd, 16.6, 8.6)	2.49 (dd, 16.7, 8.2)	0	2.49 (dd, 16.6, 8.6)	2.49 (dd, 16.6, 8.2)	0
5	2.27 (m)	2.31 (m)	0.04	2.24 (td, 7.4, 4.3)	2.29 (td, 7.2, 1.8)	0.05	2.23 (m)	2.28 (m)	0.05	2.23 (td, 7.5, 4.2)	2.29 (m)	0.06
6	0.91 (t, 7.3)	0.94 (t, 7.3)	0.03	1.41 (m)	1.44 (m)	0.03	1.42 (m)	1.46 (m)	0.04	1.41 (m)	1.45 (m)	0.04
7				1.18 (m)	1.19 (m)	0.01	1.16 (m)	1.17 (m)	0.01	1.15 (m)	1.18 (m)	0.03
8				0.78 (t, 7.3)	0.81 (t, 7.4)	0.03	1.16 (m)	1.17 (m)	0.01	1.15 (m)	1.18 (m)	0.03
9							0.77 (t, 7.2)	0.80 (t, 7.1)	0.03	1.15 (m)	1.18 (m)	0.03
10										0.78 (t, 6.9)	0.80 (t, 6.8)	0.02

[a] Eluent: hexane/ethylacetate 20/1 (v/v)

[b] Eluent: hexane/ethylacetate 25/1 (v/v)

4.4.3. Determination of Odor Thresholds

The determination of the odor thresholds of the enantiomers of 2-mercapto-4-alkanones (**1**-**5**) and 2-acetylthio-4-alkanones (**6**-**10**) was performed via GC/O in according with the procedure described by UIlrich and Grosch (1987). The values obtained for both homologous series from C6 to C10 as well as for the C5-homologs 4-mercapto-2-pentanone and 4-acetylthio-2-pentanone are compiled in Table 15. Three panelists assessed the odor thresholds of the mercapto- and the acetylthioalkanones and a fourth panelist additionally assessed the mercapto-compounds. Regarding the variability of the different panelists, a high sensitivity for the C5 and C7 homologs was observed for panelist 4, e.g. factor 49 for (*S*)-4-mercapto-2-pentanone compared to panelist 3 or factor 13 for (*S*)- and (*R*)-2-mercapto-4-heptanone **2** compared to panelist 1. However, single odor thresholds either were the same or differed only by factors between 2 and approximately 4 for the other compounds and panelists. This is equivalent to one or two dilution steps in the course of the AEDA, and therefore the sensory assessments can be considered as reproducible.

The geometric means of the odor thresholds depending on the chain lengths are presented graphically in Figure 29 (solid lines). The data revealed odor threshold minima for the chain lengths C7/C8 for 2-mercapto-4-alkanones (Figure 29A) as well as for 2-acetylthio-4-alkanones (Figure 29B). The curves for the enantiomers showed quite similar progressions; only for the (*R*)-enantiomers of the C8-homologs significantly lower odor thresholds were determined. A comparison of the geometric means of the odor thresholds determined for the enantiomers confirmed this similarity (Table 15). The calculated geometric means of the odor thresholds of the enantiomers were either the same or differed only by factors up to 2, except for 2-mercapto-4-octanone (factor 3) and 2-acetylthio-4-octanone (factor 7).

In Figures 29A and B, the previously reported odor thresholds of the homologous series of 4-mercapto-2-alkanones and 4-acetylthio-2-alkanones (Wakabayashi *et al.*, 2015) are depicted in dotted lines. The span of odor thresholds (0.1-4.9 ng/L) assessed for 4-mercapto-2-pentanone in this study is in the same order of magnitude as those previously described (0.1-2.0 ng/L). One difference can be seen in lower threshold values for the C8 and C9 representatives of 4-mercapto-2-alkanones compared to the the respective 2-mercapto-4-alkanone homologs. Another striking difference was

found for (*S*)-4-mercapto-2-hexanone which showed a very high odor threshold compared to the other mercaptoalkanones.

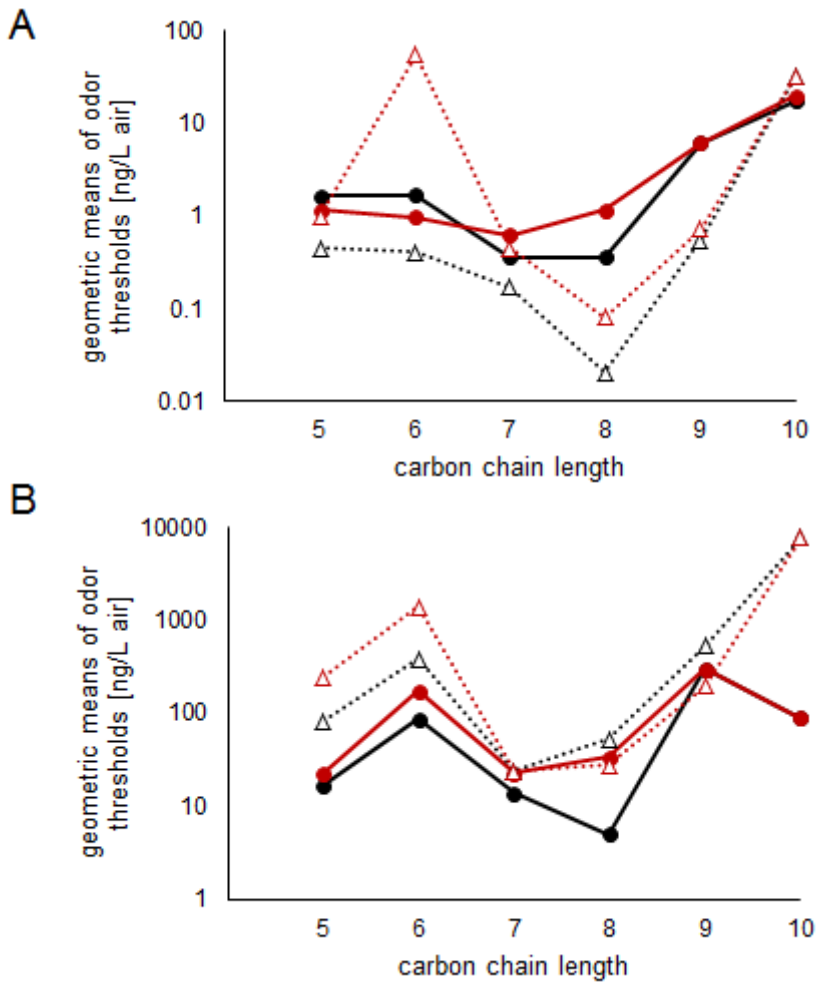

Figure 29. Geometric means of the odor thresholds of (A) 2-mercapto-4-alkanones: (*R*)-enantiomer (●), (*S*)-enantiomer (●) and 4-mercapto-2-alkanones (Wakabayashi *et al.*, 2015): (*R*)-enantiomer (Δ), (*S*)-enantiomer (Δ); (B) 2-acetylthio-4-alkanones: (*R*)-enantiomer (●), (*S*)-enantiomer (●) 4-acetylthio-2-alkanones (Wakabayashi *et al.*, 2015): (*R*)-enantiomer (Δ), (*S*)-enantiomer (Δ).

Table 15. Odor thresholds of the enantiomers of 2-mercapto-4-alkanones and 2-acetylthio-4-alkanones determined by GC/O.

		odor thresholds in air [ng/L]									
		panelist 1		panelist 2[a]		panelist 3		panelist 4[b]		geometric mean ± SD[c]	
no.	compound	(*R*)	(*S*)	(*R*)	(*S*)	(*R*)	(*S*)	(*R*)	(*S*)	(*R*)	(*S*)
11	4-mercapto-2-pentanone	4.4	2.2	1.1	1.1	4.9	4.9	0.3	0.1	1.6 ± 3.8	1.1 ± 4.6
1	2-mercapto-4-hexanone	2.5	0.6	1.0	2.7	2.4	2.4	0.5	0.6	1.3 ± 2.1	1.2 ± 2.3
2	2-mercapto-4-heptanone	1.3	1.3	0.3	0.4	0.3	2.3	0.1	0.1	0.3 ± 2.8	0.6 ± 3.7
3	2-mercapto-4-octanone	0.7	5.3	0.2	0.5	0.3	0.6	0.4	0.9	0.4 ± 1.6	1.1 ± 2.9
4	2-mercapto-4-nonanone	21	10	3.3	5.5	5.2	5.2	3.9	4.9	6.1 ± 2.3	6.1 ± 1.4
5	2-mercapto-4-decanone	39	19	16	86	10	10	14	9.0	17.2 ± 1.8	19.6 ± 2.8
13	4-acetylthio-4-pentanone	19	7.0	15	39	17	44			17 ± 1.1	23 ± 2.8
6	2-acetylthio-4-hexanone	43	43	709	712	22	178			88 ± 6.3	176 ± 4.1
7	2-acetylthio-4-heptanone	37	37	9	18	9.2	18			14 ± 2.3	23 ± 1.5
8	2-acetylthio-4-octanone	5.0	21	11	86	2.7	22			5 ± 2.0	34 ± 2.2
9	2-acetylthio-4-nonanone	149	149	596	1192	298	149			298 ± 2.0	298 ± 3.3
10	2-acetylthio-4-decanone	73	36	143	286	71	71			90 ± 1.5	90 ± 2.9

[a] Mean values calculated from duplicate analysis of mercaptoalkanones with chain lengths C6-C10
[b] Mean values calculated from duplicate analysis of mercaptoalkanones with chain lengths C5-C10
[c] Geometric standard deviation

When comparing the individual odor thresholds of 4-acetylthio-2-pentanone (7-44 ng/L) obtained in this study with those (70-200 ng/L) previously reported by (Wakabayashi *et al.*, 2015), it becomes apparent that they were significantly lower. The same results were found for the odor thresholds of (*R*)-2-acetylthio-4-octanone and the 2-acetylthio-4-decanone enantiomers; they were considerably lower than those of the respective 4-acetylthio-2-alkanone positional isomers. Except for these differences, the curves depending on the chain lengths were similar to those of the positional isomers and revealed comparable minima and maxima. In the homologous series of both positional isomers the pronounced differences in the odor thresholds of the mercaptoalkanones and the corresponding acetylthioalkanones were similarly observed.

4.4.4. Determination of Odor Qualities

Via GC/O, odor qualities of the 2-mercapto-4-alkanone and 2-acetylthio-4-alkanone enantiomers were assessed at one dilution step above the odor threshold (Tables 16 and 17). It is noteworthy that for 2-mercapto-4-alkanones the fruity and sulfury-catty notes observed for the (*R*)- and (*S*)-4-mercapto-2-alkanone enantiomers, respectively, were not percieved. The odor qualities exhibited changes from pungent, plastic (C6/C7) and roasty (C8) to earthy and mushroom (C9 and C10) depending on the chain length (Table 16). The (*R*)- and (*S*)-enantiomers showed no consistently detectable differences.

Rowe (2002) proposed structural requirements for a so-called “tropical olfactophore”, i.e., a 1,3-oxygen-sulfur functionality with specified arrangements of the substituents. This model has been extended by Robert *et al.* (2004) by including the respective acetyl compounds (Figure 30A). These requirements are not fulfilled by the 2-mercapto-4-alkanones and 2-acetylthio-4-alkanones (chain lengths C6-C10). They have alkyl groups (from ethyl to hexyl) as the substituent R_4 instead of a hydrogen, a methyl group, a ring system, or an ether moiety; this structural deviation may be the reason for the absence of tropical, fruity notes. For the investigated *β*-mercapto-alkanones, only the C5 homolog 4-mercapto-2-pentanone **11** fulfills the structural requirements proposed for the “tropical olfactophore” (Rowe, 2002). This is in accordance with the odor quality “fruity” mentioned by two of the panelists (Table 16).

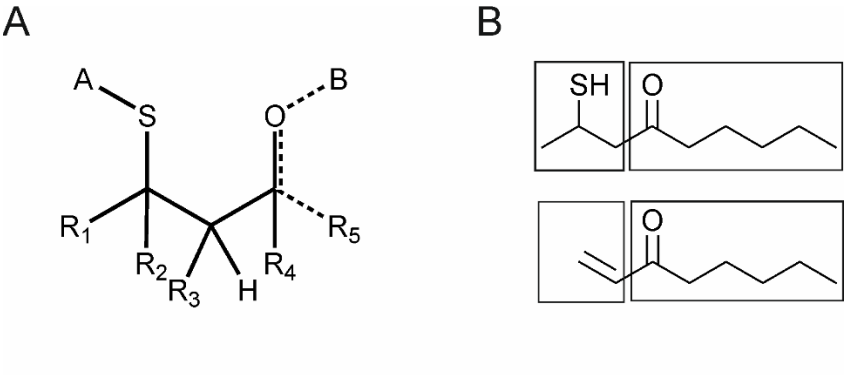

Figure 30. (A) Structural requirements for a 'tropical olfactophore' as proposed by Rowe (2002) and extended by Robert *et al.* (2004) (A: H, SCH_3, ring; B: H, CH_3, acyl, absent if carbonyl; R_1/R_2: H, alkyl; R_3: H, alkyl, ring; R_4: H, CH_3, ring, OR; R_5: H, absent if carbonyl; (B) Structures of 2-mercapto-4-nonanone **4** and 1-octen-3-one.

For both homologous series, the C9 and C10 compounds showed pronounced earthy and mushroom odor notes. An explanation for this odor quality may be the structural similarity between 2-mercapto-4-nonanone **4** and the known mushroom odorant 1-octen-3-one that is presented in Figure 30B. The alkyl chains (corresponding to the substituent R_4 in Figure 30A) have the same lengths; the function of the terminal double bond in 1-octen-3-one seems to be taken over by the *β*-mercapto group in 2-mercapto-4-nonanone **4**. The similarity between the odor qualities described for the respective homologous series of 1-alken-3-ones (Lorber *et al.*, 2014) and the odor qualities assessed for the other 2-mercapto-4-alkanones **1**-**3** and **5**, strongly supports this assumption. However, the odor thresholds of the 1-alken-3-one homologs (Lorber *et al.*, 2014) show considerably lower values than those assessed for the 2-mercapto-4-alkanones in this study. In the literature, the following odor descriptions are reported for 1-alken-3-ones: (i) pungent and plastic for 1-penten-3-one and 1-hexen-3-one (Buettner and Schieberle, 1999; Lorber *et al.*, 2014; Song and Cadwallader, 2008; Song *et al.*, 2008), (ii) vegetable-like for 1-hepten-3-one (Lorber *et al.*, 2014), and (iii) mushroom for 1-nonen-3-one (Buettner and Schieberle, 1999; Cullere *et al.*, 2013; Lorber *et al.*, 2014; Roberts and Acree, 1996; Schnermann and Schieberle, 1997; Song and Cadwallader, 2008; Song *et al.*, 2008). When comparing these descriptions with the odor qualities of the corresponding 2-mercapto-4-alkanones with one C-atom more perceived in this study, nearly perfect matches can be found. This phenomenon might also be applicable to the corresponding alcohols (data not shown) as was indicated by preliminary sensory assessments of homologous series of 2-mercapto-4-

alkanols. This is in line with the known importance of (*R*)-1-octen-3-ol as key mushroom aroma compound (Mosandl *et al.*, 1986; Zawirska-Wojtasiak, 2004). It also correlates with the mushroom-like odors described for 1-mercapto-3-octanol and 1-mercapto-3-nonanol (Polster and Schieberle, 2017).
The 2-acetylthio-4-alkanones exhibited mainly vegetable notes for the (*R*)-enantiomers (C6-C8). Earthy and mushroom odor notes were also perceived for 2-acetylthio-4-nonanone and 2-acetylthio-4-decanone. This indicates that for the acetyl-compounds the phenomenon is also applicable.

Sensory studies of 2-mercapto-4-heptanone **2** have been performed by (Naef *et al.*, 2008). The respective NaCl and sugar solutions have been tasted and flavor qualities have been reported as grapefruit, sesame, earthy, and rocket. In the course of the GC/O evaluation in the present study, the odor of this homolog was mainly associated with vegetables, onion, and pungent. However, it is noteable that one panelist described the odor of both enantiomers as bell pepper. In a previous study of (Nörenberg *et al.*, 2017a), (*S*)-2-mercapto-4-heptanone has been detected as the predominating enantiomer in cooked bell pepper. The assessement of its actual contribution to the aroma of bell pepper would require the determination of the odor threshold in water or bell pepper-type matrices and the calculation of the odor activity value.

Table 16. Odor descriptions of the enantiomers of 2-mercapto-4-alkanones determined by GC/O.

	odor descriptions[a]							
	(*R*)-enantiomer				(*S*)-enantiomer			
no.	panelist 1	panelist 2	panelist 3	panelist 4	panelist 1	panelist 2	panelist 3	panelist 4
11	urine, sweat	potatoes, earthy	tallow, cheese, sulfury	vegetables, onion	potatoes, **leek**, broth	**fruity**, **leek**, sweat	**fruity**, raspberry	sweet, onion, vegetables
1	**urine**, musk, sweet	**urine**, sweat	**pungent**, sulfury	**pungent**, garlic, onion, savory	citrus	**sweat**	**sweat**, dull	**sweat**, mustard, pungent
2	sweet, rotten	**vegetables**, cabbage	**vegetables**, **pungent**, plastic	**vegetables**, **pungent**, onion, bell pepper	**sweat**, sweet	**pungent**, **onion**	**vegetables**, plastic	**onion**, **vegetables**, **sweat**, **pungent**, bell pepper
3	**urine**, **sweet**, sweat	**urine**, cooked onion	roasty, earthy	cheese, **sweet**, vegetable broth,	sweet, rotten	**roasty**, meat	**roasty**, earthy	vegetable broth, onion, sweat
4	**mushroom**, urine, sweet	vegetables, **earthy**, celery	**mushroom**, **earthy**	**mushroom**, onion, musty	**vegetable broth**, **herbs**, sweet	**vegetables**, **mushroom**, leek	**vegetables**, plastic	**mushroom**, musty, **vegetables**, earthy
5	**earthy**, **mushroom**, **musty**, urine	**vegetables**, **dull**, onion	**mushroom**, **earthy**, **musty**, **dull**	**mushroom**, **vegetables**, **musty**	**mushroom**, **dull**, **herbs**, sweet	**vegetables**, **dull**	**mushroom**, **vegetables**, celery	**mushroom**, **vegetables**, earthy, musty,

[a] Determined at one dilution step above the odor threshold; descriptions given by at least two panelists are printed in bold

Table 17. Odor descriptions of the enantiomers of 2-acetylthio-4-alkanones determined by GC/O.

	odor descriptions[a]					
	(*R*)-enantiomer			(*S*)-enantiomer		
no.	panelist 1	panelist 2	panelist 3	panelist 1	panelist 2	panelist 3
13	**sweat**, **urine**, burnt	**sweat**, **urine**	**sweat**, tallow	potatoes, **leek**, sweat	**leek**, cabbage, dull	tallow, sulfury
6	**vegetables**, sweat, sweet	**vegetables**, sulfury	**fennel**, dull	sweat, rotten	plastic, burnt	earthy, dull, mushroom
7	**herbs**, savory, sweat, earthy	**vegetables**, leek	sulfury	sweat, sour-sweet, herbs	roasty	earthy, sulfury
8	earthy, mushroom	vegetables, onion, pungent	burnt, rubber	**rubber**, rotten	meat, dull	**rubber**
9	**earthy**, urine, sweet	**earthy**, cabbage vegetables,	mushroom	sweat, sweet, herbs	**earthy**	**earthy**, rotten, mushroom
10	earthy, sweat, slightly pungent	**mushroom**, rubber	**mushroom**, rancid	**mushroom**, acidic, pungent	**mushroom**, earthy	**mushroom**, greasy/fatty

[a] Determined at one dilution step above the odor threshold; descriptions given by at least two panelists are printed in bold

In conclusion, the sensory assessments revealed no significant changes in the odor thresholds assessed via GC/O upon the exchange of the positions of the functional groups (SH and carbonyl) in *β*-mercaptoalkanones. This is contrary to the data described for the homologous series of 3-mercapto-2-methylalkanols and 1-mercapto-2-methyl-3-alkanols (Polster and Schieberle, 2017). However, the odor qualities were considerably influenced by the positions of the functional groups.

4.5. Sensory Evaluation of Racemic 2-Mercapto-4-alkanones and 2-Acetylthio-4-alkanones

In analogy to the sensory assessments performed for the enantiomers, odor thresholds and odor qualities were also determined for racemic 2-mercapto- and 2-acetylthio-4-alkanones by using GC/O and the method described by UIlrich and Grosch (1987).

4.5.1. Determination of Odor Thresholds and Qualities of Racemic 2-Mercapto-4-alkanones

Four panelists assessed the threshold values and odor qualities of racemic 2-mercapto-4-alkanones. Threshold values were determined in duplicate by panelists 2 and 4; mean values were calculated. In Table 18, the odor thresholds determined by all panelists as well as the geometric means are presented.

Table 18. Odor thresholds of 2-mercapto-4-alkanones determined by GC/O.

	odor thresholds in air [ng/L]				
no.	panelist 1	panelist 2	panelist 3	panelist 4	geometric mean ± SD[a]
11	1.1	1.2	4.5	0.3	1.2 ± 2.0
1	4.3	8.2	8.0	4.3	5.9 ± 1.4
2	0.3	1.1	2.2	0.1	0.5 ± 4.0
3	0.3	0.6	1.1	0.1	0.3 ± 2.8
4	3.4	7.6	4.3	2.1	3.9 ± 1.7
5	8.7	28	24	4.4	12 ± 2.4

[a] geometric standard deviation

Regarding the variability, panelist 4 showed a high sensitivity for **11**, **2**, and **3**; e.g. factor 15 (**11**), factor 22 (**2**), and factor 11 (**3**) compared to panelist 3 as well as factor 7 (**2**) between panelists 1 and 3. For **5** a factor of 6 was revealed between panelists 2 and 4 as well as panelists 3 and 4. For the other compounds and panelists the individual odor thresholds either were the same or differed only by factors between 2 and approximately 4. This corresponds to one or two dilution steps in the course of the AEDA and thus indicates the reproducibility of the sensory assessments.

The evaluations of racemic 2-mercapto-4-alkanones revealed the lowest odor threshold for **3** (C8) in the range of 0.1 and 1.1 ng/L in air for all panelists. Additionally,

panelists 1 and 4 showed the lowest threshold for **2** (C7). The highest threshold was observed for **5** (C10).

In Figure 31, geometric mean values (solid line) are presented. They revealed a minimum of the odor thresholds for 2-mercapto-4-octanone **3**.

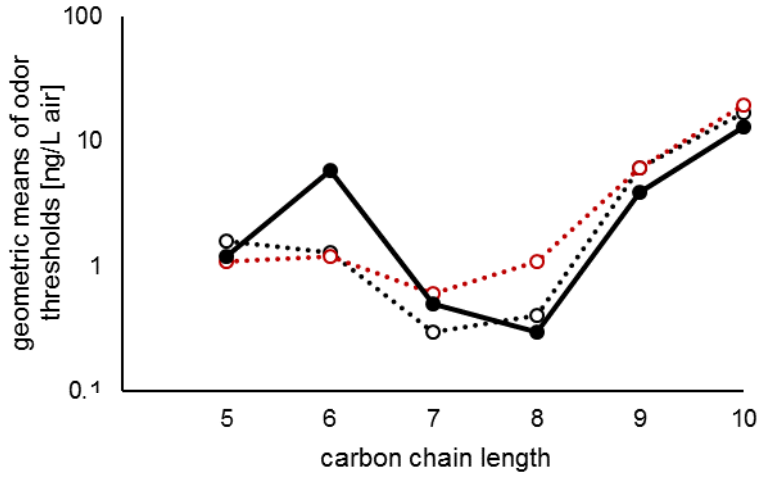

Figure 31: Geometric means of the odor thresholds of racemic 2-mercapto-4-alkanones (●), (*R*)-2-mercapto-4-alkanones (○), and (*S*)-2-mercapto-4-alkanones (○).

A comparison of the data with the odor thresholds determined for the enantiomers (Figure 31, dotted lines) shows that the curve for the racemic mercaptoalkanones is comparable to the one of the (*R*)-mercaptoalkanones. The differences of the threshold values were only marginal. The most striking difference appeared in a higher threshold value (factor 4.5) for *rac*-**1** (5.9 ng/L in air) compared to (*R*)-**1** (1.3 ng/L in air). The odor thresholds of the (*S*)-enantiomers were also comparable to those of the racemic 2-mercapto-4-alkanones, except for **1** and **3**. The threshold of *rac*-**1** (5.9 ng/L in air) was by a factor of 4.9 higher than that of (*S*)-**1** (1.2 ng/L in air), and the threshold of *rac*-**3** (0.3 ng/L in air) was lower (factor 3.7) than that of (*S*)-**3** (1.1 ng/L in air).

In Table 19, the odor qualities determined for racemic 2-mercapto-4-alkanones (C5-C10) are presented. Common odors were sweat, potatoes, and sulfury for **11**, vegetables/herbs, plastic, and pungent (**2**), sulfury (**3**), and mushroom for **4** and **5**. Every panelist described the odor quality of **1** differently. Comparing the data of **11** and **1** with previously reported odor descriptions (Vermeulen *et al.*, 2001), the smell of potatoes was also found for **11**, but greenery and black currant could not be perceived. Vermeulen *et al.* (2001) described the smell of **1** as box tree, fresh, and empyreumatic. None of these descriptions were actually given by the panelists in this study;

descriptions like roasty/herbs/bitter (panelist 3) and vegetable broth (panelist 4) may be considered to be slightly related to empyreumatic.

Table 19. Odor descriptions of racemic 2-mercapto-4-alkanones determined by GC/O.

	odor descriptions[a]			
no.	panelist 1	panelist 2	panelist 3	panelist 4
11	**potatoes**, **vegetable broth**, leek, garlic	**sweat**, fruity, **sulfury**	tallow, **sweat**, **sulfury**, meat	onion, **potatoes**, **vegetables**, pungent, **sweat**
1	sour, rotten, meat	sulfury	herbs, roasty, bitter, dull	vegetable broth, bell pepper, sweat
2	sweat, **pungent**	sulfury, savory, **herbs**	**vegetables**, **plastic**, **pungent**	**vegetable broth**, **plastic**, potatoes, onion, bell pepper
3	sweet, rubber, rotten, plastic	**sulfury**, dull, heavy, fatty	earthy, **sulfury**	vegetable broth, bell pepper, onion, potatoes, sweat, pungent
4	fruity, rotten, plastic	sulfury	**mushroom**, earthy	**mushroom**, vegetables, pungent, potatoes
5	burnt plastic, rotten, fruity	sulfury	**mushroom**, rubber, plastic	**mushroom**, earthy, vegetables

[a] Determined at one dilution step above the odor threshold; descriptions given by at least two panelists are printed in bold

Odor qualities reported for the enantiomers (cf. 4.4.3., Table 16) were similar to the common racemic descriptions of **2** (vegetables, pungent), **4** (mushroom), and **5** (mushroom). Odor qualities for *rac*-**11**, *rac*-**1**, and *rac*-**3** were different compared to the descriptions of the enantiomers. Considering the odors reported by the four panelists, it is noticeable that panelist 2 showed no common odor impressions between the racemic and enantiomeric compounds, except for **11** (sweat, fruity). Panelist 1 gave similar odor descriptions for **11** (potatoes, leek, broth), **2** (sweat), and **3** (sweet, rotten). In contrast, previously described odor properties of the enantiomers could be confirmed by the odors of racemic 2-mercapto-4-alkanones by panelists 3 and 4.

Racemic 2-mercapto-4-nonanone **4** and 2-mercapto-4-decanone **5** also revealed odors reminiscent of mushroom, as was the case for the respective enantiomers.

Therefore, the phenomenon described in 4.4.3. is also valid for the racemic 2-mercapto-4-alkanones. In contrast to the enantiomers, the odor descriptions for racemic 2-mercapto-4-alkanones with shorter chain lengths (C6-C8) were not comparable to those of the homologous series of 1-alken-3-ones. Only **2** (C7) revealed the same odor qualities as 1-hexen-3-one, i.e. plastic and pungent (Song and Cadwallader, 2008; Song *et al.*, 2008) as well as vegetables (Peterson and Reineccius, 2003) and herbaceous (Pino, 2014).

4.5.2. Determination of Odor Thresholds of Racemic 2-Acetylthio-4-alkanones

Two panelists assessed the odor thresholds and the odor qualities of racemic 2-acetylthio-4-alkanones. Threshold values were determined in duplicate by panelist 2; mean values were calculated (Table 20).

Table 20. Odor thresholds of 2-acetylthio-4-alkanones determined by GC/O.

	odor thresholds in air [ng/L]		
no.	panelist 2	panelist 3	geometric mean ± SD[a]
12	20	20	20 ± 0
6	101	82	91 ± 1.2
7	19	36	26 ± 1.6
8	5.9	11	8.1 ± 1.6
9	83	155	113 ± 1.6
10	80	77	78 ± 1.0

[a] geometric standard deviation

Regarding the variability, both panelists showed quite similar threshold values; for **7**, **8**, and **9** they differed by a factor of approximately 2. This corresponds to one dilution step in the course of the AEDA and thus indicates the reproducibility of the sensory assessments.

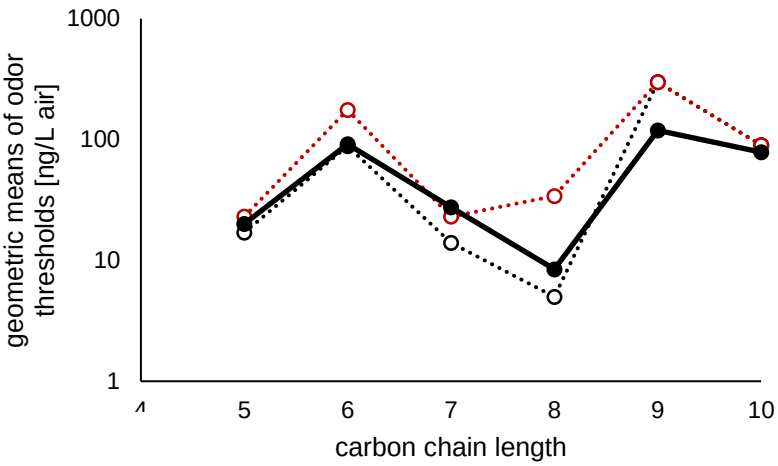

Figure 32. Geometric means of the odor thresholds of racemic 2-acetylthio-4-alkanones (●), (*R*)-2-acetylthio-4-alkanones (○), and (*S*)-2-acetylthio-4-alkanones (○).

In Figure 32 (solid line), geometric mean values calculated for both panelists are presented graphically. The data showed the lowest odor threshold for **8** (C8). Comparing the curves of the enantiomers (Figure 32, dotted lines) with the one of the racemic 2-acetylthio-4-alkanones, again, the curve of the racemic compounds is similar to the one of the (*R*)-enantiomers. Differences were found for 2-acetylthio-4-alkanones with chain lengths C7 and C9; the odor threshold is slightly lower (factor 2.9) for (*R*)-**7** (9.1 ng/L in air) than for *rac*-**7** (26 ng/L in air) and higher (factor 3.7) for (*R*)-**9** (421 ng/L in air) than for *rac*-**9** (113 ng/L in air). The (*S*)-enantiomers showed more differences compared to the racemic 2-acetylthio-4-alkanones, e.g. the lowest odor threshold was found for the chain length C7, and compounds (*S*)-**6**, (*S*)-**8**, and (*S*)-**9** exhibited higher threshold values with factors 3.9, 5.3, and 3.7, respectively, compared to the racemic homologs.

The odor qualities reported by the two panelists for 2-acetylthio-4-alkanones are shown in Table 21. The odor descriptions of both panelists were different for the homologous acetylthioalkanones (C5-C10), except for 2-acetylthio-4-heptanone **7**, described as vegetables-like. The investigation of the racemic 2-acetylthio-4-alkanones could not confirm the odor properties described for the enantiomers (cf. 4.4.3., Table 17). Panelist 3 used the same descriptions only for *rac*-**12** and (*R*)- and (*S*)-**12** (sweat and tallow) and panelist 2 described *rac*-**7** and (*R*)-**7** as vegetables and leek.

For chain lengths C9 (**9**) and C10 (**10**), the mushroom odor described for both enantiomers (cf. 4.4.3.) was not perceived for the racemic compounds by the two panelists.

Table 21. Odor descriptions of racemic 2-acetylthio-4-alkanones determined by GC/O.

	odor descriptions[a]	
no.	panelist 2	panelist 3
12	gasoline, sulfury	tallow, sweat, cheese
6	urine	herbs, savory, vegetables
7	**vegetables**, leek, herbs	**vegetables**, mushroom, earthy
8	citrus peel, fruity	sulfury
9	sulfury	rubber, burnt
10	pungent, sulfury	rubber

[a] Determined at one dilution step above the odor threshold; descriptions given by both panelists are printed in bold

The comparison of the odor properties determined for enantiomeric and racemic 2-mercapto-4-alkanones and 2-acetylthio-4-alkanones confirm that it is important to consider the stereochemistry when establishing olfactophore models.

5. SUMMARY

Absolute configurations of *β*-mercaptoalkanone enantiomers were determined, and analytical as well as sensory characterizations of homologous series of 2-mercapto-4-alkanones and the corresponding 2-acetylthio-4-alkanones were performed.

4-Mercapto-2-pentanone, 4-mercapto-2-heptanone, and the positional isomer 2-mercapto-4-heptanone were synthesized, and the enantiomers were separated via capillary gas chromatography using chiral stationary phases. Enantiomers were obtained by lipase-catalyzed kinetic resolutions of the respective acetylthioalkanones. An enzyme screening with commercially available enzyme preparations and esterases revealed lipase B from *Candida antarctica* as the appropriate biocatalyst to obtain both 2-mercapto-4-heptanone enantiomers, and lipases from *Aspergillus niger* and porcine pancreas, respectively, as suitable to obtain the enantiomers of 4-mercapto-2-heptanone. On the basis of the HPLC-elution order of the diastereoisomeric thioesters and on the assumption that the sector rule previously developed for secondary alcohols can be applied to thiols, the configurations of the reaction products were deduced after derivatizing the racemic *β*-mercaptoalkanones with (*S*)-M*α*NP. Additionally, the configurations were assigned by ^{1}H-NMR analyses after esterification with (*R*)-hydratropic acid (HTA) and 2-methoxy-2-phenylacetic acid (MPA). The assignments of the configurations were in agreement. However, they were opposite to those determined for the (*S*)-M*α*NP thioesters via the sector rule. This can be explained by the preferred *anti*-periplanar conformation of the methoxy group and the carbonyl oxygen which has been described for MPA thioesters. In contrast, the most stable and preferred conformation for MPA and M*α*NP esters is *syn*-periplanar, resulting in different anisotropy effects between the side chains and the naphthalene/aryl moiety. In consequence of the opposing configurations, the formerly assigned configurations of *β*-mercaptoalkanones determined via ^{1}H-NMR analyses of (*S*)-M*α*NP-derivatives have to be revised.

The knowledge gained for the determination of the absolute configuration of 2-mercapto-4-heptanone as well as the applied methods were used for the investigation of the homologous series of 2-mercapto-4-alkanones (chain lengths C6 and C8-C10). Lipase B of *Candida antarctica* (CAL-B) was shown to be suitable to obtain the enantiomers of 2-mercapto-4-alkanones via enzyme-catalyzed kinetic resolution of the

respective 2-acetylthio-4-alkanones. The hydrolysis products could be obtained within 0.5 h (C6-C8) and 1 h (C9 and C10) with ee values between 90.9 and 95.5% whereas the opposite enantiomers (resulting from the remaining substrates) could be obtained after 2 h (C6 and C8), 4 h (C7), and 6 h (C9 and C10) exhibiting ee values between 93.5 and 100%.

The configurations of the enantiomers were assigned via ^{1}H-NMR anisotropy-based methods using HTA, MPA, and (*S*)-M*α*NP as chiral auxiliaries. The order of elution of the enantiomers is (*S*) before (*R*) for 2-mercapto- and 2-acetylthio-4-alkanones (C6-C10) using diethyl *tert*-butylsilyl-*β*-cyclodextrin as chiral stationary phase.

Finally, the sensory properties of enantiomeric and racemic 2-mercapto- and 2-acetylthio-4-alkanones were examined. The determinations of the odor thresholds and the odor qualities of the enantiomers have been performed by capillary gas chromatography/olfactometry by applying chiral stationary phases. Minima of the odor thresholds have been obtained for the chain lengths C7/C8. The enantiomers of the homologs showed similar odor thresholds, except for chain length C8. The investigated odor properties were comparable to those known for the corresponding 1-alken-3-ones with one less C-atom and ranged from pungent (C5) to mushroom (C9/10). The studied 2-mercapto-4-alkanones do not fulfill the requirements of a “tropical olfactophore” in contrast to their positional isomers of the homologous series of 4-mercapto-2-alkanones.

Odor thresholds and odor qualities were also determined for racemic 2-mercapto-4-alkanones and 2-acetylthio-4-alkanones (C6-C10) by capillary gas chromatography/olfactometry. As for their enantiomeric homologs, there were minima of the odor thresholds of 2-mercapto-4-alkanones and 2-acetylthio-4-alkanones for the chain lengths C7/C8 and C8, respectively. Except for 2-mercapto-4-hexanone and 2-mercapto-4-octanone, the odor qualities of racemic 2-mercapto-4-alkanones were comparable to those of the enantiomers, including the mushroom note perceived for the chain lengths C9 and C10.

6. ZUSAMMENFASSUNG

Die absoluten Konfigurationen der Enantiomere von *β*-Mercaptoalkanonen wurden bestimmt. Homologe Reihen von 2-Mercapto-4-alkanonen und den entsprechenden 2-Acetylthio-4-alkanonen wurden analytisch sowie hinsichtlich ihrer sensorischen Eigenschaften charakterisiert.

4-Mercapto-2-pentanon und 4-Mercapto-2-heptanon sowie das Positionsisomer 2-Mercapto-4-heptanon wurden synthetisiert und die Enantiomere kapillargas-chromatographisch unter Einsatz chiraler stationärer Phasen getrennt. Die Enantiomere wurden mittels enzymkatalysierter kinetischer Racematspaltungen der entsprechenden Acetylthioalkanone gewonnen. Ein Enzymscreening mit handelsüblichen Lipasen und Esterasen zeigte, dass *Candida antarctica* Lipase B für die Gewinnung beider Enantiomere von 2-Mercapto-4-heptanon geeignet ist und *Aspergillus niger* Lipase bzw. Schweinepankreas-Lipase für die Gewinnung der Enantiomere von 4-Mercapto-2-heptanon. Nach Derivatisierung der racemischen *β*-Mercaptoalkanone mit (*S*)-M*α*NP wurden die Konfigurationen der Reaktionsprodukte der diastereomeren Thioester auf Basis der HPLC-Elutionsreihenfolge bestimmt. Hierfür wurde vorausgesetzt, dass die für sekundäre Alkohole entwickelte Sektorregel auch für Thiole Gültigkeit besitzt. Zusätzlich wurden die Konfigurationen mit Hilfe von ^{1}H-NMR Spektroskopie, nach Veresterung mit (*R*)-Hydratropasäure (HTA) und 2-Methoxy-2-phenylessigsäure (MPA) bestimmt. Die Konfigurationsbestimmungen mittels NMR Spektroskopie der HTA- und MPA-Thioester stimmten überein, führten jedoch zu den entgegengesetzten Konfigurationen verglichen mit denen, via (*S*)-M*α*NP-Thioester und unter Anwendung der Sektorregel ermittelt. Der Grund hierfür liegt in der für MPA-Thioester beschriebenen bevorzugten *anti*-periplanaren Anordnung der Methoxygruppe und des Carbonyl-Sauerstoffs. Im Gegensatz dazu ist die stabilste und bevorzugte Konformation der MPA- und M*α*NP-Ester *syn*-periplanar. Dies führt zu verschiedenen Anisotropieeffekten zwischen der Seitenkette und dem Naphthalin-/ Arylrest. Demzufolge müssen die mittels (*S*)-M*α*NP-Derivaten ermittelten Konfigurationen der *β*-Mercaptoalkanone revidiert werden.

Die gewonnenen Erkenntnisse zur absoluten Konfigurationsbestimmung von 2-Mercapto-4-heptanon sowie die angewendeten Methoden wurden für die Untersuchung der homologen Reihe von 2-Mercapto-4-alkanonen (Kettenlängen C6

und C8-C10) verwendet. Lipase B von *Candida antarctica* (CAL-B) war für die enzymkatalysierte Trennung der 2-Acetylthio-4-alkanone geeignet. Die Hydrolyseprodukte konnten innerhalb von 0.5 h (C6-C8) und 1 h (C9 und C10) mit Enantiomerenüberschüssen (ee) zwischen 90.9 und 95.5% gewonnen werden, wohingegen die entgegengesetzten Enantiomere (gewonnen aus dem verbliebenen Substrat) nach 2 h (C6 und C8), 4 h (C7) und 6 h (C9 und C10) mit ee Werten zwischen 93.5 und 100% erhalten wurden.

Die absoluten Konfigurationen der Enantiomere wurden mit Hilfe der ^{1}H-NMR Spektroskopie-basierten Anisotropie-Methode unter Verwendung von HTA, MPA und (*S*)-M*α*NP als chirale Reagenzien zugeordnet. Für die Enantiomere der 2-Mercapto-4-alkanone sowie 2-Acetylthio-4-alkanone (C6-C10) ist somit die Elutionsreihenfolge auf der getesteten chiralen Diethyl-*tert*-butylsilyl-*β*-Cyclodextrinphase (*S*) vor (*R*).

Schließlich wurden die sensorischen Eigenschaften sowohl der Enantiomere als auch der racemischen 2-Mercapto-4-alkanone und 2-Acetylthio-4-alkanone untersucht. Geruchsschwellenwerte sowie Geruchsqualitäten der Enantiomere wurden mit Kapillargaschromatographie/Olfaktometrie unter Verwendung chiraler Phasen bestimmt. Minima der Geruchsschwellenwerte wurden für die Kettenlängen C7/C8 gefunden. Die Geruchsschwellenwerte der Enantiomere der Homologen waren ähnlich, mit Ausnahme der Kettenlänge C8. Die untersuchten Geruchsqualitäten waren mit denen der 1-Alken-3-one, mit einem C-Atom weniger, vergleichbar und reichten von stechend (C5) bis Pilz (C9/10). Die untersuchten 2-Mercapto-4-alkanone erfüllen nicht die Anforderungen für ein „tropisches Olfactophor“, im Gegensatz zu ihren Positionsisomeren der homologen Reihe der 4-Mercapto-2-alkanone. Geruchsschwellenwerte und Geruchsqualitäten wurden ebenfalls für die racemischen 2-Mercapto-4-alkanone und 2-Acetylthio-4-alkanone (C6-C10) mittels Kapillargaschromatographie/Olfaktometrie bestimmt. Wie für die enantiomeren Homologen fanden sich Minima bei C7/C8 für die 2-Mercapto-4-alkanone und bei C8 für die 2-Acetylthio-4-alkanone. Mit Ausnahme von 2-Mercapto-4-hexanon und 2-Mercapto-4-octanon waren die Geruchsqualitäten der racemischen und enantiomeren 2-Mercapto-4-alkanone, einschließlich der für die Kettenlängen C9 und C10 wahrgenommenen Pilznoten, vergleichbar.

7. REFERENCES

Acree, T. E.; Barnard, J.; Cunningham, D. G. A procedure for the sensory analysis of gas chromatographic effluents. *Food Chem.* **1984**, *14*, 273-86.

Amoore, J. E. Stereochemical theory of olfaction. *Nature* **1963**, *198*, 271-2.

Anderson, E. M.; Larsson, K. M.; Kirk, O. One biocatalyst - many applications: the use of *Candida antarctica* B-lipase in organic synthesis. *Biocatal. Biotransform.* **1998**, *16*, 181-204.

Armstrong, D. W.; Chang, C. D.; Li, W. Y. Relevance of Enantiomeric Separations in Food and Beverage Analyses. *J. Agric. Food Chem.* **1990**, *38*, 1674-1677.

Badenhorst, C. P. S.; Bornscheuer, U. T. Getting Momentum: From Biocatalysis to Advanced Synthetic Biology. *Trends Biochem. Sci.* **2018**, *43*, 180-198.

Belitz, H.-D.; Grosch, W.; Schieberle, P. Aromastoffe. In *Lehrbuch der Lebensmittelchemie*, Belitz, H.-D.; Grosch, W.; Schieberle, P., Eds. Springer Verlag: Berlin, **2009**, pp 346-411.

Bentley, R. The nose as a stereochemist. Enantiomers and odor. *Chem. Rev.* **2006**, *106*, 4099-4112.

Berg, J. M.; Stryer, L.; Tymoczko, J. L. *Stryer Biochemie*. 7 ed.; Springer Spektrum Berlin Heidelberg, **2013**.

Bicchi, C.; Cagliero, C.; Rubiolo, P. New trends in the analysis of the volatile fraction of matrices of vegetable origin: a short overview. A review. *Flavour Fragrance J.* **2011**, *26*, 321-325.

Bicchi, C.; D'Amato, A.; Rubiolo, P. Cyclodextrin derivatives as chiral selectors for direct gas chromatographic separation of enantiomers in the essential oil, aroma and flavour fields. *J. Chromatogr. A* **1999**, *843*, 99-121.

Bicchi, C.; Manzin, V.; D'Amato, A.; Rubiolo, P. Cyclodextrin derivatives in GC separation of enantiomers of essential oil, aroma and flavor compounds. *Flavour Fragrance J.* **1995**, *10*, 127-37.

Blank, I. Gas chromatography-olfactometry in food aroma analysis. *Food Sci. Technol.* **1997**, *79*, 293-329.

Blank, I. Sensory relevance of volatile organic sulfur compounds in food. In *Heteroatomic aroma compounds* Reineccius, G. A.; Reineccius, T. A., Eds. ACS Symposium Series 826, American Chemical Society: Washington, DC, **2002**, pp 25-53.

Block, E. The organosulfur chemistry of the genus Allium and its importance to the organic chemistry of sulfur. *Angew. Chem.* **1992**, *104*, 1158-203 (See also Angew. Chem., Int. Ed. Engl., 1992, 31(9), 1135-78).

Boelens, M. H.; van Gemert, L. J. Sensory properties of optical isomers. *Perfum. Flavor.* **1993a**, *18*, 1, 3-6, 8-10, 12-14, 16.

Boelens, M. H.; van Gemert, L. J. Volatile character-impact sulfur compounds and their sensory properties. *Perfumer & Flavorist* **1993b**, *18*, 29-39.

Bommarius, A. S. Biocatalysis: A Status Report. *Annu. Rev. Chem. Biomol. Eng.* **2015**, *6*, 319-345.

Bornscheuer, U. Protein Engineering in Biocatalysis. *BIOspektrum* **2015**, *21*, 112-113.

Bornscheuer, U. T.; Huisman, G. W.; Kazlauskas, R. J.; Lutz, S.; Moore, J. C.; Robins, K. Engineering the third wave of biocatalysis. *Nature* **2012**, *485*, 185-194.

Bornscheuer, U. T.; Kazlauskas, R. J. Reaction specificity of enzymes: Catalytic promiscuity in biocatalysis: Using old enzymes to form new bonds and follow new pathways. *Angew. Chem., Int. Ed.* **2004**, *43*, 6032-6040.

Bornscheuer, U. T.; Kazlauskas, R. J. *Hydrolases in organic synthesis - regio- and stereoselective biotransformations*. 2 ed.; Wiley-VCH Verlag: Weinheim, **2006**.

Brand, G. Olfactory/trigeminal interactions in nasal chemoreception. *Neurosci Biobehav Rev* **2006**, *30*, 908-17.

Brattoli, M.; Cisternino, E.; Dambruoso, P. R.; de Gennaro, G.; Giungato, P.; Mazzone, A.; Palmisani, J.; Tutino, M. Gas chromatography analysis with olfactometric detection (GC-O) as a useful methodology for chemical characterization of odorous compounds. *Sensors* **2013**, *13*, 16759-16800.

Brenna, E.; Fuganti, C.; Serra, S. Enantioselective perception of chiral odorants. *Tetrahedron: Asymmetry* **2003**, *14*, 1-42.

Brookes, J. C.; Horsfield, A. P.; Stoneham, A. M. Odour character differences for enantiomers correlate with molecular flexibility. *J R Soc Interface* **2009**, *6*, 75-86.

Buchholz, K. B.; Poulsen, P. B. Introduction. In *Applied Biocatalysis* Straathof, A. J. J.; Adlercreutz, P., Eds. Harwood Academic Publishers: **2000**, pp 1-17.

Buettner, A.; Schieberle, P. Characterization of the Most Odor-Active Volatiles in Fresh, Hand-Squeezed Juice of Grapefruit (*Citrus paradisi* Macfayden). *J. Agric. Food Chem.* **1999**, *47*, 5189-5193.

Calcaterra, A.; D'Acquarica, I. The market of chiral drugs: Chiral switches versus de novo enantiomerically pure compounds. *J. Pharm. Biomed. Anal.* **2018**, *147*, 323-340.

Cassimjee, K. E.; Hendil-Forssell, P.; Volkov, A.; Krog, A.; Malmo, J.; Aune, T. E. V.; Knecht, W.; Miskelly, I. R.; Moody, T. S.; Svedendahl Humble, M. Streamlined Preparation of Immobilized *Candida antarctica* Lipase B. *ACS Omega* **2017**, *2*, 8674-8677.

Chen, C. S.; Fujimoto, Y.; Girdaukas, G.; Sih, C. J. Quantitative analyses of biochemical kinetic resolutions of enantiomers. *Journal of the American Chemical Society* **1982**, *104*, 7294-7299.

Cooper, A. J. L. Mechanisms of cysteine S-conjugate β-lyases. *Adv. Enzymol. Relat. Areas Mol. Biol.* **1998**, *72*, 199-238.

Cullere, L.; Fernandez de Simon, B.; Cadahia, E.; Ferreira, V.; Hernandez-Orte, P.; Cacho, J. Characterization by gas chromatography-olfactometry of the most odor-active compounds in extracts prepared from acacia, chestnut, cherry, ash and oak woods. *LWT-Food Sci. Technol.* **2013**, *53*, 240-248.

Cygler, M.; Grochulski, P.; Kazlauskas, R. J.; Schrag, J. D.; Bouthillier, F.; Rubin, B.; Serreqi, A. N.; Gupta, A. K. A Structural Basis for the Chiral Preferences of Lipases. *J. Am. Chem. Soc.* **1994**, *116*, 3180-6.

Darriet, P.; Tominaga, T.; Lavigne, V.; Boidron, J.-N.; Dubourdieu, D. Identification of a powerful aromatic component of *Vitis vinifera* L. var. Sauvignon wines: 4-mercapto-4-methylpentan-2-one. *Flavour Fragrance J.* **1995**, *10*, 385-92.

Delahunty, C. M.; Eyres, G.; Dufour, J.-P. Gas chromatography-olfactometry. *J. Sep. Sci.* **2006**, *29*, 2107-2125.

DeMaria, S.; Ngai, J. The cell biology of smell. *J. Cell Biol.* **2010**, *191*, 443-452.

Demole, E.; Enggist, P.; Ohloff, G. 1-*p*-Menthene-8-thiol: a powerful flavor impact constituent of grapefruit juice (*Citrus paradisi* Macfayden). *Helv. Chim. Acta* **1982**, *65*, 1785-94.

Dimoglo, A. S.; Gorbachov, M.; Bersuker, I. B.; Greni, A. I.; Vysotskaya, L. E.; Stepanova, O. V.; Lukash, E. Structural and electronic origin of meat odour of organic hetero-atomic compounds. *Nahrung* **1988**, *32*, 461-73.

Dodziuk, H. Molecules with holes-cyclodextrins. In *Cyclodextrins and Their Complexes: Chemistry, Analytical Methods, Applications*, Dodziuk, H., Ed. Wiley-VCH Verlag: Weinheim, **2006**, pp 1-30.

Dunkel, A.; Steinhaus, M.; Kotthoff, M.; Nowak, B.; Krautwurst, D.; Schieberle, P.; Hofmann, T. Nature's Chemical Signatures in Human Olfaction: A Foodborne Perspective for Future Biotechnology. *Angew. Chem., Int. Ed.* **2014**, *53*, 7124-7143.

Ema, T.; Kobayashi, J.; Maeno, S.; Sakai, T.; Utaka, M. Origin of the Enantioselectivity of Lipases Explained by a Stereo-Sensing Mechanism Operative at the Transition State. *Bull. Chem. Soc. Jpn.* **1998**, *71*, 443-453.

Emura, M.; Yaguchi, Y.; Nakahashi, A.; Sugimoto, D.; Miura, N.; Monde, K. Stereochemical studies of odorous 2-substituted-3(2H)-furanones by vibrational circular dichroism. *J. Agric. Food Chem.* **2009**, *57*, 9909-9915.

Engel, K. H.; Tressl, R. Identification of new sulfur-containing volatiles in yellow passionfruit (*Passiflora edulis* f. *flavicarpa*). *J. Agric. Food Chem.* **1991**, *39*, 2249-2252.

Escher, S.; Niclass, Y.; van de Waal, M.; Starkenmann, C. Combinatorial synthesis by nature: volatile organic sulfur-containing constituents of *Ruta chalepensis* L. *Chem. Biodivers.* **2006**, *3*, 943-957.

Ferreira, V.; Ortin, N.; Escudero, A.; Lopez, R.; Cacho, J. Chemical characterization of the aroma of Grenache rose wines: aroma extract dilution analysis, quantitative determination, and sensory reconstitution studies. *J Agric Food Chem* **2002**, *50*, 4048-54.

Gal, J. The Discovery of Stereoselectivity at Biological Receptors: Arnaldo Piutti and the Taste of the Asparagine Enantiomers-History and Analysis on the 125th Anniversary. *Chirality* **2012**, *24*, 959-976.

Gal, J. Molecular Chirality in Chemistry and Biology: Historical Milestones. *Helv. Chim. Acta* **2013**, *96*, 1617-1657.

Ghanem, A.; Aboul-Enein, H. Y. Application of lipases in kinetic resolution of racemates. *Chirality* **2005**, *17*, 1-15.

Gil-Av, E.; Charles-Sigler, R.; Fischer, G.; Nurok, D. Resolution of optical isomers by gas liquid partition chromatography. *J. Gas Chromatogr.* **1966**, *4*, 51-8.

Goeke, A. Sulfur-containing odorants in fragrance chemistry. *Sulfur Rep.* **2002**, *23*, 243-278.

Grosch, W. Aroma compound analysis. *Chem. unserer Zeit* **1990**, *24*, 82-89.

Grosch, W. Detection of potent odorants in foods by aroma extract dilution analysis. *Trends in Food Science & Technology* **1993**, *4*, 68-73.

Grosch, W. Evaluation of the key odorants of foods by dilution experiments, aroma models and omission. *Chem. Senses* **2001**, *26*, 533-545.

Gunst, F.; Verzele, M. On the sunstruck flavor of beer. *J. Inst. Brew.* **1978**, *84*, 291-2.

Guth, H. Quantitation and Sensory Studies of Character Impact Odorants of Different White Wine Varieties. *J. Agric. Food Chem.* **1997**, *45*, 3027-3032.

Guth, H.; Grosch, W. A comparative study of the potent odorants of different virgin olive oils. *Fett Wiss. Technol.* **1991**, *93*, 335-9.

Haeffner, F.; Norin, T.; Hult, K. Molecular modeling of the enantioselectivity in lipase-catalyzed transesterification reactions. *Biophys. J.* **1998**, *74*, 1251-1262.

Hanefeld, U.; Gardossi, L.; Magner, E. Understanding enzyme immobilisation. *Chem Soc Rev* **2009**, *38*, 453-68.

Hansen, T. V.; Waagen, V.; Partali, V.; Anthonsen, H. W.; Anthonsen, T. Cosolvent enhancement of enantioselectivity in lipase-catalyzed hydrolysis of racemic esters. A process for production of homochiral C-3 building blocks using lipase B from *Candida antarctica*. *Tetrahedron: Asymmetry* **1995**, *6*, 499-504.

Harada, N.; Watanabe, M.; Kuwahara, S.; Sugio, A.; Kasai, Y.; Ichikawa, A. 2-Methoxy-2-(1-naphthyl)propionic acid, a powerful chiral auxiliary for enantioresolution of alcohols and determination of their absolute cofigurations by the 1H NMR anisotropy method. *Tedrahedron: Asymmetry* **2000**, *11*, 1249-1253.

Hatt, H. Geschmack und Geruch. In *Physiologie des Menschen*, Schmidt, R. F.; Lang, F.; Heckmann, M., Eds. Springer Verlag Berlin, **2010**, Vol. 31, pp 421-436.

Helmchen, G.; Schmierer, R. Determination of the absolute configuration of chiral thiols by proton nuclear magnetic resonance spectroscopy of diastereomeric thiol esters. *Angew. Chem.* **1976**, *88*, 770-771.

Heusinger, G.; Mosandl, A. Chiral, sulfur-containing aroma substances of the yellow passion fruit (*Passiflora edulis* f. *flavicarpa*). Preparation of enantiomers and absolute configuration. *Tetrahedron Lett.* **1984**, *25*, 507-510.

Hjorth, A.; Carriere, F.; Cudrey, C.; Woldike, H.; Boel, E.; Lawson, D. M.; Ferrato, F.; Cambillau, C.; Dodson, G. G.; et, a. A structural domain (the lid) found in pancreatic lipases is absent in the guinea pig (phospho)lipase. *Biochemistry* **1993**, *32*, 4702-7.

Holscher, W.; Vitzthum, O. G.; Steinhart, H. Prenyl alcohol - source for odorants in roasted coffee. *J. Agric. Food Chem.* **1992**, *40*, 655-8.

Hult, K.; Norin, T. Enantioselectivity of some lipases: control and prediction. *Pure Appl. Chem.* **1992**, *64*, 1129-34.

Hutt, A. J.; Valentova, J. The chiral switch: the development of single enantiomer drugs from racemates. *Universitas Comeniana. Acta Facultatis Pharmaceuticae* **2003**, *50*, 7-23.

Jaeger, K. E.; Dijkstra, B. W.; Reetz, M. T. Bacterial biocatalysts: molecular biology, three-dimensional structures, and biotechnological applications of lipases. *Annu. Rev. Microbiol.* **1999**, *53*, 315-351.

Jung, K.; Fastowski, O.; Engel, K.-H. Occurrence of 4-methoxy-2-methyl-2-butanethiol in blackcurrant (*Ribes nigrum* L.) berries. *Flavour Fragrance J.* **2016**, *31*, 438-441.

Juvancz, Z.; Petersson, P. Enantioselective gas chromatography. *Journal Microcolumn Sep.* **1996**, *8*, 99-114.

Kasai, Y.; Sugio, A.; Sekiguchi, S.; Kuwahara, S.; Matsumoto, T.; Watanabe, M.; Ichikawa, A.; Harada, N. Conformational analysis of MαNP esters, powerful chiral resolution and 1H NMR anisotropy tools – aromatic geometry and solvent effects on Δδ values. *Eur. J. Org. Chem.* **2007**, 1811-1826.

Kasai, Y.; Taji, H.; Fujita, T.; Yamamoto, Y.; Akagi, M.; Sugio, A.; Kuwahara, S.; Watanabe, M.; Harada, N.; Ichikawa, A.; Schurig, V. MαNP Acid, a Powerful chiral molecular tool for preparation of enantiopure alcohols by resolution and determination of their absolute configurations by the 1H NMR anisotropy method. *Chirality* **2004**, *16*, 569-585.

Kazlauskas, R. J. Elucidating structure-mechanism relationships in lipases: prospects for predicting and engineering catalytic properties. *Trends Biotechnol.* **1994**, *12*, 464-72.

Kazlauskas, R. J.; Weissfloch, A. N. E.; Rappaport, A. T.; Cuccia, L. A. A rule to predict which enantiomer of a secondary alcohol reacts faster in reactions catalyzed by cholesterol esterase, lipase from Pseudomonas cepacia, and lipase from *Candida rugosa*. *J. Org. Chem.* **1991**, *56*, 2656-65.

Kirk, O.; Christensen, M. W. Lipases from *Candida antarctica*: Unique Biocatalysts from a Unique Origin. *Org. Process Res. Dev.* **2002**, *6*, 446-451.

Kiske, C.; Riegel, A. D.; Hopf, R.; Kvindt, A.; Poplacean, I.; Taniguchi, T.; Swamy, M. M. M.; Monde, K.; Eisenreich, W.; Engel, K.-H. Determination of the Absolute Configurations and Sensory Properties of the Enantiomers of a Homologous Series (C6-C10) of 2-Mercapto-4-alkanones. *J. Agric. Food Chem.* **2019**, *67*, 1187-1196.

Kleinhenz, J. K.; Kuo, C. J.; Harper, W. J. Evaluation of polyfunctional thiol compounds in aged Cheddar cheese: identification. *Milchwissenschaft* **2006**, *61*, 300-304.

Kleinhenz, J. K.; Kuo, C. J.; Harper, W. J. Evaluation of polyfunctional thiol compounds in aged Cheddar cheese: estimated concentrations. *Milchwissenschaft* **2007**, 181-183.

Koenig, W. A.; Hochmuth, D. H. Enantioselective gas chromatography in flavor and fragrance analysis: Strategies for the identification of known and unknown plant volatiles. *J. Chromatogr. Sci.* **2004**, *42*, 423-439.

Koppenhoefer, B.; Behnisch, R.; Epperlein, U.; Holzschuh, H.; Bernreuther, A.; Piras, P.; Roussel, C. enantiomeric odor differences and gas chromatographic properties of flavors and fragrances. *Perfum. Flavor.* **1994**, *19*, 1-2, 4, 6-8, 10-12, 14.

Koscielski, T.; Sybilska, D.; Jurczak, J. Separation of α- and β-pinene into enantiomers in gas-liquid chromatography systems via α-cyclodextrin inclusion complexes. *J. Chromatogr.* **1983**, *280*, 131-4.

Kovac, A.; Scheib, H.; Pleiss, J.; Schmid, R. D.; Paltauf, F. Molecular basis of lipase stereoselectivity. *Eur. J. Lipid Sci. Technol.* **2000**, *102*, 61-77.

Lamparsky, D.; Schudel, P. *p*-Menthan-8-thiol-3-one. New component of Buchu leaf oil. *Parfums, Cosmet., Savons Fr.* **1972**, *2*, 465-7.

Lee, G. H.; Suriyaphan, O.; Cadwallader, K. R. Aroma Components of Cooked Tail Meat of American Lobster (*Homarus americanus*). *J. Agric. Food Chem.* **2001**, *49*, 4324-4332.

Leffingwell, J. C. Chirality and Odour Perception. www.leffingwell.com/chirality/chirality.htm (Accessed: 8 May 2018),

Lehmann, D.; Dietrich, A.; Hener, U.; Mosandl, A. Stereoisomeric flavor compounds. LXX: 1-*p*-menthene-8-thiol: separation and sensory evaluation of the enantiomers by enantioselective gas chromatography-olfactometry. *Phytochem. Anal.* **1995**, *6*, 255-7.

Leitereg, T. J.; Guadagni, D. G.; Harris, J.; Mon, T. R.; Teranishi, R. Evidence for the difference between the odors of the optical isomers (+)- and (-)-carvone. *Nature* **1971**, *230*, 455-6.

Li, S.; Purdy, W. C. Cyclodextrins and their applications in analytical chemistry. *Chem.l Rev.* **1992**, *92*, 1457-70.

Linssen, J. P. H.; Janssens, J. L. G. M.; Roozen, J. P.; Posthumus, M. A. Combined gas chromatography and sniffing port analysis of volatile compounds of mineral water packed in polyethylene laminated packages. *Food Chem.* **1993**, *46*, 367-71.

Lorber, K.; Schieberle, P.; Buettner, A. Influence of the Chemical Structure on Odor Qualities and Odor Thresholds in Homologous Series of Alka-1,5-dien-3-ones, Alk-1-en-3-ones, Alka-1,5-dien-3-ols, and Alk-1-en-3-ols. *J. Agric. Food Chem.* **2014**, *62*, 1025-1031.

Luan, B.; Zhou, R. A novel self-activation mechanism of *Candida antarctica* lipase B. *Phys. Chem. Chem. Phys.* **2017**, *19*, 15709-15714.

Maga, J. A. The role of sulfur compounds in food flavor. Part III: Thiols. *CRC Crit. Rev. Food Sci. Nutr.* **1976**, *7*, 147-92.

Magnusson, A.; Hult, K.; Holmquist, M. Creation of an Enantioselective Hydrolase by Engineered Substrate-Assisted Catalysis. *J. Am. Chem. Soc.* **2001**, *123*, 4354-4355.

Magnusson, A. O.; Rotticci-Mulder, J. C.; Santagostino, A.; Hult, K. Creating space for large secondary alcohols by rational redesign of *Candida antarctica* lipase B. *ChemBioChem* **2005**, *6*, 1051-1056.

Mahattanatawee, K.; Perez-Cacho, P. R.; Davenport, T.; Rouseff, R. Comparison of three lychee cultivar odor profiles using gas chromatography-olfactometry and gas chromatography-sulfur detection. *J Agric Food Chem* **2007**, *55*, 1939-44.

Mane, S. Racemic drug resolution: a comprehensive guide. *Anal. Methods* **2016**, *8*, 7567-7586.

Marchelli, R.; Dossena, A.; Palla, G. The potential of enantioselective analysis as a quality control tool. *Trends Food Sci. Technol.* **1996**, *7*, 113-119.

Martinelle, M.; Holmquist, M.; Hult, K. On the interfacial activation of *Candida antarctica* lipase A and B as compared with *Humicola lanuginosa* lipase. *Biochim. Biophys. Acta, Lipids Lipid Metab.* **1995**, *1258*, 272-6.

Martinez, C.; De Geus, P.; Lauwereys, M.; Matthyssens, G.; Cambillau, C. Fusarium solani cutinase is a lipolytic enzyme with a catalytic serine accessible to solvent. *Nature* **1992**, *356*, 615-18.

Mayer, F.; Czerny, M.; Grosch, W. Sensory study of the character impact aroma compounds of a coffee beverage. *Eur. Food Res. Technol.* **2000**, *211*, 272-276.

McGorrin, R. J. The significance of volatile sulfur compounds in food flavors. An overview. In *Volatile Sulfur Compounds in Food*, ACS Symposium Series 1068, American Chemical Society: Washington, DC, **2011**, pp 3-31.

Meilgaard, M. C. Flavor chemistry of beer. II. Flavor and threshold of 239 aroma volatiles. *Tech. Q., Master Brew. Assoc. Am.* **1975**, *12*, 151-68.

Mestres, M.; Busto, O.; Guasch, J. Analysis of organic sulfur compounds in wine aroma. *J. Chromatogr. A* **2000**, *881* 569-581.

Milo, C.; Reineccius, G. A. Identification and Quantification of Potent Odorants in Regular-Fat and Low-Fat Mild Cheddar Cheese. *J. Agric. Food Chem.* **1997**, *45*, 3590-3594.

Mori, K. Molecular asymmetry and pheromone science. *Biosci., Biotechnol., Biochem.* **1996**, *60*, 1925-1932.

Mori, K. Organic Synthesis and Chemical Ecology. *Acc. Chem. Res.* **2000**, *33*, 102-110.

Mortimer, C. E.; Müller, U. *Chemie: Das Basiswissen der Chemie*. Thieme-Verlag: Stuttgart, **2010**.

Mosandl, A. Capillary gas chromatography in quality assessment of flavors and fragrances. *J. Chromatogr.* **1992**, *624*, 267-92.

Mosandl, A.; Heusinger, G.; Gessner, M. Analytical and sensory differentiation of 1-octen-3-ol enantiomers. *J. Agric. Food Chem.* **1986**, *34*, 119-22.

Mottram, D. S.; Mottram, H. R. An overview of the contribution of sulfur-containing compounds to the aroma in heated foods. In *Heteroatomic Aroma Compounds*, ACS Symposium Series 826, American Chemical Society: Washington, D.C., **2002**, pp 73-92.

Munafo, J. P.; Didzbalis, J.; Schnell, R. J.; Schieberle, P.; Steinhaus, M. Characterization of the Major Aroma-Active Compounds in Mango (*Mangifera indica* L.) Cultivars Haden, White Alfonso, Praya Sowoy, Royal Special, and Malindi by Application of a Comparative Aroma Extract Dilution Analysis. *J. Agric. Food Chem.* **2014**, *62*, 4544-4551.

Muralidhar, R. V.; Chirumamilla, R. R.; Marchant, R.; Ramachandran, V. N.; Ward, O. P.; Nigam, P. Understanding lipase stereoselectivity. *World J. Microbiol. Biotechnol.* **2002**, *18*, 81-97.

Mussinan, C. J.; Keelan, M. E. Sulfur compounds in foods. An overview. In *Sulfur Compounds in Foods* ACS Symposium Series 564, American Chemical Society: Washington, DC, **1994**, pp 1-6.

Naef, R.; Velluz, A.; Jaquier, A. New volatile sulfur-containing constituents in a simultaneous distillation-extraction extract of red bell peppers (*Capsicum annuum*). *J. Agric. Food Chem.* **2008**, *56*, 517-527.

Nakahashi, A.; Yaguchi, Y.; Miura, N.; Emura, M.; Monde, K. A vibrational circular dichroism approach to the determination of the absolute configurations of flavorous 5-substituted-2(5H)-furanones. *J. Nat. Prod.* **2011**, *74*, 707-711.

Nelson, D.; Cox, M. *Lehninger Biochemie*. Springer-Verlag: Berlin, **2009**.

Nestl, B. M.; Nebel, B. A.; Hauer, B. Recent progress in industrial biocatalysis. *Curr. Opin. Chem. Biol.* **2011**, *15*, 187-193.

Nguyen, L. A.; He, H.; Chuong, P.-H. Chiral drugs. An overview. *Int. J. Biomed. Sci.* **2006**, *2*, 85-100.

Nijssen, L. M.; Maarse, H. Volatile compounds in black currant products. An additional factor in authenticity control of fruit juices. *Flavour Fragrance J.* **1986**, *1*, 143-8.

Nörenberg, S.; Kiske, C.; Burmann, A.; Poplacean, I.; Engel, K.-H. Distributions of the Stereoisomers of β-Mercaptoheptanones and β-Mercaptoheptanols in Cooked Bell Pepper (*Capsicum annuum*). *J. Agric. Food Chem.* **2017a**, *65*, 10250-10257.

Nörenberg, S.; Kiske, C.; Reichardt, B.; Andelfinger, V.; Pfeiffer, A.; Schmidts, F.; Eisenreich, W.; Engel, K.-H. Analysis and Sensory Evaluation of the Stereoisomers of a Homologous Series (C5-C10) of 4-Mercapto-2-alkanols. *J. Agric. Food Chem.* **2017b**, *65*, 8913-8922.

Nörenberg, S.; Reichardt, B.; Andelfinger, V.; Eisenreich, W.; Engel, K.-H. Influence of the stereochemistry on the sensory properties of 4-mercapto-2-heptanol and its acetyl-derivatives. *J. Agric. Food Chem.* **2013**, *61*, 2062-2069.

Nowotny, H. P.; Schmalzing, D.; Wistuba, D.; Schurig, V. Extending the scope of enantiomer separation on diluted methylated β-cyclodextrin derivatives by high-resolution gas chromatography. *J. High Resolut. Chromatogr.* **1989**, *12*, 383-93.

Ohloff, G. Structure-odor relationships. In *Scent and Fragrances: the fascination of odorants and their chemical perspectives*, Ohloff, G., Ed. Springer Verlag: Berlin, **1994**, pp 9-56.

Oikawa, Y.; Sugano, K.; Yonemitsu, O. Meldrum's acid in organic synthesis. 2. A general and versatile synthesis of β-keto esters. *J. Org. Chem.* **1978**, *43*, 2087-2088.

Ollis, D. L.; Cheah, E.; Cygler, M.; Dijkstra, B.; Frolow, F.; Franken, S. M.; Harel, M.; Remington, S. J.; Silman, I.; et, a. The α/β hydrolase fold. *Protein Eng.* **1992**, *5*, 197-211.

Orrenius, C.; Haeffner, F.; Rotticci, D.; Ohrner, N.; Norin, T.; Hult, K. Chiral recognition of alcohol enantiomers in acyl transfer reactions catalysed by *Candida antarctica* lipase B. *Biocatal. Biotransform.* **1998**, *16*, 1-15.

Patton, S.; Josephson, D. V. A method for determining significance of volatile flavor compounds in foods. *J. Food Sci.* **1957**, *22*, 316-318.

Peterson, D. G.; Reineccius, G. A. Determination of the aroma impact compounds in heated sweet cream butter. *Flavour Fragrance J.* **2003**, *18*, 320-324.

Pino, J. A. Odour-active compounds in papaya fruit cv. Red Maradol. *Food Chem.* **2014**, *146*, 120-126.

Polster, J.; Schieberle, P. Structure-odor correlations in homologous series of alkanethiols and attempts to predict odor thresholds by 3D-QSAR studies. *J. Agric. Food Chem.* **2015**, *63*, 1419-1432.

Polster, J.; Schieberle, P. Structure-Odor Correlations in Homologous Series of Mercaptoalkanols. *J. Agric. Food Chem.* **2017**, *65*, 4329-4340.

Porto, S.; Quiñoá, A.; Riguera, R. Designing chiral derivatizing agents (CDA) for the NMR assignment of the absolute configuration: a theoretical and experimental approach with thiols as a case study. *Tetrahedron* **2014**, *70*, 3276-3283.

Porto, S.; Seco, J. M.; Ortiz, A.; Quiñoá, A.; Riguera, R. Chiral thiols: the assignment of their absolute configuration by 1H NMR. *Org. Lett.* **2007**, *9*, 5015-5018.

Preininger, M.; Rychlik, M.; Grosch, W. Potent odorants of the neutral volatile fraction of Swiss cheese (Emmentaler). *Dev. Food Sci.* **1994**, *35*, 267-70.

Prelog, V. Chirality in chemistry. *Science* **1976**, *193*, 17-24.

Qian, M.; Reineccius, G. A. Quantification of aroma compounds in Parmigiano Reggiano cheese by a dynamic headspace gas chromatography-mass spectrometry technique and calculation of odor activity value. *J. Dairy Sci.* **2003**, *86*, 770-776.

Rakels, J. L. L.; Straathof, A. J. J.; Heijnen, J. J. A simple method to determine the enantiomeric ratio in enantioselective biocatalysis. *Enzyme Microb. Technol.* **1993**, *15*, 1051-1056.

Reetz, M. T. Lipases as practical biocatalysts. *Curr. Opin. Chem. Biol.* **2002**, *6*, 145-150.

Reetz, M. T. Biocatalysis in Organic Chemistry and Biotechnology: Past, Present, and Future. *J. Am. Chem. Soc.* **2013**, *135*, 12480-12496.

Rienacker, R.; Ohloff, G. Optically active β-citronellol from d- or l-pinane. *Angew. Chem.* **1961**, *73*, 240.

Rigaud, J.; Etievant, P.; Henry, R.; Latrasse, A. 4-Methoxy-2-methyl-2-butanethiol, a major constituent of the aroma of the black currant bud (*Ribes nigrum* L.). *Sci. Aliments* **1986**, *6*, 213-20.

Robert, F.; Heritier, J.; Quiquerez, J.; Simian, H.; Blank, I. Synthesis and sensorial properties of 2-alkylalk-2-enals and 3-(acetylthio)-2-alkyl alkanals. *J. Agric. Food Chem.* **2004**, *52*, 3525-3529.

Roberts, D. D.; Acree, T. E. Effects of Heating and Cream Addition on Fresh Raspberry Aroma Using a Retronasal Aroma Simulator and Gas Chromatography Olfactometry. *J. Agric. Food Chem.* **1996**, *44*, 3919-3925.

Rossiter, K. J. Structure-Odor Relationships. *Chem. Rev.* **1996**, *96*, 3201-3240.

Rothe, M.; Thomas, B. Aromastoffe des Brotes. *Z Lebensm Unters Forsch* **1963**, *119*, 302-310.

Rotticci, D.; Haeffner, F.; Orrenius, C.; Norin, T.; Hult, K. Molecular recognition of sec-alcohol enantiomers by *Candida antarctica* lipase B. *J. Mol. Catal. B: Enzym.* **1998**, *5*, 267-272.

Rowe, D.; Tangel, B. Aroma chemicals for the sweet field. *Perfum. Flavor.* **1999**, *24*, 36-38,40-44.

Rowe, D. J. High impact aroma chemicals. In *Advances in Flavours and Fragrances–From the Sensation to the Synthesis*, Swift, K. A. D., Ed. Royal Society of Chemistry: Cambridge, UK, **2002**, pp 202-226.

Sakoda, Y.; Hayashi, S. Relationship of odour and chemical Structure in 1- and 2-alkyl alcohols and thiols. In *In Advances in Flavours and Fragrances: From the Sensation To the Synthesis;* , Swift, K. A. D., Ed. The Royal Society of Chemistry: Cambridge, U.K., **2002**, pp 15-24.

San-Juan, F.; Cacho, J.; Ferreira, V.; Escudero, A. 3-Methyl-2-butene-1-thiol: Identification, analysis, occurrence and sensory role of an uncommon thiol in wine. *Talanta* **2012**, *99*, 225-231.

Sarda, L.; Desnuelle, P. Actions of pancreatic lipase on esters in emulsions. *Biochim Biophys Acta* **1958**, *30*, 513-21.

Schmid, R. D.; Verger, R. Lipases: interfacial enzymes with attractive applications. *Angew. Chem., Int. Ed.* **1998**, *37*, 1609-1633.

Schnermann, P.; Schieberle, P. Evaluation of Key Odorants in Milk Chocolate and Cocoa Mass by Aroma Extract Dilution Analyses. *J. Agric. Food Chem.* **1997**, *45*, 867-872.

Schoenauer, S.; Schieberle, P. Structure-Odor Activity Studies on Monoterpenoid Mercaptans Synthesized by Changing the Structural Motifs of the Key Food Odorant 1-*p*-Menthene-8-thiol. *J. Agric. Food Chem.* **2016**, *64*, 3849-3861.

Schrag, J. D.; Cygler, M. Lipases and α/β hydrolase fold. *Methods Enzymol.* **1997**, *284*, 85-107.

Schreier, P.; Bernreuther, A.; Huffer, M. Techniques used in analysis of optically active compounds. In *Analysis of chiral organic molecules: methodology and applications*, Schreier, P.; Bernreuther, A.; Huffer, M., Eds. de Gruyter, Berlin: **1995**, pp 132-233.

Schulze, B.; Wubbolts, M. G. Biocatalysis for industrial production of fine chemicals. *Curr. Opin. Biotechnol.* **1999**, *10*, 609-615.

Schurig, V. enantiomer separation by gas chromatography on chiral stationary phases. *J. Chromatogr. A* **1994**, *666*, 111-29.

Schurig, V. Separation of enantiomers by gas chromatography. *J.Chromatogr. A* **2001**, *906*, 275-299.

Schurig, V.; Nowotny, H. P. Gas-chromatographic separation of enantiomers on stationary phases without metal complexes. 2. Gas-chromatographic separation of enantiomers on cyclodextrin derivatives. *Angew. Chem.* **1990**, *102*, 969-86.

Scriba, G. K. E. Chiral recognition mechanisms in analytical separation sciences. *Chromatographia* **2012**, *75*, 815-838.

Shankaranarayana, M. L.; Raghavan, B.; Abraham, K. O.; Natarajan, C. P. Volatile sulfur compounds in food flavors. *CRC Critical Reviews in Food Technology* **1974**, *4*, 395-435.

Simian, H.; Robert, F.; Blank, I. Identification and synthesis of 2-heptanethiol, a new flavor compound found in bell peppers. *J. Agric. Food Chem.* **2004**, *52*, 306-310.

Song, H.; Cadwallader, K. R. Aroma components of American country ham. *J. Food Sci.* **2008**, *73*, C29-C35.

Song, H.; Cadwallader, K. R.; Singh, T. K. Odour-active compounds of Jinhua ham. *Flavour Fragrance J.* **2008**, *23*, 1-6.

Starkenmann, C.; Troccaz, M.; Howell, K. The role of cysteine and cysteine-S conjugates as odour precursors in the flavour and fragrance industry. *Flavour Fragrance J.* **2008**, *23*, 369-381.

Stauch, B.; Fisher, S. J.; Cianci, M. Open and closed states of *Candida antarctica* lipase B: protonation and the mechanism of interfacial activation. *J. Lipid Res.* **2015**, *56*, 2348-2358.

Stecher, H.; Faber, K. Biocatalytic deracemization techniques. Dynamic resolutions and stereoinversions. *Synthesis* **1997**, 1-16.

Straathof, A. J. J.; Jongejan, J. A. The enantiomeric ratio: origin, determination and prediction. *Enzyme Microb. Technol.* **1997**, *21*, 559-571.

Sundt, E.; Willhalm, B.; Chappaz, R.; Ohloff, G. Organoleptic principle of cassia flavor in buchu oil. *Helv. Chim. Acta* **1971**, *54*, 1801-5.

Szejtli, J. Utilization of cyclodextrins in industrial products and processes. *J. Mater. Chem.* **1997**, *7*, 575-587.

Szejtli, J. Introduction and General Overview of Cyclodextrin Chemistry. *Chem. Rev.* **1998**, *98*, 1743-1753.

Szente, L.; Szeman, J. Cyclodextrins in Analytical Chemistry: Host-Guest Type Molecular Recognition. *Anal. Chem.* **2013**, *85* 8024-8030.

Taji, H.; Kasai, Y.; Sugio, A.; Kuwahara, S.; Watanabe, M.; Harada, N.; Ichikawa, A. Practical enantioresolution of alcohols with 2-methoxy-2-(1-naphthyl)propionic acid and determination of their absolute configurations by the 1H NMR anisotropy method. *Chirality* **2002**, *14*, 81-84.

Tominaga, T.; Darriet, P.; Dubourdieu, D. Identification of 3-mercaptohexyl acetate in Sauvignon wine, a powerful aromatic compound exhibiting box-tree odor. *Vitis* **1996**, *35*, 207-210.

Tominaga, T.; Dubourdieu, D. Identification of 4-mercapto-4-methylpentan-2-one from the box tree (*Buxus sempervirens* L.) and broom (*Sarothamnus scoparius* (L.) Koch.). *Flavour Fragr. J.* **1997**, *12*, 373-376.

Tominaga, T.; Dubourdieu, D. Identification of cysteinylated aroma precursors of certain volatile thiols in passion fruit juice. *J Agric Food Chem* **2000**, *48*, 2874-6.

Tominaga, T.; Furrer, A.; Henry, R.; Dubourdieu, D. Identification of new volatile thiols in the aroma of *Vitis vinifera* L. var. Sauvignon blanc wines. *Flavour Fragr. J.* **1998**, *13*, 159-162.

Tominaga, T.; Niclass, Y.; Frerot, E.; Dubourdieu, D. Stereoisomeric Distribution of 3-Mercaptohexan-1-ol and 3-Mercaptohexyl Acetate in Dry and Sweet White Wines Made from Vitis vinifera (Var. Sauvignon Blanc and Semillon). *J. Agric. Food Chem.* **2006**, *54*, 7251-7255.

Tromelin, A. Odour perception: A review of an intricate signalling pathway. *Flavour Fragr. J.* **2016**, *31*, 107-119.

Tsai, S.-W. Enantiopreference of *Candida antarctica* lipase B toward carboxylic acids: Substrate models and enantioselectivity thereof. *J. Mol. Catal. B: Enzym.* **2016**, *127*, 98-116.

Turner, N. J. Directed evolution of enzymes for applied biocatalysis. *Trends Biotechnol.* **2003**, *21*, 474-478.

UIlrich, F.; Grosch, W. Identification of the most intense volatile flavour compounds formed during autoxidation of linoleic acid. *Z Lebensm Unters Forsch* **1987**, *184*, 277-282.

Uppenberg, J.; Hansen, M. T.; Patkar, S.; Jones, T. A. The sequence, crystal structure determination and refinement of two crystal forms of lipase B from *Candida antarctica*. *Structure* **1994**, *2*, 293-308.

Uppenberg, J.; Oehrner, N.; Norin, M.; Hult, K.; Kleywegt, G. J.; Patkar, S.; Waagen, V.; Anthonsen, T.; Jones, T. A. Crystallographic and molecular-modeling studies of lipase B from *Candida antarctica* reveal a stereospecificity pocket for secondary alcohols. *Biochemistry* **1995**, *34*, 16838-51.

van den Dool, H.; Kratz, P. D. A generalization of the retention index system including linear temperature programmed gas-liquid partition chromatography. *J. Chromatogr. A* **1963**, *11*, 463-471.

Van Ruth, S. M. Methods for gas chromatography-olfactometry: a review. *Biomol. Eng.* **2001**, *17*, 121-128.

Vermeulen, C.; Collin, S. Synthesis and Sensorial Properties of Mercaptoaldehydes. *J. Agric. Food Chem.* **2002**, *50*, 5654-5659.

Vermeulen, C.; Collin, S. Combinatorial synthesis and screening of novel odorants such as polyfunctional thiols. *Comb. Chem. High Throughput Screen.* **2006**, *9*, 583-590.

Vermeulen, C.; Gijs, L.; Collin, S. Sensorial contribution and formation pathways of thiols in foods: A review. *Food Rev. Int.* **2005**, *21*, 69-137.

Vermeulen, C.; Guyot-Declerck, C.; Collin, S. Combinatorial Synthesis and Sensorial Properties of Mercapto Primary Alcohols and Analogues. *J. Agric. Food Chem.* **2003**, *51*, 3623-3628.

Vermeulen, C.; Lejeune, I.; Tran, T. T. H.; Collin, S. Occurrence of Polyfunctional Thiols in Fresh Lager Beers. *J. Agric. Food Chem.* **2006**, *54*, 5061-5068.

Vermeulen, C.; Pellaud, J.; Gijs, L.; Collin, S. Combinatorial synthesis and sensorial properties of polyfunctional thiols. *J. Agric. Food Chem.* **2001**, *49*, 5445-5449.

Wakabayashi, H.; Wakabayashi, M.; Eisenreich, W.; Engel, K.-H. Stereoselectivity of the generation of 3-mercaptohexanal and 3-mercaptohexanol by lipase-catalyzed hydrolysis of 3-acetylthioesters. *J. Agric. Food Chem.* **2003**, *51*, 4349-4355.

Wakabayashi, M.; Wakabayashi, H.; Eisenreich, W.; Morimitsu, Y.; Kubota, K.; Engel, K.-H. Determination of the absolute configurations of 4-mercapto-2-alkanones using the 1H NMR anisotropy method and enzyme-catalyzed kinetic resolution of the corresponding 4-acetylthio-2-alkanones. *Eur. Food Res. Technol.* **2011**, *232*, 753-760.

Wakabayashi, M.; Wakabayashi, H.; Noerenberg, S.; Reichardt, B.; Kubota, K.; Engel, K. H. Analytical and sensory characterization of chiral 4-mercapto-2-alkanones, 4-acetylthio-2-alkanones, and the corresponding alcohols. In *Recent Advances in the Analysis of Food and Flavors*, ACS Symposium Series 1098, American Chemical Society: Washington, D.C., **2012**, pp 27-39.

Wakabayashi, M.; Wakabayashi, H.; Nörenberg, S.; Kubota, K.; Engel, K.-H. Comparison of odour thresholds and odour qualities of the enantiomers of 4-mercapto-2-alkanones and 4-acetylthio-2-alkanones. *Flavour Fragr. J.* **2015**, *30*.

Waldeck, B. Three-dimensional pharmacology, a subject ranging from ignorance to overstatements. *Pharmacol. Toxicol.* **2003**, *93*, 203-210.

Wannagat, U.; Damrath, V.; Schliephake, A.; Harder, U. Sila-substituted perfumes and isosteric compounds of perfumes. XI. Comparison of carbinols and silanols with thiocarbinols and silanethiols. *Monatsh. Chem.* **1987**, *118*, 779-88.

Weber, B.; Haag, H. P.; Mosandl, A. Stereoisomeric flavor compounds. Part 59. 3-Mercaptohexyl- and 3-methylthiohexylalkanoates. Structure and properties of the enantiomers. *Z. Lebensm.-Unters. Forsch.* **1992**, *195*, 426-8.

Weber, B.; Maas, B.; Mosandl, A. Stereoisomeric Flavor Compounds. 72. Stereoisomeric Distribution of Some Chiral Sulfur-Containing Trace Components of Yellow Passion Fruits. *J. Agric. Food Chem.* **1995**, *43*, 2438-41.

Weiss, T.; Snitz, K.; Yablonka, A.; Khan, R. M.; Gafsou, D.; Schneidman, E.; Sobel, N. Perceptual convergence of multi-component mixtures in olfaction implies an olfactory white. *Proc. Natl. Acad. Sci. U. S. A.* **2012**, *109*, 19959-19964, S19959/1-S19959/25.

Werkhoff, P.; Guentert, M.; Krammer, G.; Sommer, H.; Kaulen, J. Vacuum headspace method in aroma research: flavor chemistry of yellow passion fruits. *J. Agric. Food Chem.* **1998**, *46*, 1076-1093.

Widder, S.; Luentzel, C. S.; Dittner, T.; Pickenhagen, W. 3-Mercapto-2-methylpentan-1-ol, a New Powerful Aroma Compound. *J. Agric. Food Chem.* **2000**, *48*, 418-423.

Winter, M.; Furrer, A.; Willhalm, B.; Thommen, W. Identification and synthesis of two new organic sulfur compounds from the yellow passion fruit (*Passiflora edulis* f. *flavicarpa*). *Helv. Chim. Acta* **1976**, *59*, 1613-20.

Wright, R. H. Odour and chemical constitution. *Nature* **1954**, *173*, 831.

Zawirska-Wojtasiak, R. Optical purity of (*R*)-(-)-1-octen-3-ol in the aroma of various species of edible mushrooms. *Food Chem.* **2004**, *86*, 113-118.

8. APPENDIX

Table 22. ^{1}H-NMR data and Δδ values of (*R*)- and (*S*)-MPA thioesters of (*R*)-(-)-2-mercapto-4-heptanone **2**-E1.

H	δ (*R*,*R*)-36	δ (*S*,*R*)-35	$\Delta\delta^{RS}$
1	1.201 (d, 7.0)	1.252 (d, 6.9)	-0.051
2	3.801 (m)	3.806 (m)	-0.005
3	2.708 (dd, 16.7, 5.3)	2.601 (dd, 16.7, 4.9)	0.107
3'	2.521 (dd, 16.7, 8.2)	2.478 (dd, 16.7, 8.4)	0.043
5	2.281 (td, 7.1, 1.0)	2.218 (m)	0.063
6	1.508 (h, 7.3)	1.456 (dt, 14.8, 7.4)	0.052
7	0.823 (t, 7.4)	0.788 (t, 7.4)	0.035

Table 23. ^{1}H-NMR data and Δδ values of (*R*)- and (*S*)-MPA thioesters of (*R*)-(-)-2-heptanethiol.

H	δ (*R*,*R*)-34	δ (*S*,*R*)-33	$\Delta\delta^{RS}$
1	1.149	1.150	-0.001
2	3.398 (m)	3.428 (m)	-0.03
3	1.451 (m)	1.450 (m)	0.001
4	1.320 (m)	1.318 (m)	0.002
5	1.176 (m)	1.151 (m)	0.025
6	1.302 (m)	1.261 (m)	0.041
7	0.806 (m)	0.757 (m)	0.049

Table 24. ^{1}H-NMR data and Δδ values of (*R*)- and (*S*)-MαNP thioesters of (*R*)-(-)-2-heptanethiol.

H	δ (*R*,*R*)-26	δ (*S*,*R*)-25	$\Delta\delta^{RS}$
1	1.182	1.194	-0.012
2	3.421 (m)	3.426 (m)	-0.005
3	1.467 (m)	1.466 (m)	0.001
4	1.252 (m)	1.246 (m)	0.006
5	n.d.[a]	n.d.[a]	n.d.[a]
6	1.208 (m)	1.184 (m)	0.024
7	0.792 (m)	0.764 (m)	0.028

[a] not determined

Table 25. ^{1}H-NMR data and Δδ values of (*R*)- and (*S*)-MαNP thioesters of (*R*)-(-)-2-mercapto-4-heptanone **2**-E1.

H	δ **(*R*,*R*)-21**	δ **(*S*,*R*)-19**	$\Delta\delta^{RS}$
1	1.224 (d, 6.9)	1.236 (d, 7.0)	-0.012
2	3.801 (m)	3.794 (m)	0.007
3	2.672 (dd, 16.5, 5.5)	2.639 (dd, 16.6, 4.9)	0.033
3'	2.484 (dd, 16.5, 8.2)	2.485 (dd, 16.6, 8.6)	-0.001
5	2.265 (td, 7.2, 1.5)	2.220 (td, 7.3, 3.0)	0.045
6	1.489 (m)	1.457 (q, 7.4)	0.032
7	0.813 (t, 7.0)	0.775 (t, 7.4)	0. 038

Table 26. ^{1}H-NMR data and Δδ values of (*R*)- and (*S*)-MαNP esters of (*R*)-(-)-2-heptanol.

H	δ **(*R*,*R*)-22**	δ **(*S*,*R*)-24**	$\Delta\delta^{RS}$
1	1.042 (d, 6.2)	0.810 (d, 6.2)	0.232
2	4.792 (m)	4.841 (m)	-0.049
3	1.095 (m)	1.307 (m)	-0.212
4	0.462 (m)	1.036 (m)	-0.574
5	0.820 (m)	1.199 (m)	-0.379
6	0.724 (dt, 14.7, 7.4)	1.102 (m)	-0.378
7	0.601 (t, 7.2)	0.747 (t, 7.1)	-0.146

Table 27. ^{1}H-NMR data and Δδ values of (*R*)- and (*S*)-MPA thioesters of (*R*)-(-)-2-mercapto-4-hexanone **1**-E1.

H	δ **(*R*,*R*)-45**	δ **(*S*,*R*)-46**	$\Delta\delta^{RS}$
1	1.204 (d, 7.1)	1.255 (d, 7.0)	-0.051
2	3.803 (dqd, 8.2, 7.0, 5.3)	3.806 (m)	-0.003
3	2.713 (dd, 16.7, 5.3)	2.607 (dd, 16.7, 5.3)	0.106
3'	2.535 (dd, 16.6, 8.1)	2.490 (dd, 16.7, 8.4)	0.045
5	2.325 (qd, 7.3, 1.7)	2.264 (m)	0.061
6	0.962 (t, 7.3)	0.915 (t, 7.3)	0.047

Table 28. ^{1}H-NMR data and Δδ values of (*R*)- and (*S*)-MPA thioesters of (*R*)-(-)-2-mercapto-4-octanone **3**-E1.

H	δ (*R*,*R*)-47	δ (*S*,*R*)-48	$\Delta\delta^{RS}$
1	1.198 (d, 7.0)	1.250 (d, 7.1)	-0.052
2	3.797 (m)	3.803 (m)	-0.006
3	2.710 (dd, 16.7, 5.3)	2.605 (dd, 16.7, 4.9)	0.105
3'	2.526 (dd, 16.7, 8.2)	2.483 (dd, 16.8, 8.4)	0.043
5	2.297 (td, 7.2, 1.2)	2.237 (m)	0.060
6	1.457 (m)	1.415 (m)	0.042
7	1.217 (m)	1.183 (m)	0.034
8	0.819 (t, 7.3)	0.796 (t, 7.3)	0.023

Table 29. ^{1}H-NMR data and Δδ values of (*R*)- and (*S*)-MPA thioesters of (*R*)-(-)-2-mercapto-4-nonanone **4**-E1.

H	δ (*R*,*R*)-49	δ (*S*,*R*)-50	$\Delta\delta^{RS}$
1	1.199 (d, 7.0)	1.249 (d, 6.9)	-0.050
2	3.793 (m)	3.805 (m)	-0.012
3	2.708 (dd, 16.7, 5.3)	2.602 (dd, 16.8, 4.9)	0.106
3'	2.525 (dd, 16.7, 8.2)	2.480 (dd, 16.8, 8.4)	0.045
5	2.292 (td, 7.2, 1.1)	2.234 (td, 7.4, 3.7)	0.058
6	1.476 (dt, 15.0, 7.5)	1.432 (dt, 15.1, 7.5)	0.044
7	1.231 (m)	1.202 (m)	0.029
8	1.166 (m)	1.136 (m)	0.030
9	0.811 (t, 7.2)	0.795 (t, 7.2)	0.016

Table 30. ^{1}H-NMR data and Δδ values of (*R*)- and (*S*)-MPA thioesters of (*R*)-(-)-2-mercapto-4-decanone **5**-E1.

H	δ (*R*,*R*)-51	δ (*S*,*R*)-52	$\Delta\delta^{RS}$
1	1.195 (d, 7.0)	1.249 (d, 6.9)	-0.054
2	3.799 (m)	3.806 (m)	-0.007
3	2.705 (dd, 16.7, 5.3)	2.603 (dd, 16.8, 4.9)	0.102
3'	2.522 (dd, 16.8, 8.1)	2.480 (dd, 16.8, 8.5)	0.042
5	2.291 (td, 7.2, 1.0)	2.236 (td, 7.3, 3.6)	0.055
6	1.466 (m)	1.428 (m)	0.038
7	1.195 (m)	1.170 (m)	0.025
8	1.195 (m)	1.170 (m)	0.025
9	1.195 (m)	1.170 (m)	0.025
10	0.804 (t, 7.0)	0.796 (t, 7.0)	0.008

Table 31. Conversion rates (c and c_{ee}), enantiomeric excesses of substrates and respective products (ee_S and ee_P) as well as enantioselectivities (E) calculated according to the different equations in the course of the enzyme-catalyzed kinetic resolution of 2-acetylthio-4-hexanone **6** by using GC/FID V.

2-acetylthio-4-hexanone **6**								
						enantioselectivity E		
enzyme	time [h]	c [%]	ee_S [%]	ee_P [%]	c_{ee} [%]	equation 5	equation 6	equation 7
CAL-B	0.5	33.8	49.9	93.6	34.6	55	50	50
	0.75	41.8	70.3	91.7	43.3	50	48	49
	1	46.7	84.1	89.4	48.4	48	47	48
	2	57.4	98.4	80.4	55.0	43	43	43
	4	69.0	99.8	63.7	61.0	28	28	28
	8	79.9	100	41.9	70.5	n.d.	n.d.	n.d.
	24	89.0	100	10.9	90.2	n.d.	n.d.	n.d.
PPL	0.5	41.5	43.2	53.1	44.7	5	5	5
	0.75	49.9	55.9	49.2	53.2	5	5	5
	1	54.1	62.8	46.6	57.4	5	5	5
	2	64.6	80.0	37.5	68.0	5	5	5
	4	75.0	93.4	26.1	78.2	5	5	5
	8	83.8	98.1	14.6	87.1	4	4	4
	24	91.2	99.0	4.8	95.4	3	3	3
WGL	0.5	17.8	4.8	12.6	27.5	1	1	1
	0.75	25.0	5.6	9.3	37.7	1	1	1
	1	30.2	5.9	6.6	47.4	1	1	1
	2	48.3	4.7	1.8	71.9	1	1	1
	4	70.0	0.3	1.0	19.3	1	1	1
	8	92.4	9.4	1.5	86.1	1	1	1
	24	98.9	12.0	1.2	90.1	1	1	1

Table 32. Conversion rates (c and c_{ee}), enantiomeric excesses of substrates (ee_S) and respective products (ee_P) as well as enantioselectivities (E) (calculated according to the different equations, cf. 3.3.1.4.) in the course of the enzyme-catalyzed kinetic resolution of 2-acetylthio-4-heptanone **7** by using GC/FID V.

2-acetylthio-4-heptanone **7**								
						enantioselectivity E		
enzyme	time [h]	c [%]	ee_S [%]	ee_P [%]	c_{ee} [%]	equation 5	equation 6	equation 7
CAL-B	0.5	43.5	61.4	93.7	39.6	58	58	58
	0.75	50.3	80.1	91.3	46.7	54	54	54
	1	52.2	79.2	89.5	46.5	51	43	44
	2	56.2	97.7	81.0	54.7	42	42	42
	4	60.6	99.9	66.6	60.0	43	44	43
	8	67.5	100	47.3	67.9	n.d.	n.d.	n.d.
	24	81.8	100	19.1	84.0	n.d.	n.d.	n.d.
PPL	0.5	44.0	28.7	31.4	47.7	2	2	2
	0.75	53.1	35.8	26.9	57.1	2	2	2
	1	58.2	37.8	23.9	61.3	2	2	2
	2	71.2	49.1	17.1	74.1	2	2	2
	4	80.2	59.8	11.7	83.6	2	2	2
	8	87.1	67.3	7.4	90.0	2	2	2
	24	92.6	68.8	3.3	95.4	2	2	2
WGL	0.5	25.1	10.5	27.5	27.7	2	2	2
	0.75	31.8	12.9	24.8	34.2	2	2	2
	1	38.2	15.4	21.1	42.2	2	2	2
	2	55.3	18.2	13.1	58.2	2	2	2
	4	66.3	17.7	6.4	73.3	1	1	1
	8	82.1	14.9	1.7	90.1	1	1	1
	24	96.2	4.4	0.2	97.1	1	1	1

Table 33. Conversion rates (c and c_{ee}), enantiomeric excesses of substrates (ee_S) and respective products (ee_P) as well as enantioselectivities (E) (calculated according to the different equations, cf. 3.3.1.4.) in the course of the enzyme-catalyzed kinetic resolution of 2-acetylthio-4-octanone **8** by using GC/FID V.

2-acetylthio-4-octanone **8**								
						enantioselectivity E		
enzyme	time [h]	c [%]	ee_S [%]	ee_P [%]	c_{ee} [%]	equation 5	equation 6	equation 7
CAL-B	0.5	36.3	50.0	90.9	35.4	47	47	35
	0.75	43.6	66.6	89.7	42.6	51	51	37
	1	49.8	79.1	88.1	47.3	50	50	38
	2	57	94.2	81.1	53.7	42	42	34
	4	61.5	95.8	68.7	58.2	23	23	20
	8	64	100	50.5	66.5	n.d.	n.d.	n.d.
	24	78.7	100	19.0	84.1	n.d.	n.d.	n.d.
PPL	0.5	22.7	5	13.2	27.3	1	1	1
	0.75	30.8	5.1	9.1	35.8	1	1	1
	1	36.3	4.8	6.3	43.6	1	1	1
	2	47.3	2.9	1.5	67.8	1	1	1
	4	59.9	1.0	1.7	30.0	1	1	1
	8	69.3	6.9	3.5	66.1	1	1	1
	24	82.3	17.6	3.5	83.6	1	1	1
WGL	0.5	9.1	2.5	18.9	11.6	2	2	2
	0.75	13.9	3.2	16.7	16.2	1	1	1
	1	17.6	3.9	15.6	19.8	1	1	1
	2	23.9	5.5	13.0	29.9	1	1	1
	4	35.3	7.7	10.0	43.4	1	1	1
	8	49.3	9.7	6.3	60.6	1	1	1
	24	69.9	7.1	1.2	85.9	1	1	1

Table 34. Conversion rates (c and c_{ee}), enantiomeric excesses of substrates (ee_S) and respective products (ee_P) as well as enantioselectivities (E) (calculated according to the different equations, cf. 3.3.1.4.) in the course of the enzyme-catalyzed kinetic resolution of 2-acetylthio-4-nonanone **9** by using GC/FID VI.

2-acetylthio-4-nonanone **9**								
						enantioselectivity E		
enzyme	time [h]	c [%]	ee_S [%]	ee_P [%]	c_{ee} [%]	equation 5	equation 6	equation 7
CAL-B	0.5	34.4	48.8	95.5	33.7	77	71	71
	0.75	36.8	60.5	94.6	38.9	70	67	67
	1	44.9	86.8	93.0	48.2	92	88	89
	1.5	45.3	86.8	93.0	48.2	79	78	78
	2	51.2	94.4	91.6	50.7	82	82	82
	4	54.4	99.2	84.0	54.2	62	62	62
	8	58.4	99.8	72.6	57.9	42	43	42
	24	67.5	99.9	49.0	67.1	19	15	19
PPL	1	3.4	0.2	10.5	1.5	1	1	1
	2	2.9	0.5	15.2	3.0	1	1	1
	4	6.1	1.0	20.4	4.9	2	2	2
	8	7.9	2.1	29.2	6.8	2	2	2
	24	11.3	4.8	39.7	10.7	2	2	2
WGL	1	23.0	6.0	21.7	21.7	2	2	2
	2	39.1	11.0	19.2	36.5	2	2	2
	4	52.5	15.4	14.8	50.9	2	2	2
	8	62.8	16.0	10.2	60.8	1	1	1
	24	79.6	15.4	4.0	79.4	1	1	1

Table 35. Conversion rates (c and c_{ee}), enantiomeric excesses of substrates (ee_S) and respective products (ee_P) as well as enantioselectivities (E) (calculated according to the different equations, cf. 3.3.1.4.) in the course of the enzyme-catalyzed kinetic resolution of 2-acetylthio-4-decanone **10** by using GC/FID VI.

2-acetylthio-4-decanone **10**								
						enantioselectivity E		
enzyme	time [h]	c [%]	ee_S [%]	ee_P [%]	c_{ee} [%]	equation 5	equation 6	equation 7
CAL-B	0.5	23.7	40.1	86.1	32.3	17	20	20
	0.75	32.9	52.0	94.3	35.2	74	57	57
	1	35.2	73.5	91.9	44.2	95	79	79
	1.5	38.3	73.5	18.5	21.4	60	52	52
	2	40.0	73.8	94.4	43.4	117	76	78
	4	47.5	92.8	90.1	50.7	66	64	65
	6	49.2	93.5	83.5	52.8	38	38	38
	8	50.7	98.5	82.9	54.3	51	52	52
	24	58.6	99.7	57.6	63.4	21	22	21
PPL	1	8.6	1.0	12.9	7.6	1	1	1
	2	12.8	2.4	10.6	18.1	1	1	1
	4	19.3	3.2	10.6	23.1	1	1	1
	8	25.8	4.5	10.1	31.0	1	1	1
	24	32.3	6.3	10.3	37.9	1	1	1
WGL	1	13.4	2.0	17.2	10.7	1	1	1
	2	18.7	2.0	9.0	18.3	1	1	1
	4	23.3	1.4	5.3	28.1	1	1	1
	8	30.2	0.7	3.6	9.3	1	1	1
	24	38.4	8.1	7.1	54.9	1	1	1

Table 36. Conversion rates (c and c_{ee}), enantiomeric excesses of substrates (ee_S) and respective products (ee_P) as well as enantioselectivities (E) (calculated according to the different equations, cf. 3.3.1.4.) in the course of the enzyme-catalyzed kinetic resolution of 4-acetylthio-2-heptanone **13** by using GC/FID IV.

4-acetylthio-2-heptanone **13**								
						enantioselectivity E		
enzyme	time [h]	c [%]	ee_S [%]	ee_P [%]	c_{ee} [%]	equation 5	equation 6	equation 7
CAL-B	1	0.2	7.7	n.d.[a]	n.d.[a]	n.d.[a]	n.d.[a]	n.d.[a]
	2	0.3	6.9	n.d.[a]	n.d.[a]	n.d.[a]	n.d.[a]	n.d.[a]
	4	0.4	6.3	100.0	5.9	n.d.[a]	n.d.[a]	n.d.[a]
	8	1.1	5.2	68.6	7.1	6	6	6
	24	4.3	2.4	70.9	3.3	6	6	6
PPL	1	57.5	39.8	39.0	50.5	3	3	3
	2	69.9	64.1	31.1	67.3	3	3	3
	4	79.3	82.1	21.4	79.4	3	3	3
	8	85.7	89.0	13.5	86.8	3	3	3
	24	88.2	85.0	8.5	90.7	2	2	2
WGL	1	30.2	12.3	8.1	60.4	1	1	1
	2	46.4	14.3	6.4	69.0	1	1	1
	4	67.4	17.3	4.0	81.1	1	1	1
	8	88.9	28.2	1.9	93.6	1	1	1
	24	98.2	34.4	0.4	98.7	1	1	1

[a] not determinable

Publications (Peer-Reviewed)

Kiske, C.; Nörenberg, S.; Ecker, M.; Ma, X.; Taniguchi, T.; Monde, K.; Eisenreich, W.; Engel, K.-H. Reinvestigation of the Absolute Configurations of Chiral *β*-Mercaptoalkanones Using Vibrational Circular Dichroism and ^{1}H NMR Analysis.
J. Agric. Food Chem. **2016**, *64*, 8563-8571.
Copyright permission from American Chemical Society 2016.

Kiske, C.; Riegel, A. D.; Hopf, R., Kvindt, A.; Poplacean, I.; Taniguchi, T.; Swamy, M. M. M.; Monde, K.; Eisenreich, W.; Engel, K.-H. Determination of the Absolute Configurations and the Sensory Properties of the Enantiomers of a Homologous Series (C6–C10) of 2-Mercapto-4-alkanones. *J. Agric*. *Food Chem*. **2019**, *67*, 1187-1196.
Copyright permission from American Chemical Society 2019.

Nörenberg, S.; **Kiske, C.**; Reichardt, B.; Andelfinger, V.; Pfeiffer, A.; Schmidts, F.; Eisenreich, W.; Engel, K.-H. Analysis and Sensory Evaluation of the Stereoisomers of a Homologous Series (C5-C10) of 4-Mercapto-2-alkanols.
J. Agric. Food Chem. **2017**, *65*, 8913-8922.

Nörenberg, S.; **Kiske, C.**; Burmann, A.; Poplacean, I.; Engel, K.-H. Distributions of the Stereoisomers of *β*-Mercaptoheptanones and *β*-Mercaptoheptanols in Cooked Bell Pepper (*Capsicum annuum*).
J. Agric. Food Chem. **2017**, *65*, 10250-10257.